OUKA
The University of Osaka
Institutional Knowledge Archive

Title	REACTI0N MECHANISM OF F_1-ATPASE
Author(s)	Matsuoka, Ichiro
Citation	大阪大学, 1982, 博士論文
Version Type	VoR
URL	https://hdl.handle.net/11094/27705
rights	
Note	

The University of Osaka Institutional Knowledge Archive : OUKA

https://ir.library.osaka-u.ac.jp/

The University of Osaka

REACTION MECHANISM OF F_1-ATPASE

ICHIRO MATSUOKA

DEPARTMENT OF BIOLOGY, FACULTY OF SCIENCE, OSAKA UNIVERSITY

FEBRUARY 1982

CONTENTS

GENERAL INTRODUCTION

In oxidative phosphorylation and photophosphorylation, exergonic oxidation-reduction reactions are coupled to the endergonic synthesis of ATP. The chemiosmotic hypothesis of Peter Mitchell(1) best describes the manner in which energy is conserved during ATP synthesis; that is, a transmembrane electrochemical gradient serves as a required intermediate in the following energy conversion processes (Reaction 1 & 2).

$$A_{red} + B_{ox} \rightleftharpoons A_{ox} + B_{red} + \Delta\mu H^{+} \qquad 1$$

$$ADP + P_i + \Delta\mu H^{+} \rightleftharpoons ATP + H_2O \qquad 2$$

The vectorial transport of protons across the membrane associated with electron transport gives rise to a electrochemical gradient, $\Delta\mu H^{+}$(Reaction 1). The energy stored in this gradient is used by membrane-bound coupling factors, F_1-F_o, to drive the net synthesis of ATP(Reaction 2). As this reaction is reversible, the proton gradient is also formed during the net hydrolysis of ATP(1).

The complex of coupling factors that catalyzes Reaction 2 has two empirically defined components. F_o is an integral membrane complex of three distinct subunits, and has shown to play an essential role in the translocation of protons(2). F_1 can be detached from the membrane as a water soluble complex of five subunits, α to ε (2). The enzyme, F_1, contains catalytic site for ATP synthesis and hydrolysis. However, the major question still to be answered is, How does the F_1-F_o complex catalyze the synthesis of ATP? When physically separated from membrane, soluble F_1 is only capable of catalyzing the net hydrolysis of ATP. However, if we assume the mechanism of ATP synthesis is the

reversal of that of ATP hydrolysis, we can elucidate the mechanism of ATP synthesis from the detailed analysis on the mechanism of ATP hydrolysis catalyzed by soluble F_1. Thus, the reaction mechanism of F_1-ATPase is the subject of this thesis.

I attempted to clarify the reaction mechanism of F_1-ATPase using a fluorescent analog of ATP. Thus, 2'-(5-dimethylamino-naphthalene-1-sulfonyl) amino-2'-deoxyATP (DNS-ATP) was synthesized by Watanabe and coworkers(3). DNS-ATP has the following advantages for the present purpose. (1) The fluorescence intensity of DNS-ATP increases markedly on its bunding to F_1, and it reflects the environment of nucleotide binding site of F_1. (2) DNS-ATP is hydrolyzed by F_1 very slowly, making kinetic measurements easier than with ATP. (3) DNS-AT^{32}P can be easily synthesized enzymatically.

In this thesis, following conclusions were drawn from the analysis of the reactions of DNS-ATP with F_1 (isolated from beef heart mitochondria) and EF_1 (isolated from E. coli plasma membrane): (1) F_1 contains two identical DNS-ATP binding sites. The affinity of the sites for DNS-ATP is very high, and the DNS-ATP bound to this site is hydrolyzed according to the following reaction scheme:

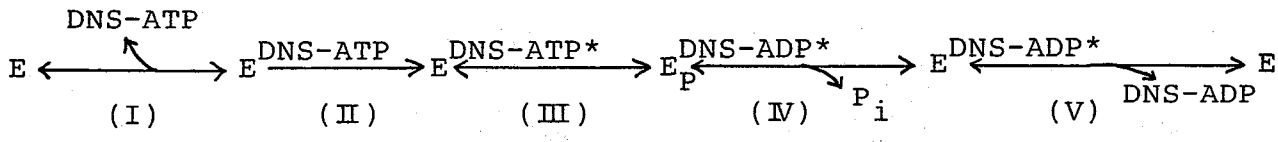

This scheme is quite resembles that of myosin ATPase. (2) High concentrations of nucleotide, such as ATP, accelerate the steps (III), (IV), and (V) in the above scheme. Thus, the low affinity regulatory site(s) is suggested to exist, besides the high affinity catalytic sites. (3) DNS-ATP binds to α subunit of EF_1 with very high affinity and not to β subunit. The chemical modification of

β subunit of EF_1 with DCCD does not change the binding of DNS-ATP to EF_1 (steps (I) and (II)), and does not inhibit the single turnover of DNS-ATP cleavage (step (III)). However, this modifi= cation leads to the inhibition of accelerating effect of ATP on the DNS-nucleotide release from EF_1 (step (V)), and leads to the inhibition of EF_1-ATPase activity at steady state. Therefore, it is suggested that the high affinity catalytic site and low affinity regulatory site exist in the α subunit and β subunit, respectively.

1. Mitchell, P. (1977) Ann. Rev. Biochem. 46, 996-1005
2. Kagawa, Y. (1978) Biochim. Biophys. Acta 505, 45-93
3. Watanabe, T., Inoue, A., Tonomura, Y., Uesugi, S., & Ikehara, M. (1981) J. Biochem. 90, 957-965

ABBREVIATIONS

ATP	adenosinetriphosphate
ADP	adenosinediphosphate
$AT^{32}P$	[γ-^{32}P]ATP
DNS-ATP and DNS-ADP	2'-(5-dimethylaminonaphthalene-1-sulfonyl) amino-2'-deoxyATP and -deoxyADP
DNS-$AT^{32}P$	[γ-^{32}P]DNS-ATP
CTP	cytidinetriphosphate
GTP	guanosinetriphosphate
ITP	inosinetriphosphate
NTP and NDP	nucleoside tri- and diphosphate
AMPPNP	adenylyl-5'-imidodiphosphate
F_1	coupling factor 1 (soluble mitochondrial ATPase)
EF_1	F_1 of E. coli
EDTA	ethylenediaminetetraacetic acid
DCCD	dicyclohexylcarbodiimido
PEP	phosphoenolpyruvate
SDS	sodium dodecyl sulfate
TCA	trichloroacetic acid
Tris	tris(hydroxymethyl)aminomethane
P_i	inorganic phosphate
PP_i	inorganic pyrophosphate

PART I.

Reaction Mechanism of the ATPase Activity of Mitochondrial F_1, Studied by Using a Fluorescent ATP Analog, 2'-(5-Dimethylamino-naphthalene-1-Sulfonyl) Amino-2'-DeoxyATP: Its Striking Resemblance to That of Myosin ATPase.

SUMMARY

The reaction mechanism of beef heart mitochondrial F_1-ATPase was studied by using a fluorescent ATP analog, 2'-(5-dimethylamino=naphthalene-1-sulfonyl)amino-2'-deoxyATP (DNS-ATP), as a substrate. The following results were obtained.

1. In the presence of Mg^{2+}, 2 mol of DNS-ATP bind to 1 mol of F_1 with an apparent dissociation constant of 0.44 μM. Upon binding, the fluorescence emission spectrum of DNS-ATP shifted to shorter wavelengths, and the fluorescence intensity at 520 nm increased 4.8 fold. On the other hand, in the absence of Mg^{2+}, the apparent dissociation constant of F_1-DNS-ATP was 16 μM, and the extent of fluorescence enhancement was 1.3- to 1.9-fold.

2. The initial rate of fluorescence enhancement, v_f, upon addition of Mg^{2+} to a mixture of F_1 and DNS-ATP was given by the following equation:

$$v_f = \frac{V_f}{(1 + \frac{K_f}{[\text{DNS-ATP}]})}$$

where V_f = 0.34 s^{-1} and K_f = 3.3 μM. Following the fluorescence enhancement, TCA-P_i and free P_i were liberated consecutively. The fluorescence intensity maintained its enhanced level even after the free P_i liberation and, on addition of an excess amount of EDTA, decreased slowly to the original level From these findings, the following reaction mechanism for F_1-DNS-ATPase was proposed:

$$E+DNS\text{-}ATP \rightleftharpoons E^{DNS\text{-}ATP} \rightarrow E^{DNS\text{-}ATP*} \rightleftharpoons E_P^{DNS\text{-}ADP*} \searrow^{P_i} \quad E^{DNS\text{-}ADP*} \searrow^{DNS\text{-}ADP} E$$

rapid. eq. fast fast slow very slow

where an asterisk indicates the state of bound DNS-nucleotide with enhanced fluorescence and $E_P^{DNS\text{-}ADP*}$ is a TCA-unstable reaction intermediate. This reaction mechanism resembles that of myosin ATPase. In accordance with the reaction mechanism and the stoichiometry of DNS-ATP binding, an initial burst of TCA-P_i liberation of 2 mol/mol F_1 was observed.

3. The addition of an excess of ATP to F_1-DNS-nucleotide in the presence of Mg^{2+} accelerated markedly the liberation of both TCA-P_i and free P_i. ATP also accelerated the fluorescence decrease of F_1-DNS nucleotide. Direct measurements of released free DNS-nucleotide indicated that the fluorescence decrease was due to the release of DNS-ADP from F_1. ADP, AMPPNP, ITP, and GTP accelerated the F_1-DNS-ATPase reaction in a similar manner. On addition of these NTP, the release of DNS-ADP from F_1 proceeded in rapid and slow steps. CTP and PPi largely or completely failed to accelerate the conversion of $E^{DNS\text{-}ATP*}$ into $E_P^{DNS\text{-}ADP*}$. Furthermore, CTP and PP_i induced only the slow release of DNS-ADP. Therefore, we concluded that several nucleotides including ATP bind to the regulatory site(s) on F_1 to induce a conformational change at the catalytic sites and accelerate each of the following steps: $E^{DNS\text{-}ATP*} \rightleftharpoons E_P^{DNS\text{-}ADP*} \searrow^{P_i} E^{DNS\text{-}ADP*} \searrow^{DNS\text{-}ADP} E$. On the other hand, PP_i and CTP mainly accelerate the release of DNS-ADP from $E^{DNS\text{-}ADP*}$ by displacement. AMP did not affect the F_1-DNS-ATPase reaction.

4. The steady-state rate of F_1-DNS-ATPase, v_o, increased linearly with increase in the concentration of DNS-ATP and was 1 s^{-1} at 200 μM DNS-ATP exceeding than V_f (0.34 s^{-1}). The time course of ATP hydrolysis after addition of ATP to F_1-DNS-nucleotide showed no lag phase which corresponds to the release of DNS-ADP. These two findings indicate that F_1-NTPase can also occur through a reaction path in which E_P^{NDP} is not formed.

5. P_i enhanced the fluorescence of F_1-DNS-nucleotide and inhibited the displacement of bound DNS-ADP with ATP or PP_i. The extent of fluorescence enhancement by P_i was maximal at 1 mol DNS-ATP/mol F_1. This finding implies that the two DNS-ATP binding sites on F_1 are heterogenous at least with respect to the interaction with P_i.

INTRODUCTION

It is widely accepted that a mitochondrial F_1-F_o complex catalyzes the ATP synthesis in oxidative phosphorylation (for reviews see 1,2). When isolated from membrane, F_1 catalyzes only the hydrolysis of ATP, although the reaction center of ATP synthesis is supposed to be remaining in the isolated enzyme.

Recently important information has been accumulated on the structure and function of each subunit in F_1-ATPase [EC 3.6.1.3] from thermophilic bacteria (2) and E. coli (3) by use of a reconstitution technique. Furthermore, many features of nucleotide binding to F_1 were reported by Slater (4) and others (for review see 5). Boyer and coworkers (6) investigated the reaction mechanism of F_1-ATPase mainly utilizing the oxygen exchange reaction, and Slater and coworkers (7) analyzed kinetic properties of the presteady state of ATP hydrolysis. Several authors (6-10) suggested regulatory effects of ATP and ADP on the reaction rate, nucleotide binding, and P_i binding to F_1. Boyer and coworkers (11) have proposed a possible catalytic cooperativity among subunits in the reaction of F_1-ATPase.

Boyer and coworkers (11) suggested that there was a similarity between F_1-ATPase and myosin ATPase in their reaction mechanisms. In myosin ATPase, each reaction step is identified and conformational change of the enzyme induced by nucleotide binding is directly measured (12-15). On the other hand, details of the reaction mechanism of F_1-ATPase are not known despite numerous efforts as mentioned above. Therefore, we attempted to clarify the reaction mechanism of F_1-ATPase by using the methods developed

in the research of myosin ATPase (12-15). One of them was to use a fluorescent analog of ATP, 2'-(5-dimethylaminonaphtalene-1-sulfonyl) amino-2'-deoxyATP (DNS-ATP) which was synthesized by substituting the 2'-hydroxy group of ATP with an amino group and introducing a dimethyl amino naphtalene sulfonyl group (16). DNS-ATP has the following advantages serving the present purpose: (1) The fluorescence intensity of DNS-ATP increases markedly on its binding to F_1, and the extent of enhancement depends on experimental conditions. (2) DNS-ATP is hydrolyzed by F_1 very slowly, enabling easier kinetic measurements than using ATP. (3) DNS-AT^{32}P can be easily synthesized enzymatically.

MATERIALS AND METHODS

Materials — DNS-ATP and DNS-ADP were synthesized as described previously (16). DNS-AT^{32}P was synthesized by the same enzymatic method as described by Glynn and Chapell for AT^{32}P synthesis (17). Specific radioactivity of DNS-AT^{32}P was about 2 μCi/nmol. Adequate purity of DNS-ATP, DNS-ADP, and DNS-AT^{32}P was confirmed by paper electrophoresis run in 50 mM triethylamine bicarbonate at pH 7.6 (16).

Pyruvate kinase [EC 2.7.1.40] was prepared according to the method of Tietz and Ochoa (18). Luciferase [EC 1.13.12.7] was prepared from firefly lantern as described previously (19). ATP, ADP, and AMP were purchased from Khojin Ltd.(Tokyo). AMPPNP, ITP, GTP, PEP, and luciferin were purchased from Sigma Chemicals Co.(St. Louis). [^{3}H]Glucose was purchased from New England Nuclear Co.(London). All other chemicals were of reagent grade purity.

Purification of F_1— Submitochondrial particles were prepared from beef heart mitochondria as described by Beyer (20). F_1 was extracted from submitochondrial particles with chloroform as described by Beechy et al. (21). After 30-60% ammonium sulfate fractionation, the concentrated extract was subjected to gel filtration on a Sephacryl S-300 Superfine column (3.2x75 cm) equilibrated with 100 mM Tris-HCl, 5mM EDTA, and 50% glycerol at pH 8.0 and 20°C. The eluted enzyme was concentrated by ultrafiltration on an Amicon Diaflo XM-100A membrane, and stored at 0°C. The protein concentration of purified F_1 was determined by the biuret method (22) with bovine serum

albumin ($A_{279\ nm}$ = 0.667 $cm^2 \cdot mg^{-1}$) as a standard. The concentration of F_1 was calculated by using a molecular weight of 360,000 (1). The purified enzyme was subjected to SDS-gel electrophoresis on 10% polyacrylamide gel according to the method of Weber and Osborne (23).

The nucleotide content of purified F_1 was measured as follows: To 0.5 ml of F_1 solution at 22 mg/ml, 0.5 ml of 8% $HClO_4$ was added. After centrifugation at 2000 x g for 20 min, the supernatant was neutralized to pH 7.6 with 4 N KOH. Total nucleotide content was determined spectrophotometrically by using $\varepsilon_{259\ nm}$ = 15.4 $mM^{-1}cm^{-1}$ for adenine nucleotides, since the UV absorption spectrum of the supernatant was the same as that for adenine nucleotides. The contents of ATP and ADP were determined by the firefly luciferase system, as described by Furukawa et al. (19), after convertion of ADP to ATP by 0.1 mg/ml pyruvate kinase and 4 mM PEP.

Fluorescence Measurement — Usually measurement solutions were prepared by addition of reagents in 5-20 µl portions to 2.0 ml of 50 mM Tris-HCl, pH 8.0 containing 2 mM EDTA. The measurements were performed at 30°C. To initiate a reaction, a reagent was stirred into a cuvette containing the rest of a reaction mixture with the aid of a magnetic stirrer (mixing time $\leq$ 0.2 s). Fluorescence intensity was measured on a Hitachi MPF-4 spectrofluorometer equipped with a thermostated cuvette hodler. The slit widths on the excitation and emission monochrometers were 6 and 8 nm, respectively. The fluorescence intensity at 520 nm of DNS-ATP and DNS ADP was measured with excitation at 340 nm.

Partial Reaction of F_1-DNS-ATPase — All the concentrations were expressed in terms of final concentrations, unless otherwise stated, throughout the text and figure legends. The composition of a reaction mixture was 5 mM $MgCl_2$, 2 mM EDTA, 50 mM Tris-HCl at pH 8.0 and appropriate concentrations of DNS-ATP and F_1. After adding 0.1 ml of F_1 solution to 0.85 ml of a solution containing EDTA and DNS-AT^{32}P in Tris-HCl, it was incubated for 30 s at 30°C. The F_1-DNS-ATPase reaction was started by addition of 0.05 ml of 100 mM $MgCl_2$. At appropriate intervals the reaction was stopped by addition of 1 ml of 10% TCA. After centrifugation, $^{32}P_i$ in the supernatant (TCA-$^{32}P_i$) was measured as described by Nakamura and Tonomura (24).

The concentration of total free ^{32}P (free $^{32}P_i$ + free DNS-ATP^{32}P) was measured by a double membrane filtration method developed by Yamaguchi and Tonomura (25). By using a set of two membrane filters (upper Amicon Diaflo XM-100A membrane; lower Millipore filter, pore size 0.8 μm), this technique enabled the separation of free ^{32}P remaining on the Millipore filter from the F_1-bound form on the Amicon membrane. The diameter of both membranes was 10 mm. The reaction mixture was the same as used in the TCA-$^{32}P_i$ measurement, except that 10 mM [^{3}H]glucose was added to measure the volume of a filtrate. At appropriate times, 50 μl of the reaction mixture was withdrawn and applied on the upper membrane and filtrated by vacuum sucking for 4 s. A small volume (0.5-3 μl) of filtrate remained on the Millipore filter was dried, and the residues were solubilized in 1 ml of dimethyl formamide. The concentration of total free ^{32}P in the filtrate was determined from the ratio of radioactivities, $^{32}P/^{3}H$ (25).

The reaction mixture for measurement of the concentration of free DNS-nucleotide was the same as that for the TCA-$^{32}P_i$ measurement, except that 10 mM [^{3}H]glucose was added and DNS-ATP was used instead of DNS-AT^{32}P. The diameter of the membranes was 25 mm, and the volume of a reaction mixture applied on the membranes was 500 µl, leaving 10-30 µl on the Millipore filter after sucking. The dried Millipore filter was solubilized by 2 ml of dimethyl formamide.

The amount of free DNS-nucleotide in the filtrate was determined by measuring the fluorescence intensity at 530 nm after correcting the fluorescence due to Millipore filter solubilized by dimethyl formamide. The volume of the filtrate was determined from the radioactivity of [^{3}H]glucose.

ATPase Activity — The ATPase activity of F_1 was measured in the presence of a pyruvate kinase system (0.1 mg/ml pyruvate kinase and 4 mM PEP) as a feeder, and the amount of P_i liberated was measured by the method of Fiske and Subbarow (26).

RESULTS

Properties of Purified F_1 — The specific activity of purified F_1 measured in the presence of 5 mM ATP at pH 8.0 and 30 °C was 120-150 U/mg, which was similar to that already reported (7). When kept in 50% glycerol, F_1 was quite stable. At 0 °C the activity did not change at all for more than three months. As is widely accepted, purified F_1 was composed of 5 subunits (Fig. 1), and the intrinsic inhibitor protein which is usually seen between δ and ε subunits in SDS-gel electrophoresis (27) was completely removed by gel filtration on Sephacryl S-300. The adenine nucleotide content calculated from ΔA at 259 nm was 2.4 mol/mol F_1. The ATP content of the sample measured by the luciferin-luciferase method was 2.3 mol/mol F_1. The ADP content was less than 0.3 mol/mol F_1.

Fluorescence Change of DNS-ATP on Its Binding to F_1 — Figure 2 shows that the addition of 1.5 μM F_1 to 3.2 μM DNS-ATP in the presence of 2 mM EDTA increased the fluorescence intensity at 520 nm 24% from the level of free DNS-ATP, and that this increase consisted of an initial rapid change and the following slow one. This fluorescence increase was completely reversed by addition of 0.2 mM ATP, 0.2 mM ADP, 1 mM PP_i or 1 mM P_i (data not shown). On further addition of 5 mM $MgCl_2$ to the above mixture of F_1 and DNS-ATP, the fluorescence was markedly enhanced with a halftime of about 10 s, and reached a plateau within about 1 min. The Mg^{2+}-dependent fluorescence enhancement was observed only in the presence of F_1. Subsequent addition of P_i slowly enhanced the fluorescence intensity as will be

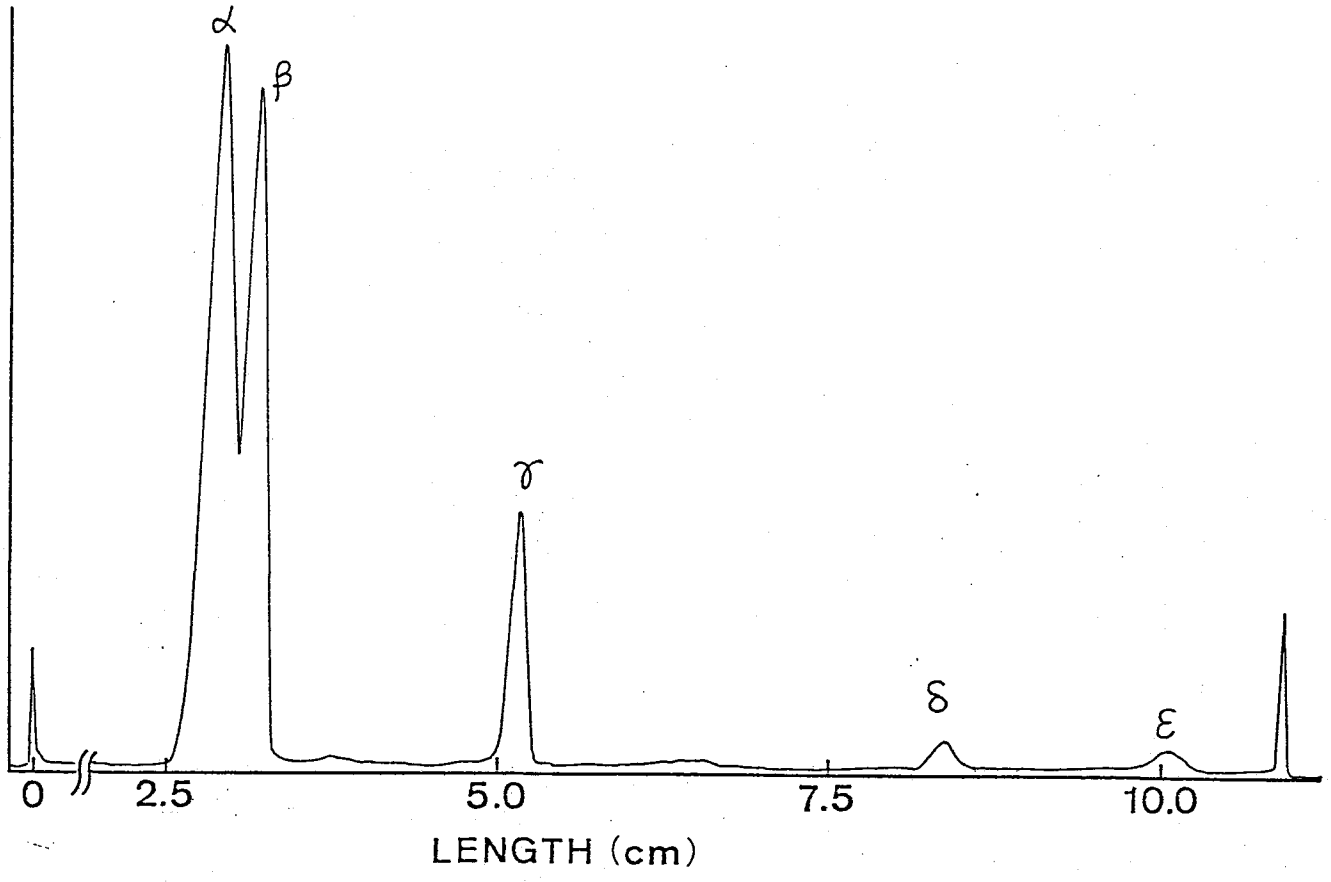

Fig. 1. SDS-gel electrophoretic pattern of purified F_1-ATPase. The amount of the applied protein was 5 μg. The length is the migration distance from the origin. The gel was stained by Coomassie Brilliant Blue, and scanned at 550 nm at 0.05 mm slit width.

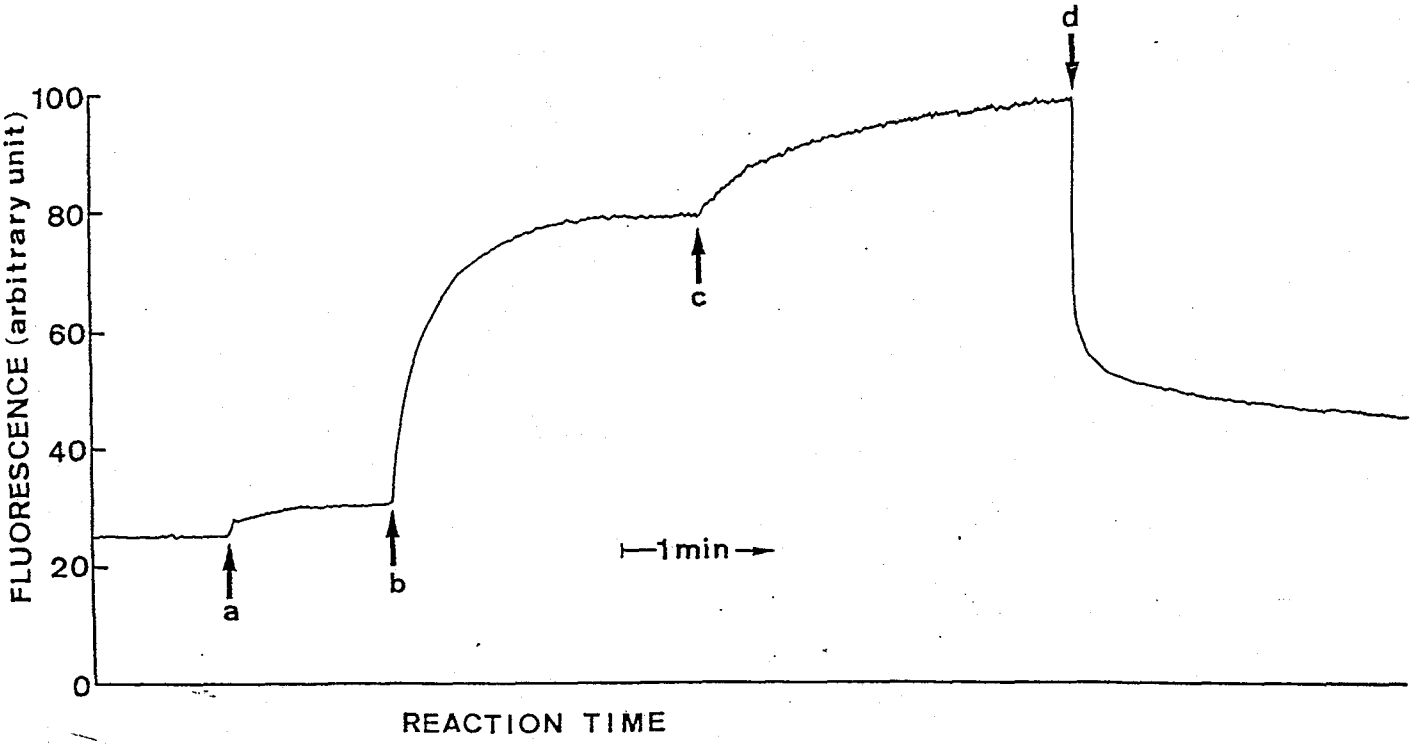

Fig. 2. Fluorescence intensity change of DNS-ATP on its binding to F_1. To mixture containing 3.2 μM DNS-ATP and 2 mM EDTA in 50 mM Tris-HCl, pH 8.0, following additions were made: a, 1.5 μM F_1; b, 5 mM $MgCl_2$; c, 4 mM K-P_i; d, 0.2 mM ATP.

detailed later. During this series of reaction, fluorescence emission spectra were recorded at various stages as shown in Fig. 3. DNS-ATP in 2 mM EDTA had an emission peak at around 555 nm (trace a) (16), which shifted to 545 nm with a slight increase in fluorescence intensity by addition of F_1 (trace b). Addition of 5 mM $MgCl_2$ markedly enhanced the fluorescence the maximum shifting to 525 nm (trace c). Finally by addition of 2mM Pi, the fluorescence maximum shifted to 520 nm with an intensity increase (trace d). As reported previously (12), addition of dioxane to an aqueous solution of DNS-ATP enhanced its fluorescence and caused a blue shift reflecting a hydrophobic interaction. Therefore hydrophobicity of the DNS-ATP binding site in F_1 was suggested to be very high (see Table I in DISCUSSION).

When F_1 was added to DNS-ATP in the presence of 2 mM EDTA at pH 6.5 or 7.5 (Fig. 4, arrow a), the fluorescence intensity increased rapidly followed by a slow decrease (Fig. 4). The fluorescence intensities at 1 min after addition of F_1 were 1.8- and 2.1-fold greater than those of free DNS-ATP at pH 7.5, and 6.5, respectively. At pH 8.0 this increase was 1.3-fold. The extent and time course of the fluorescence enhancement on addition of 5 mM $MgCl_2$ (arrow b) were almost the same at these pHs. All the following experiments were carried out at pH 8.0, where the fluorescence of DNS-ATP changed only slightly on addition of F_1 in the absence of Mg^{2+}.

The stoichiometry of DNS-ATP binding to F_1 was determined by fluorometric titration of o.75 or 1.5 uM F_1 with DNS-ATP in the presence of Mg^{2+} (Fig. 5.). The data were analyzed based on the quadratic equation:

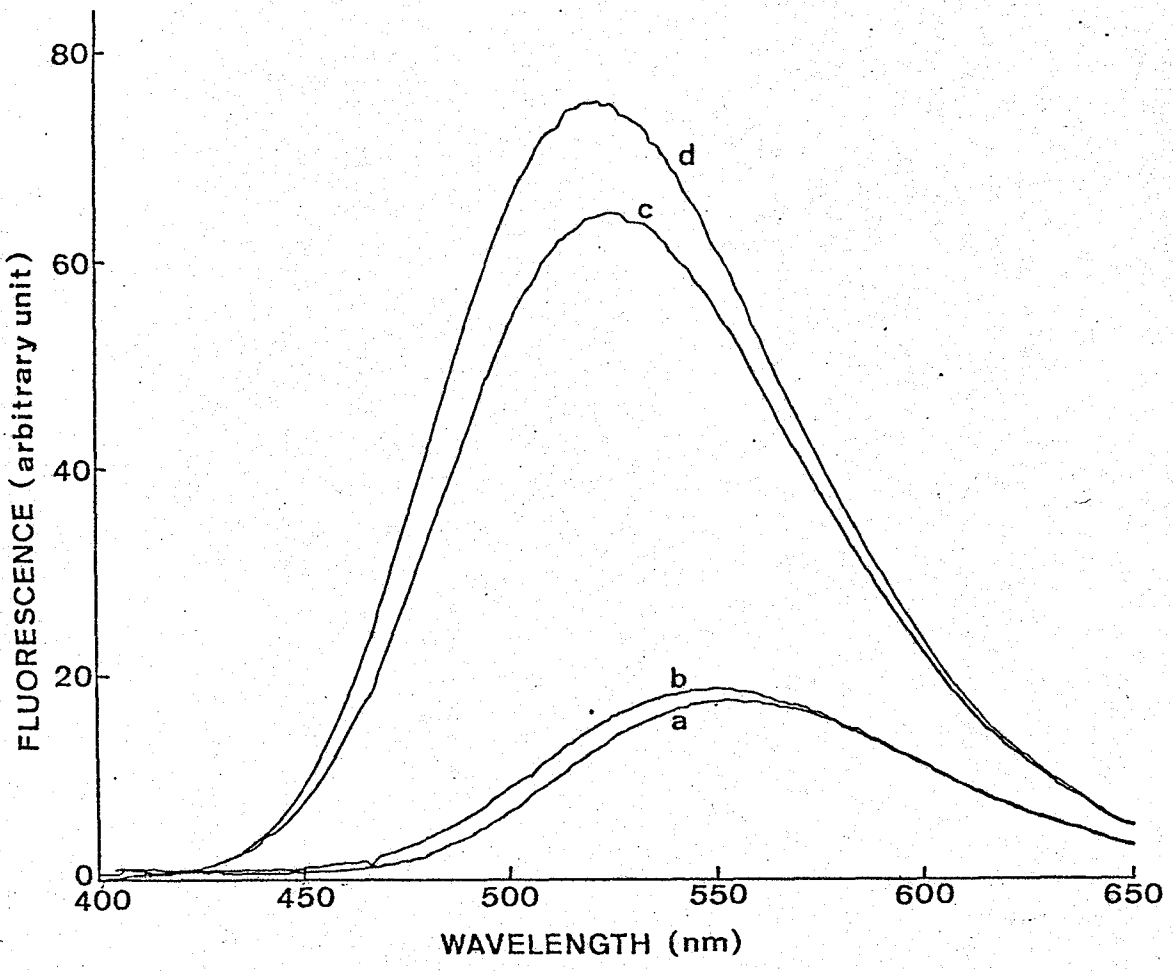

Fig. 3. Fluorescence emission spectra recorded during a course of reaction of DNS-ATP with F_1. Spectra were recorded in the following order; curve a, 2.1 μM DNS-ATP alone; curve b, 1 min after addition of 2.3 μM F_1; curve c, 2 min after addition of 5 mM $MgCl_2$; curve d, 2 min after addition of 2 mM K-P_i. The excitation wavelength was 340 nm.

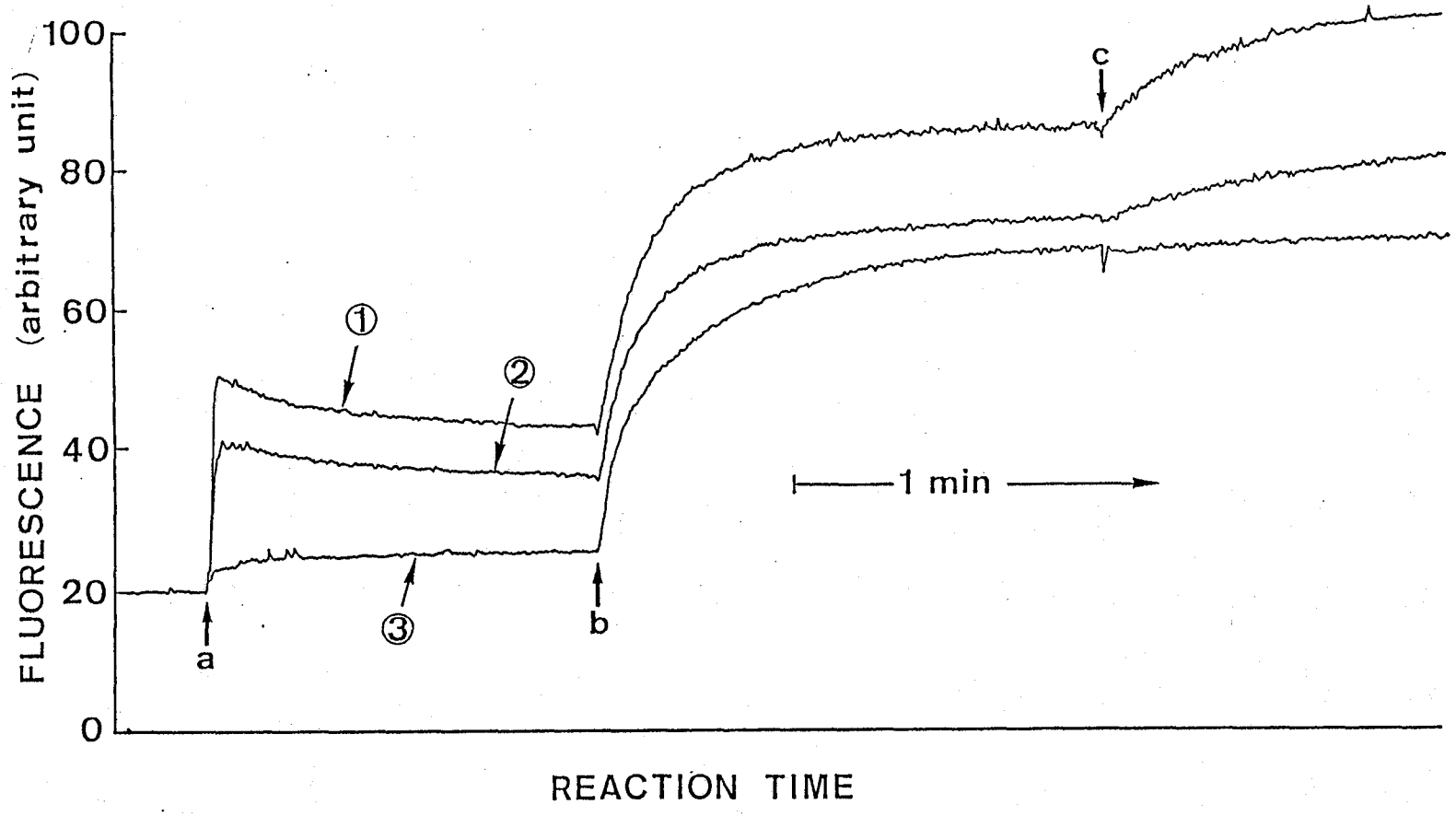

Fig. 4. pH Dependence of reaction of DNS-ATP with F_1. The pH of a mixture containing 2.1 μM DNS-ATP and 2 mM EDTA at 30°C was adjusted to 6.5 with 50 mM Tris-acetate (curve 1), 7.5 with 50 mM Tris-HCl (curve 2) and 8.0 with 50 mM Tris-HCl (curve 3). Following additions were made; a, 1.5 μM F_1; b, 5 mM $MgCl_2$; c, 50 μM K-P_i.

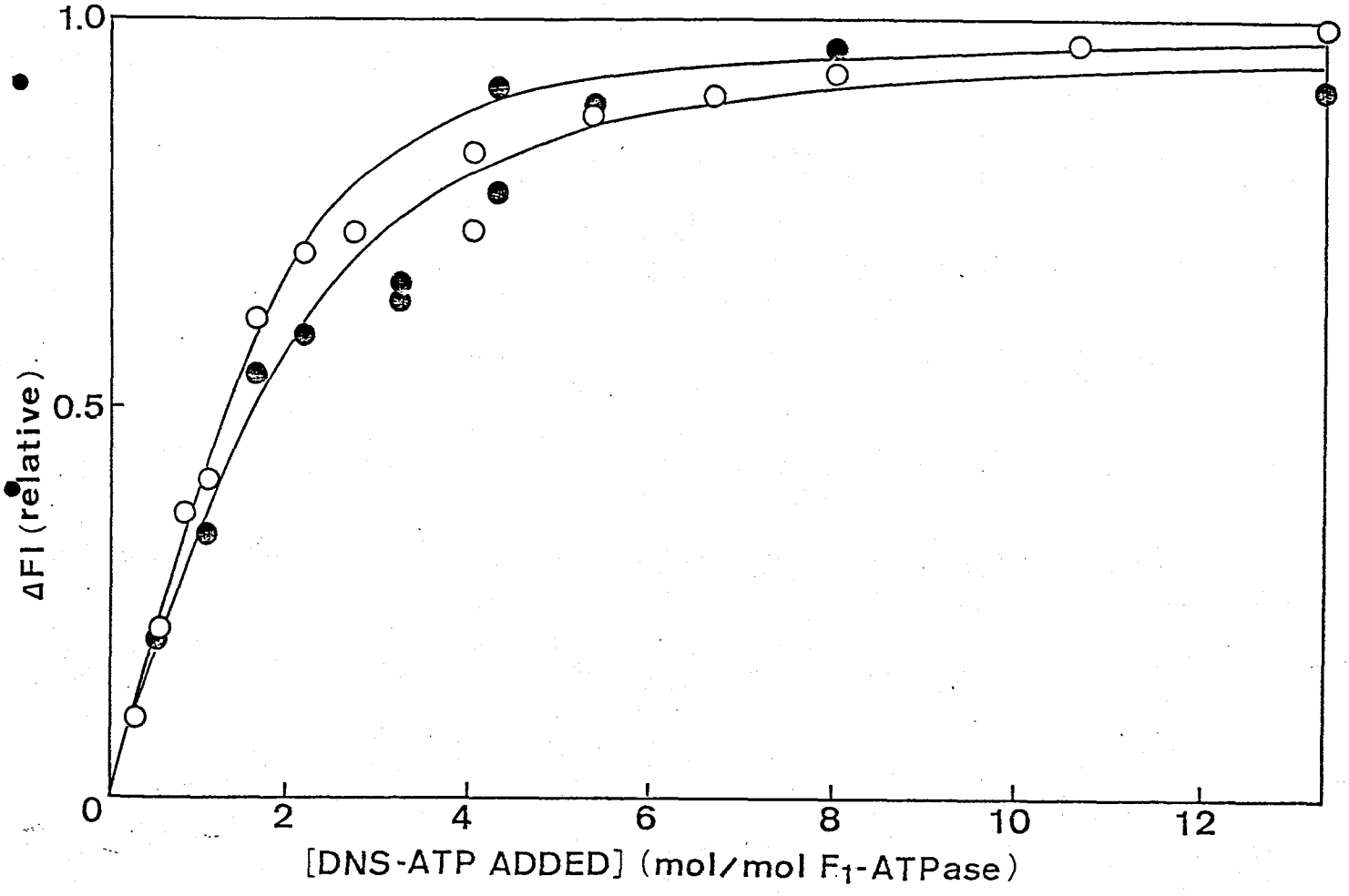

Fig. 5. Fluorometric titration of F_1 by DNS-ATP in the presence of $MgCl_2$. The extent of fluorescence enhancement 2 min after addition of 5 mM $MgCl_2$ was plotted against the amount of DNS-ATP added. The reaction mixture contained 0.75 (●) or 1.5 μM (○) F_1 in 2 mM EDTA, 50 mM Tris-HCl at pH 8.0. The solid lines are the theoretical curves (see text). The upper is for 1.5 μM F_1, and the lower for 0.75 μM F_1.

$$\Delta F = \frac{R}{2}\left\{(nE_o + S_o + \phi_{DNS\text{-}ATP}) - [(nE_o + S_o + \phi_{DNS\text{-}ATP})^2 - 4nE_oS_o]^{1/2}\right\} \quad (1)$$

where ΔF is the extent of fluorescence enhancement, and is assumed to be proportional to the amount of the F_1-DNS-nucleotide. R is the fluorescence parameter dependent upon experimental conditions, n is the number of independent and equivalent binding sites of DNS-ATP on F_1, E_o and S_o are the total concentrations of F_1 and DNS-ATP, respectively, and $\phi_{DNS\text{-}ATP}$ is the dissociation constant for the complex. It was also postulated that the fluorescence intensity of DNS-ATP during the course of interaction did not change. The curves in Fig. 5 are the best fits of the data to Eqn. 1 with n = 2 and $\phi_{DNS\text{-}ATP}$ = 0.44 μM. With n values other than 2, the fit was poor.

When PP_i had been added to the F_1-DNS-ATP system in advance, the extent of fluorescence enhancement on addition of Mg^{2+} decreased with increasing concentration of PP_i (Fig. 6). The results were explained by a competitive binding of PP_i to the DNS-ATP binding site on F_1:

$$\phi'_{DNS\text{-}ATP} = \phi_{DNS\text{-}ATP}\left(1 + \frac{[PP_i]}{\phi_{PP_i}}\right) \quad (2)$$

where $\phi'_{DNS\text{-}ATP}$ is the apparent dissociation constant for F_1-DNS-nucleotide in the presence of PP_i and ϕ_{PP_i} is the dissociation constant for F_1-PP_i. The data in Fig. 6 were analyzed based on Eqn. 1, where $\phi_{DNS\text{-}ATP}$ was replaced by $\phi'_{DNS\text{-}ATP}$ of Eqn. 2. The curve in Fig. 6 is the best fit to the data obtained with ϕ_{PP_i} = 39 μM.

DNS-ADP was also bound to F_1 and brought about similar fluorescence changes as DNS-ATP. In Fig. 7, the extents of

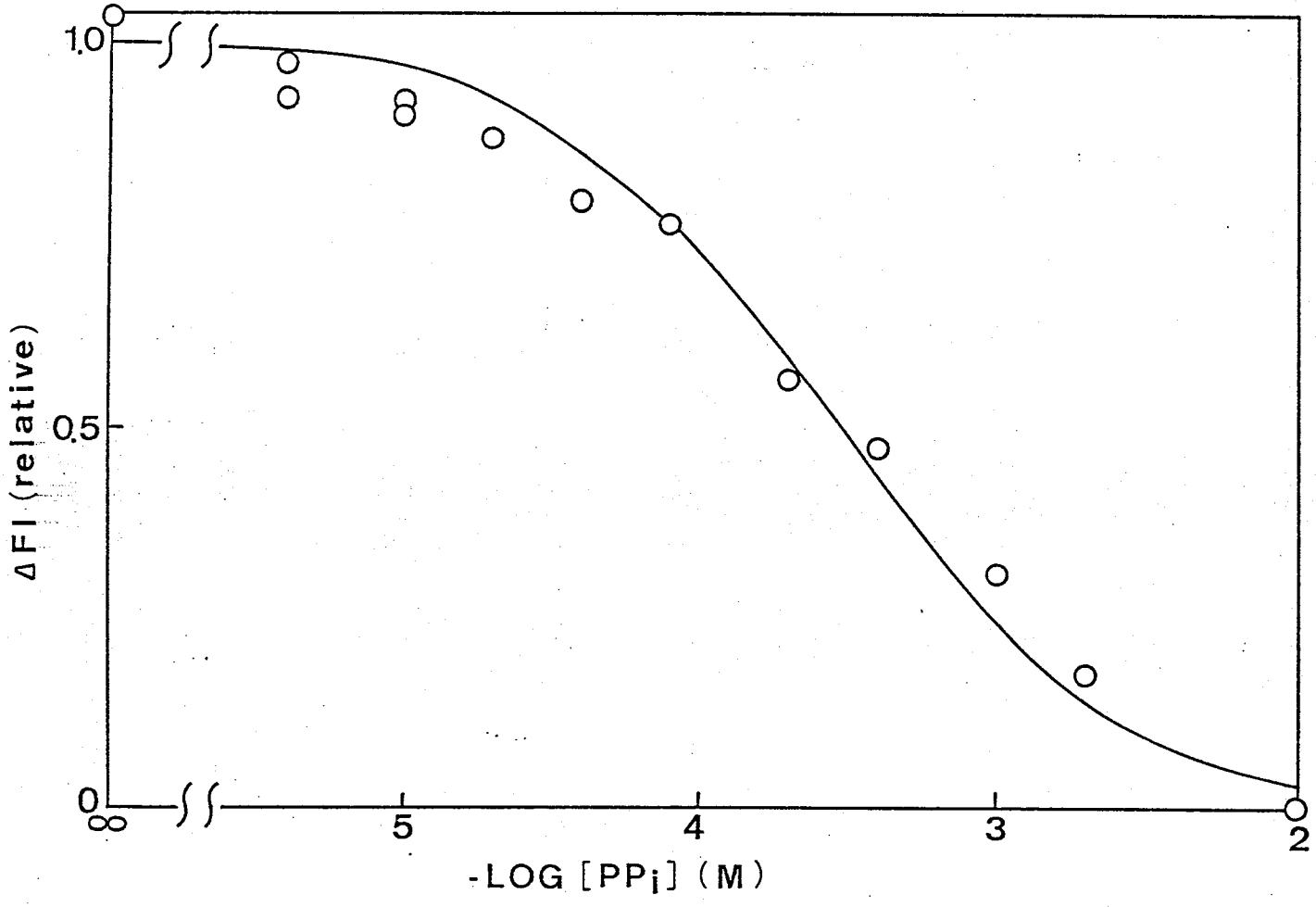

Fig. 6. Competitive binding of PP_i to the DNS-ATP binding site on F_1. The extent of fluorescence enhancement of DNS-ATP after addition of 5 mM $MgCl_2$ was plotted against the concentration of PP_i. The reaction mixture contained 3.2 μM DNS-ATP and 0.75 μM F_1. The solid line is the theoretical curve (see text).

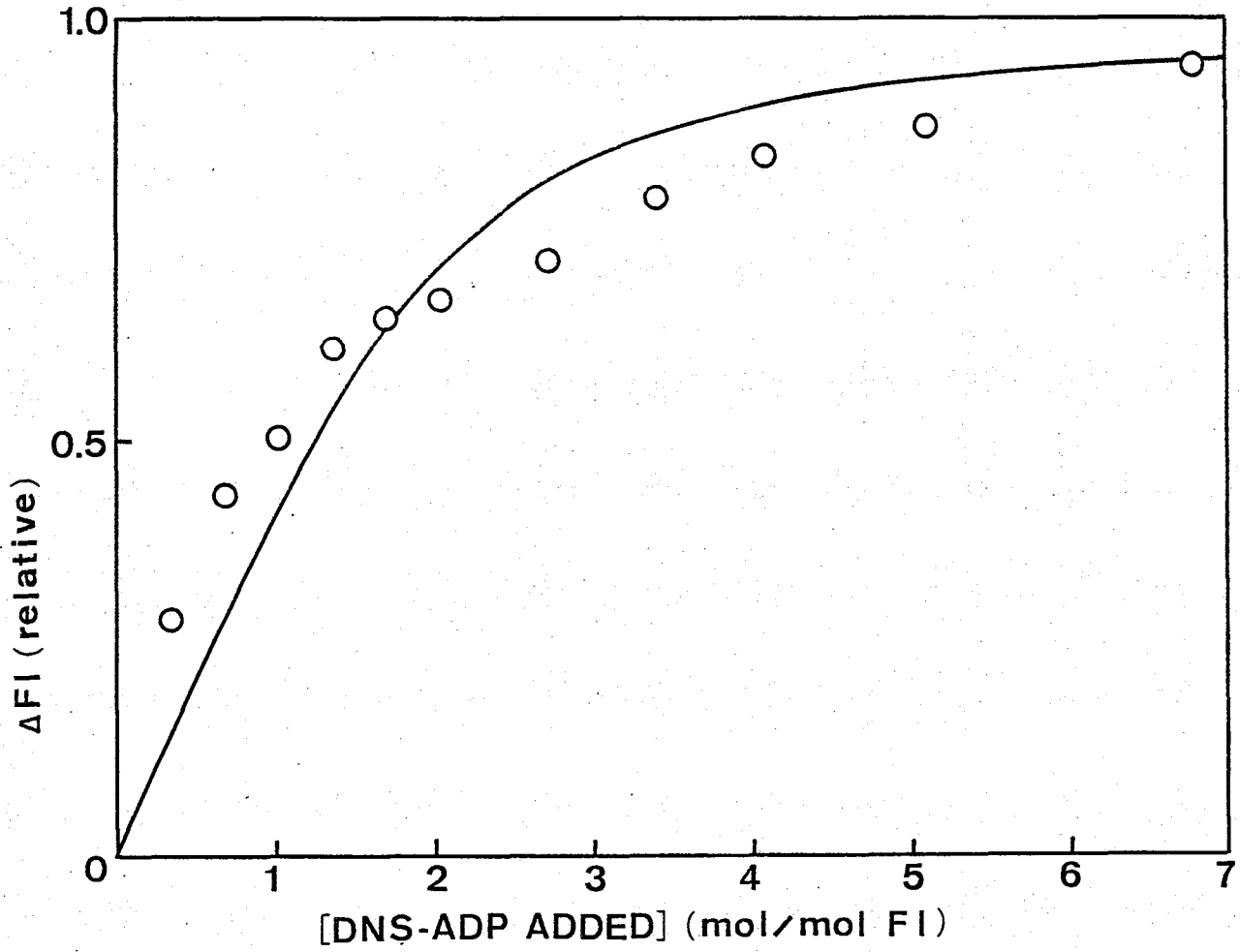

Fig. 7. Fluorometric titration of F_1 with DNS-ADP in the presence of $MgCl_2$. The extent of fluorescence enhancement 2 min after addition of 5 mM $MgCl_2$ was plotted against the amount of DNS-ADP added. The reaction mixture contained 1.5 μM F_1. The solid line is the teoretical curve (see text).

fluorescence enhancement on addition of 5 mM $MgCl_2$ to mixtures containing 1.5 μM F_1 and various amounts of DNS-ADP were plotted against the amounts of DNS-ADP added. The theoretical curve was obtained by using Eqn. 1, where parameters for DNS-ATP were taken as those for DNS-ADP, with n = 2 and $\phi_{DNS\text{-}ADP}$ = 0.4 μM. However, the measured values deviated somewhat from the curve.

Reaction Sequence of F_1-DNS-ATPase — We measured the initial rates of fluorescence enhancement, v_f, on addition of 5 mM $MgCl_2$ to mixtures containing 1.5 μM F_1 and various concentrations of DNS-ATP. The double reciprocal plot of v_f against the concentration of DNS-ATP gave a straight line as shown in Fig. 8. This result may be explained by the following reaction scheme,

$$E + \text{DNS-ATP} \underset{K_f}{\rightleftharpoons} E\cdot\text{DNS-ATP} \xrightarrow[V_f]{} E\cdot\text{DNS-ATP}^*.$$

By assuming that the first step is in rapid equilibrium (see DISCUSSION), we obtain

$$v_f = \frac{V_f}{1 + \dfrac{K_f}{[\text{DNS-ATP}]}} \qquad (3)$$

where K_f is the dissociation constant of E·DNS-ATP, V_f is the rate constant of the fluorescence enhancement, and an asterisk indicates a complex with an enhanced fluorescence intensity. The values of K_f and V_f were estimated as 3.3 μM and 0.34 s^{-1}, respectively, from the results in Fig. 8.

In Fig. 9, the initial phase of fluorescence enhancement on addition of 5 mM $MgCl_2$ to a mixture of 4.28 uM DNS-AT^{32}P and 6.78 uM F_1 is compared with the TCA-$^{32}P_i$ liberation

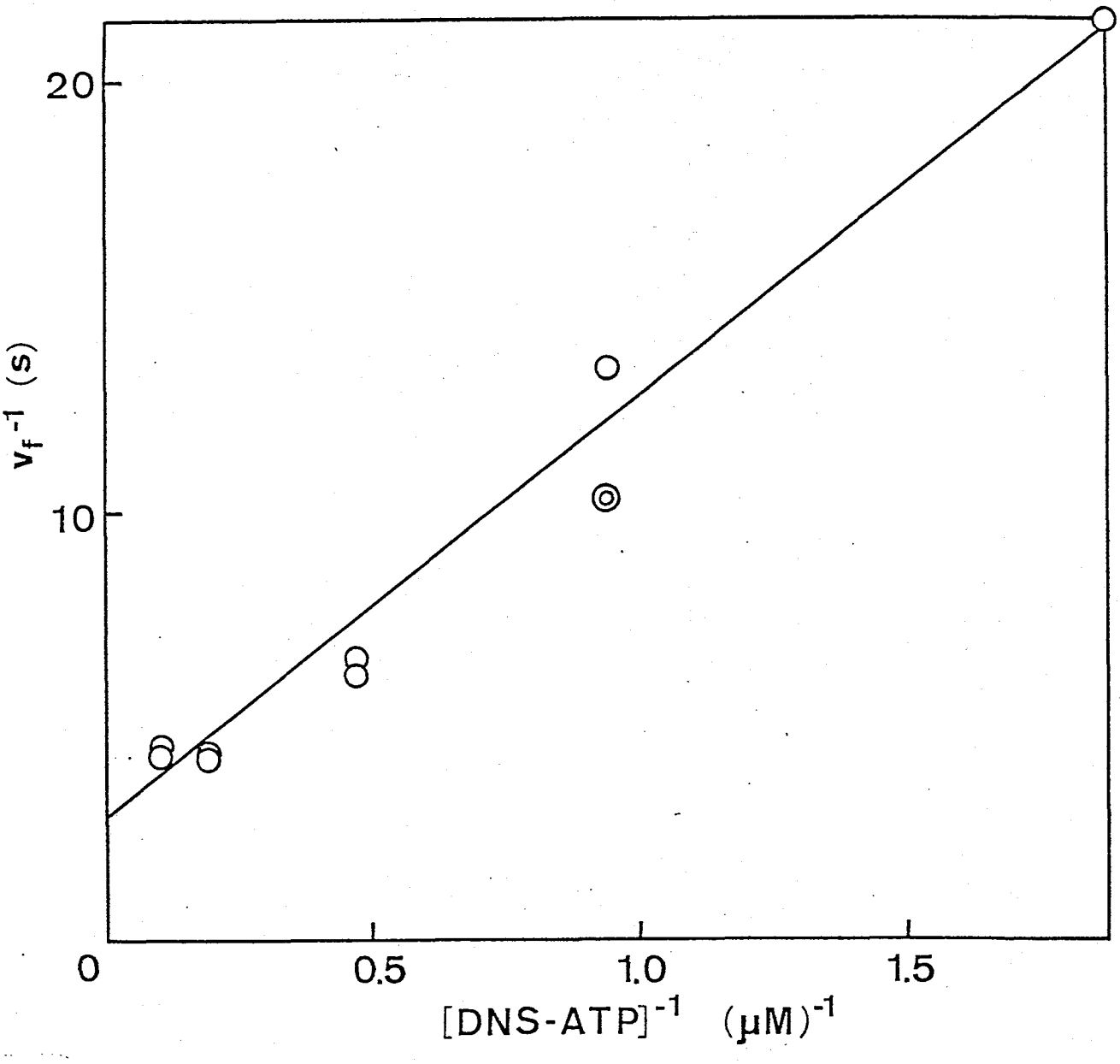

Fig. 8. Double reciprocal plot of the initial rate of fluorescence enhancement against DNS-ATP concentration. The reciprocal of the initial rate of fluorescence enhancement of DNS-ATP on addition of 5 mM $MgCl_2$, v_f, was plotted against the reciprocal of the concentration of DNS-ATP added. The concentration of F_1 was 1.5 μM.

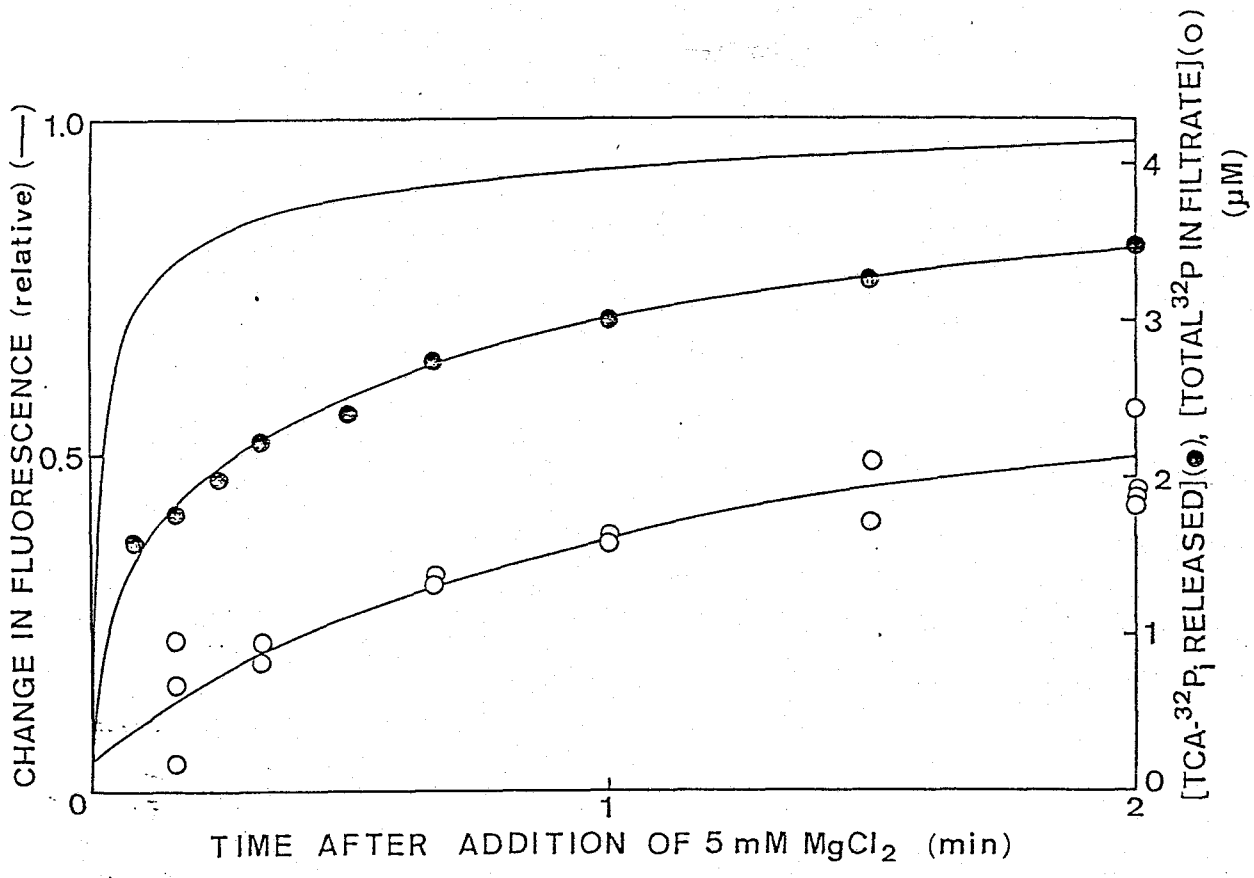

Fig. 9. Time course of fluorescence enhancement, TCA-$^{32}P_i$ liberation and total free ^{32}P liberation in the initial phase of the reaction of DNS-AT^{32}P with F_1. The reaction mixture contained 4.28 μM DNS-AT^{32}P, 6.78 μM F_1, and 10 mM [^{3}H]glucose in 2 mM EDTA and 50 mM Tris-HCl at pH 8.0. The reaction was started by addition of 5 mM $MgCl_2$, and stopped by addition of 5% TCA (TCA-$^{32}P_i$) or filtration through an XM-100A membrane (total free ^{32}P) at the indicated time. The time course of fluorescence enhancement was measured separately under the same conditions.

and release of total ^{32}P into the filtrate of the reaction mixture (see MATERIALS and METHODS). The percentages of DNS-AT^{32}P bound to F_1 immediately after addition of Mg^{2+} and at the steady state were calculated by using K_f = 3.3 μM [Eqn. (3)] and $\phi_{DNS\text{-}ATP}$ = 0.44 μM [Eqn. (1)] to be 73% and 95%, respectively. Even if the initial concentration of free DNS-AT^{32}P is 27%, this is expected to decrease rapidly corresponding to an initial rapid increase in the fluorescence intensity. Therefore, we concluded that the amount of total ^{32}P in the filtrate was almost equal to or slightly higher than the amount of free $^{32}P_i$ released from F_1 to the medium. Thus, after the addition of 5 mM $MgCl_2$ the fluorescence enhancement, liberation of TCA-$^{32}P_i$ due to hydrolysis of DNS-ATP, and liberation of free $^{32}P_i$ seem to occur sequentially in this order. Since the fluorescence intensity maintained its enhanced level for most of the reaction, it is clear that DNS-ADP formed by hydrolysis of DNS-AT^{32}P was still bound to F_1 and that the release of DNS-ADP from F_1 was very slow.

Figure 10A shows the time courses of TCA-$^{32}P_i$ liberation after addition of 2.83, 5.65 or 11.3 mol DNS-AT^{32}P/mol F_1 to 0.75 μM F_1. In Fig. 10B, the logarithm of the remaining fraction of DNS-AT^{32}P, ([total ^{32}P] - [TCA-$^{32}P_i$])/[total ^{32}P], was plotted against time after addition of 5 mM $MgCl_2$. At all DNS-AT^{32}P concentrations examined, the time course of TCA-$^{32}P_i$ liberation deviated from a single exponential curve, exhibiting rapid and subsequent slow phases. The amount of TCA-$^{32}P_i$ liberated during the rapid phase was estimated by extrapolating the second

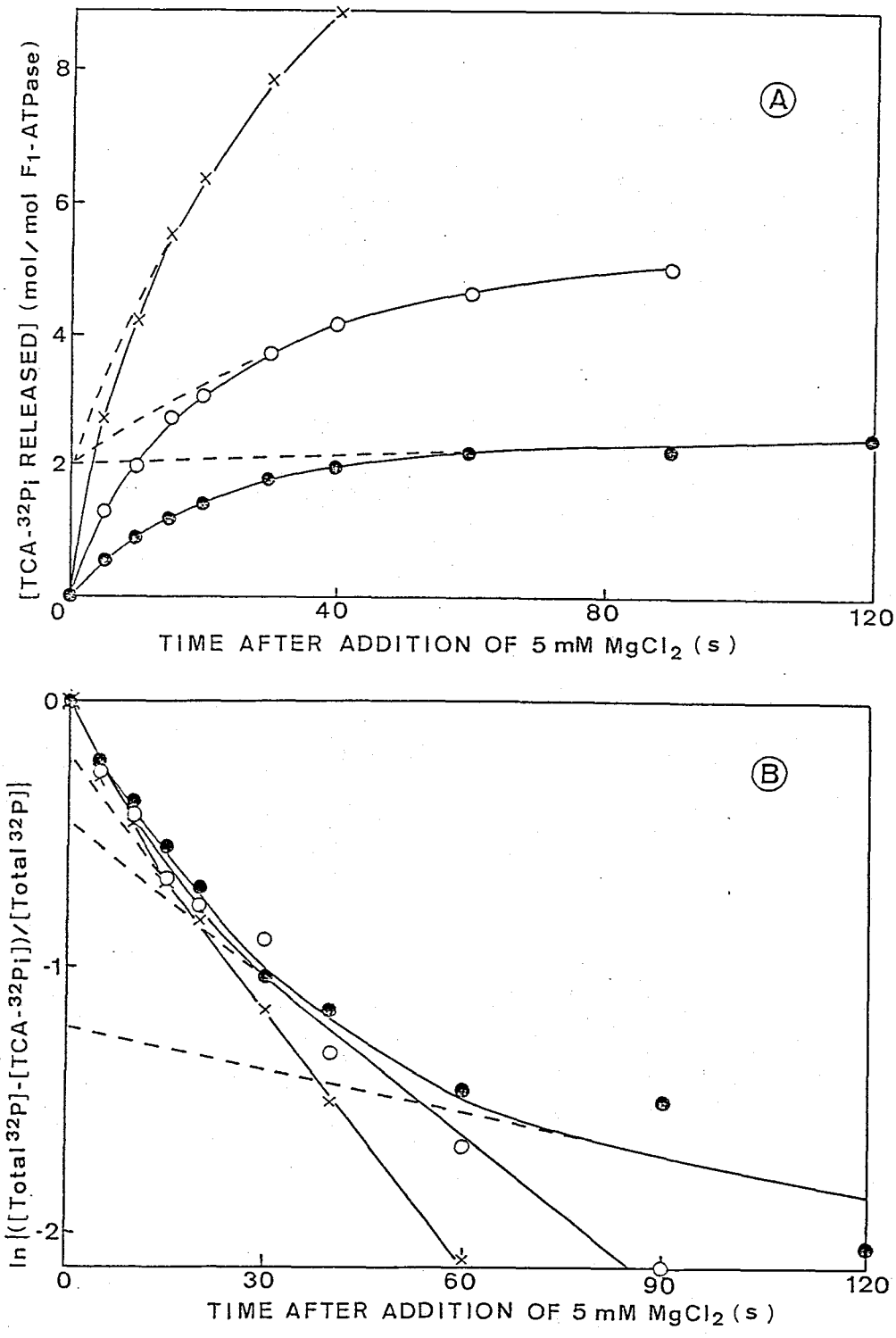

Fig. 10. Initial phase of TCA-$^{32}P_i$ liberation from DNS-AT^{32}P by F_1. A: The reaction mixture contained 2.83 (●), 5.65 (○) or 11.3 (×) mol DNS-AT^{32}P/mol F_1 and 0.75 μM F_1. The reaction was started by addition of 5 mM $MgCl_2$. B: The data in A were plotted as the logarithm of the fraction of remaining amount of DNS-AT^{32}P versus reaction time. The P_i-burst size was obtained by extrapolating the linear portion of a slow change to time 0 (broken line).

slow linear part to time 0. It was independent of the DNS-ATP concentration used, and was about 2 mol/mol F_1.

When the fluorescence intensity reached a plateau after addition of 5 mM $MgCl_2$, an excess amount of EDTA was added to remove free Mg^{2+} (Fig. 11). The fluorescence intensity then decreased very slowly ($t_{1/2} \approx 6$ min).

When 4 mM $CaCl_2$ was added to a reaction mixture containing 1.1 μM DNS-ATP and 1.1 μM F_1, the fluorescence intensity increased rapidly and reached the maximal level within 20 s (Fig. 12), followed by a spontaneous decrease. This result suggests spontaneous decomposition of F_1-DNS-ADP in the presence of Ca^{2+}.

Acceleration of TCA-P_i and Free P_i Liberation by Addition of High Concentration of Nucleotides — Figure 13 shows the effect of ATP on the time course of TCA-$^{32}P_i$ liberation in a reaction mixture containing 4.28 μM DNS-AT^{32}P and 6.78 μM F_1. When 0.2 mM ATP was added 2 min after addition of 5 mM $MgCl_2$, all the remaining DNS-AT^{32}P was immediately recovered as TCA-$^{32}P_i$ and as free $^{32}P_i$ as shown in Fig. 15. At this moment, more than 95% of DNS-AT^{32}P added was estimated to be bound to F_1 as DNS-AT^{32}P and DNS-ADP on the basis of $\phi_{DNS\text{-}ATP}$ = 0.44 μM.

In the experiments shown in Fig. 14, 5 mM $MgCl_2$ was added to a mixture of 1.8 μM DNS-AT^{32}P and 1.2 μM F_1 followed by addition of 0.2 mM ATP 15 s or 30 s later. The rate of TCA-$^{32}P_i$ liberation after the ATP addition was faster in the latter case than in the former. The total amount of TCA-$^{32}P_i$ liberated after addition of 0.2 mM ATP was 1.06 mol/mol F_1 in the latter case, and this value was equal to the amount of DNS-AT^{32}P bound to F_1 as

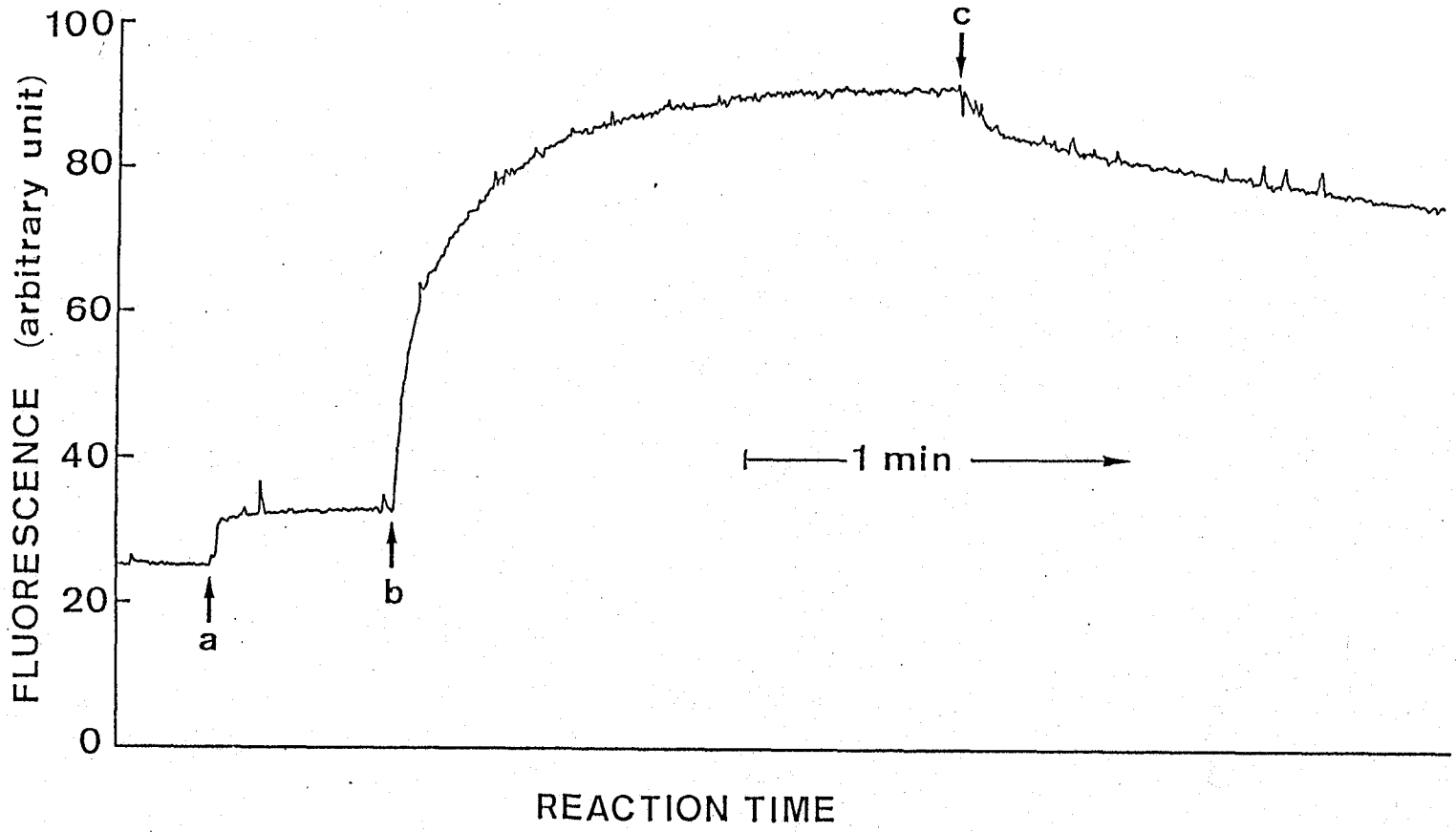

Fig. 11. Fluorescence decay on addition of EDTA to F_1-DNS-nucleotide. The reaction mixture contained 2.12 μM DNS-ATP in 2 mM EDTA, 50 mM Tris-HCl at pH 8.0. Following additions were made; a, 1.36 μM F_1; b, 4 mM $MgCl_2$; c, 7 mM EDTA.

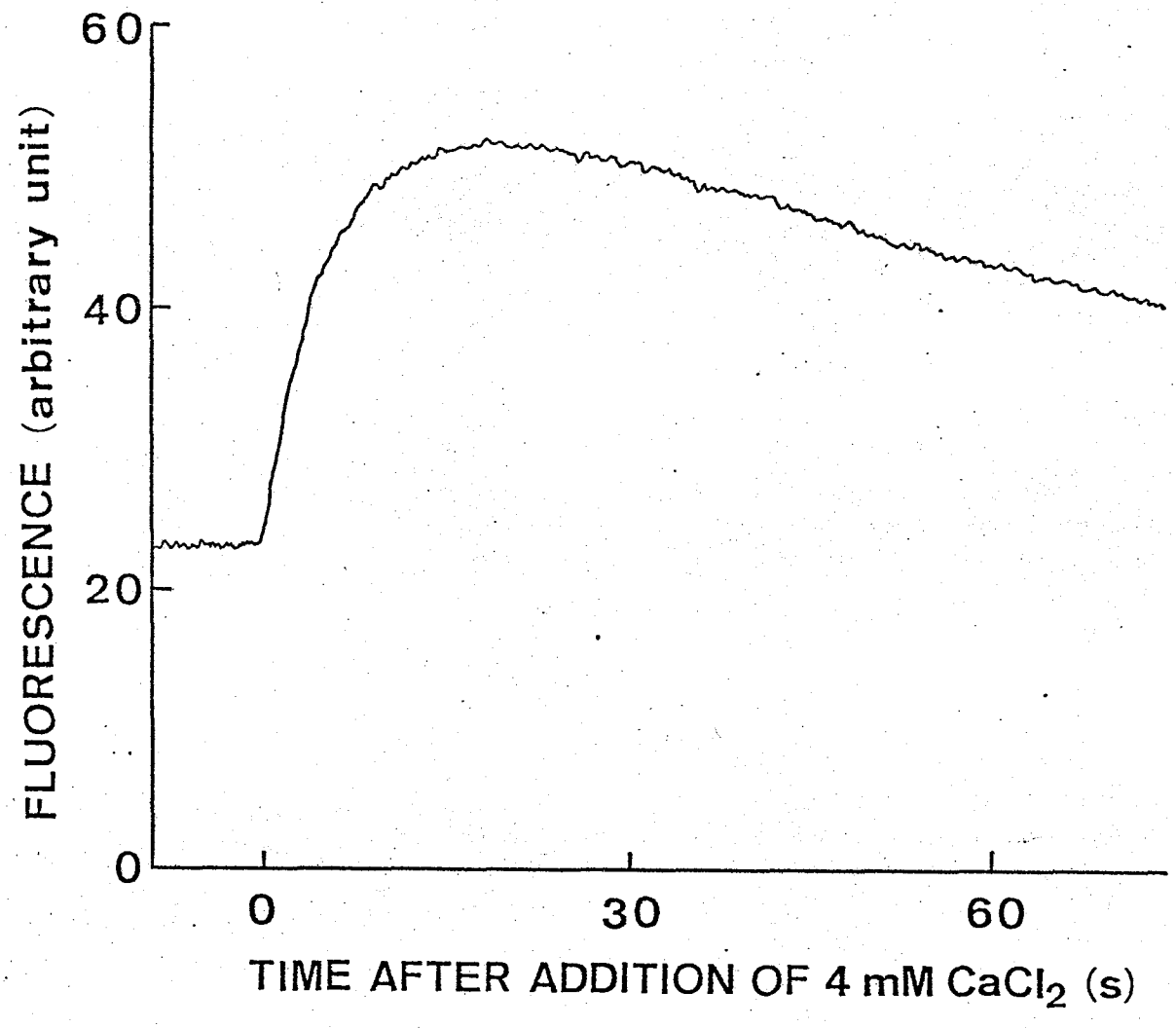

Fig. 12. Time course of change in fluorescence on reaction of DNS-ATP with F_1 in the presence of $CaCl_2$. The reaction mixture contained 1.1 μM DNS-ATP and 1.1 μM F_1. The reaction was started by addition of 4 mM $CaCl_2$.

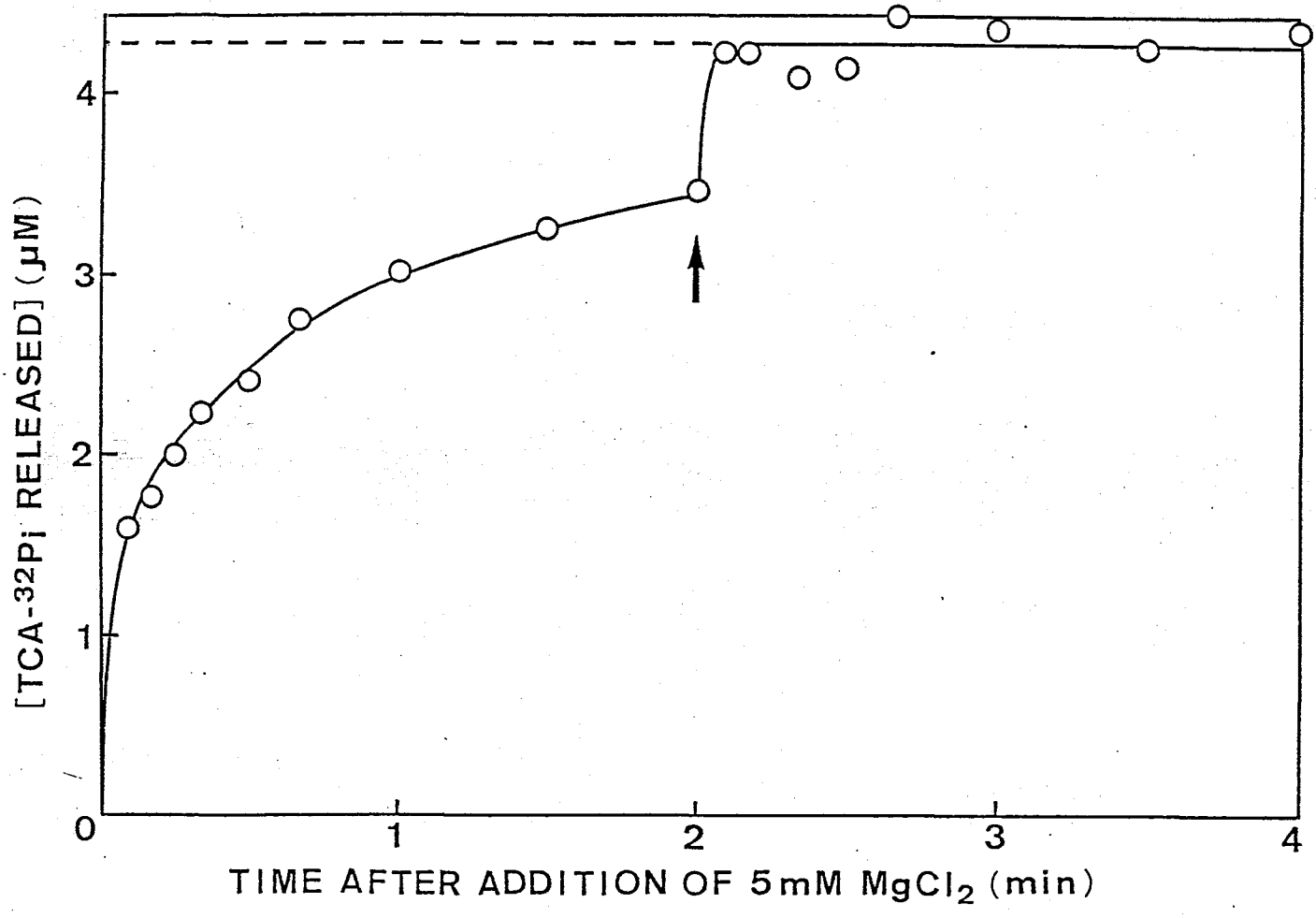

Fig. 13. Acceleration by ATP of TCA-$^{32}P_i$ liberation from the F_1-DNS-AT^{32}P system. The reaction mixture contained 4.28 μM DNS-AT^{32}P and 6.78 μM F_1. The reaction was started by addition of 5 mM $MgCl_2$. At the arrow (2 min) 0.2 mM ATP was added. The broken line shows the level of 4.28 μM.

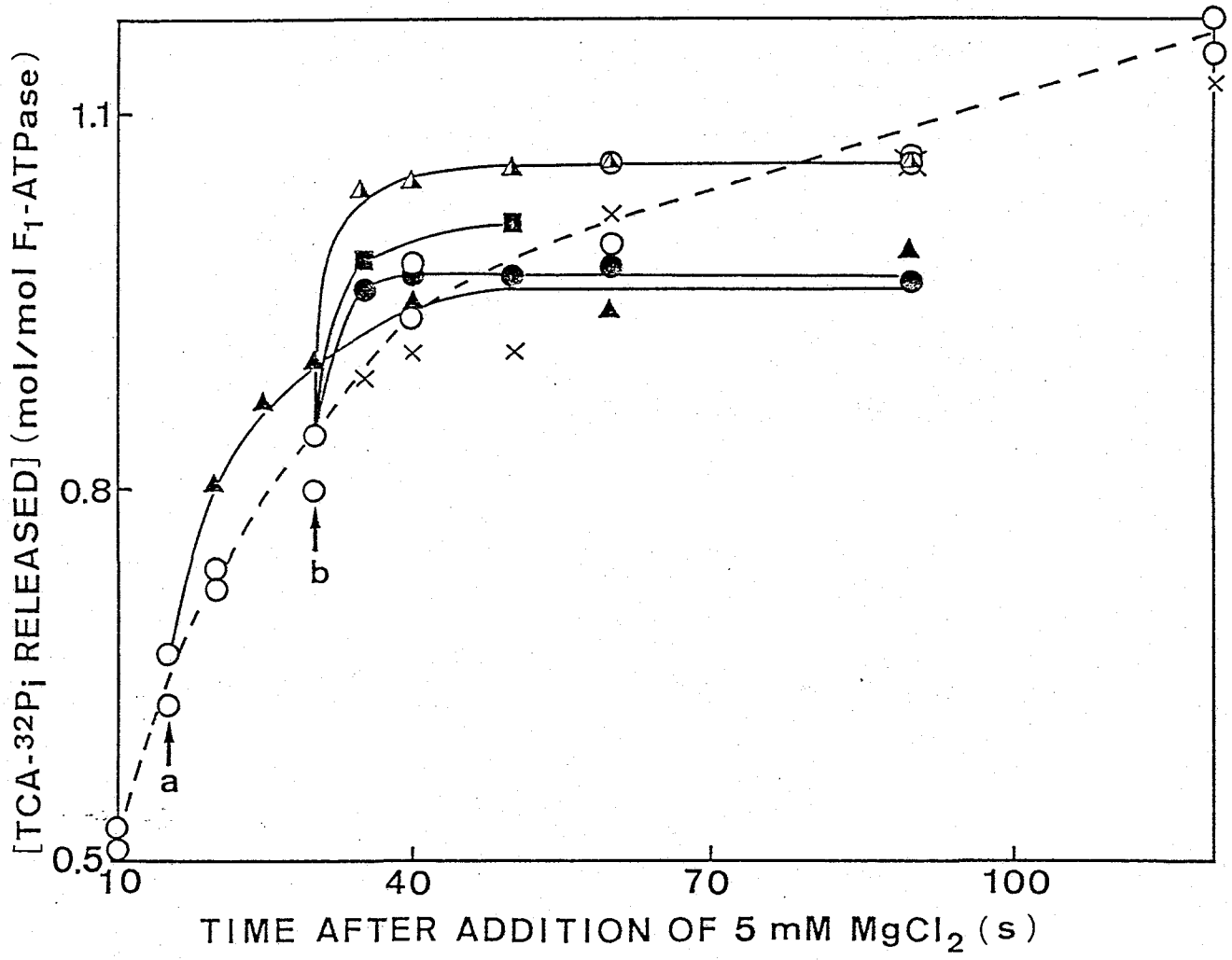

Fig. 14. Acceleration by various phosphate compounds of TCA-$^{32}P_i$ liberation from the F_1-DNS-AT^{32}P system. The reaction mixture contained 1.8 μM DNS-AT^{32}P and 1.22 μM F_1. The reaction was started by addition of 5 mM $MgCl_2$. At the arrow a (15 s) 0.2 mM ATP (▲) was added. At the arrow b (30 s) 0.2 mM ATP (▲), 0.2 mM AMPPNP (■), 0.2 mM ADP (●) or 1 mM PP_i (×) was added. The control (○) is also indicated.

calculated by using $\phi_{DNS\text{-}ATP}$ = 0.44 μM. The rate of TCA-$^{32}P_i$ liberation also increased by addition of 0.2 mM ADP or 0.2 mM AMPPNP but to a lesser extent. Addition of 0.2 mM PP_i showed no effect. The results in Figs. 13-15 clearly demonstrate that DNS-AT^{32}P bound to F_1 is hydrolyzed very rapidly on addition of 0.2 mM ATP, and that [γ-^{32}P]phosphoryl group is rapidly released as free $^{32}P_i$.

Acceleration of DNS-ADP Release from F_1-DNS-Nucleotide Complex by Addition of High Concentration of ATP — A decrease in fluorescence intensity and release of DNS-nucleotide occurred concomitantly on addition of 0.2 mM ATP to a mixture of 8.6 μM DNS-ATP, 9.2 μM F_1, and 5 mM Mg^{2+}, which had been incubated for 2 min (Fig. 16). The fluorescence intensity decreased rapidly to about 50% of the original level within the response time of an apparatus ($\lesssim$ 0.5 s), followed by a slow decrease approaching a level of free DNS-ATP. Since F_1-DNS-ATP was readily converted into F_1-DNS-ADP + P_i by addition of ATP as mentioned above, the observed changes correspond to the release of DNS-ADP from F_1-DNS-ADP.

When increasing concentrations of ATP was added to F_1-DNS-nucleotide, the extent of the first rapid decrease of the fluorescence increased accompanying an increase in the rate of slow change (Fig. 17), but did not reach 100% even on addition of 0.2 mM ATP.

Acceleration of DNS-ADP Release from F_1-DNS-Nucleotide Complex by Addition of Various Phosphate Compounds — ATP, ADP, AMPPNP, ITP, and GTP, 0.2 mM each, added to F_1-DNS-nucleotide induced a fluorescence decrease consisting of rapid and slow

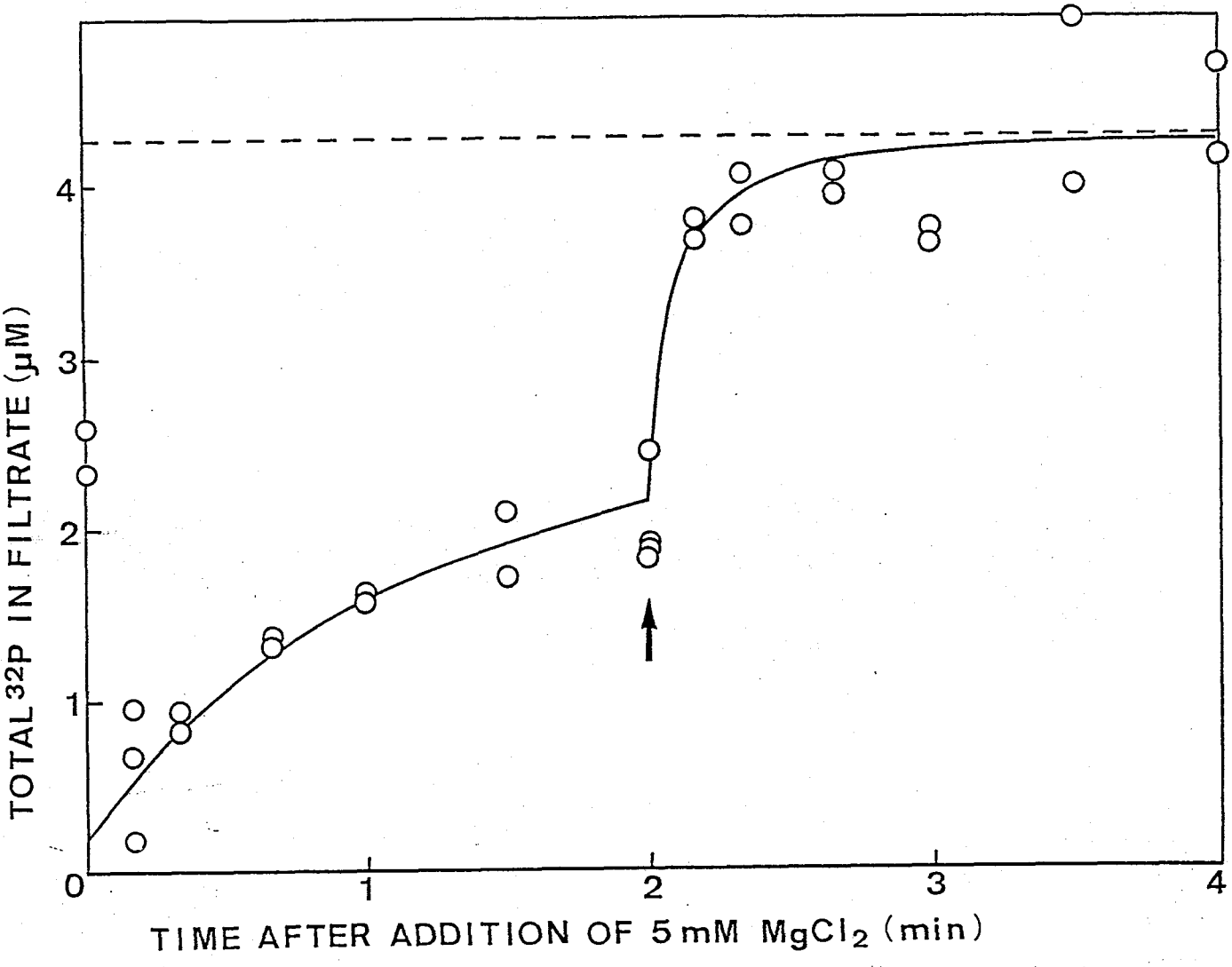

Fig. 15. Acceleration by ATP of free ^{32}P liberation from the F_1-DNS-AT^{32}P system. The reaction was carried out under the identical conditions as described in the legend to Fig. 13 except that the reaction was stopped by filtration through an XM-100A membrane.

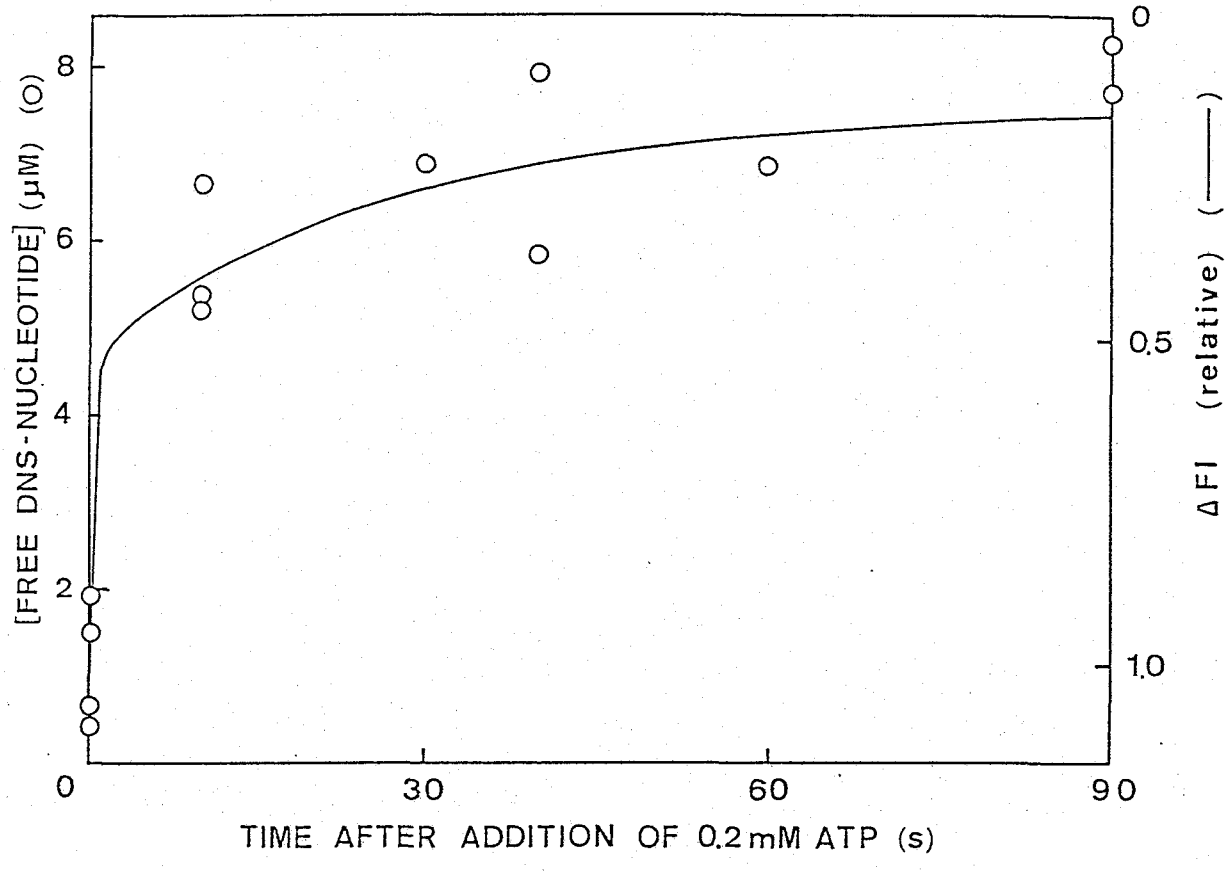

Fig. 16. Comparison of the time course of a decrease in fluorescence with that of release of DNS-nucleotide on addition of ATP to F_1-DNS-ATP. A mixture containing 8.6 μM DNS-ATP, 9.2 μM F_1, and 10 mM [^{3}H]glucose was incubated with 5 mM $MgCl_2$ for 90 s, and then 0.2 mM ATP was added. The reaction was stopped by filtration through an XM-100A membrane at the time indicated. The extent of a decrease in fluorescence intensity, ΔFl, is plotted as relative to difference between the intensity before addition of 0.2 mM ATP (1.0) and that of free DNS-ADP (0).

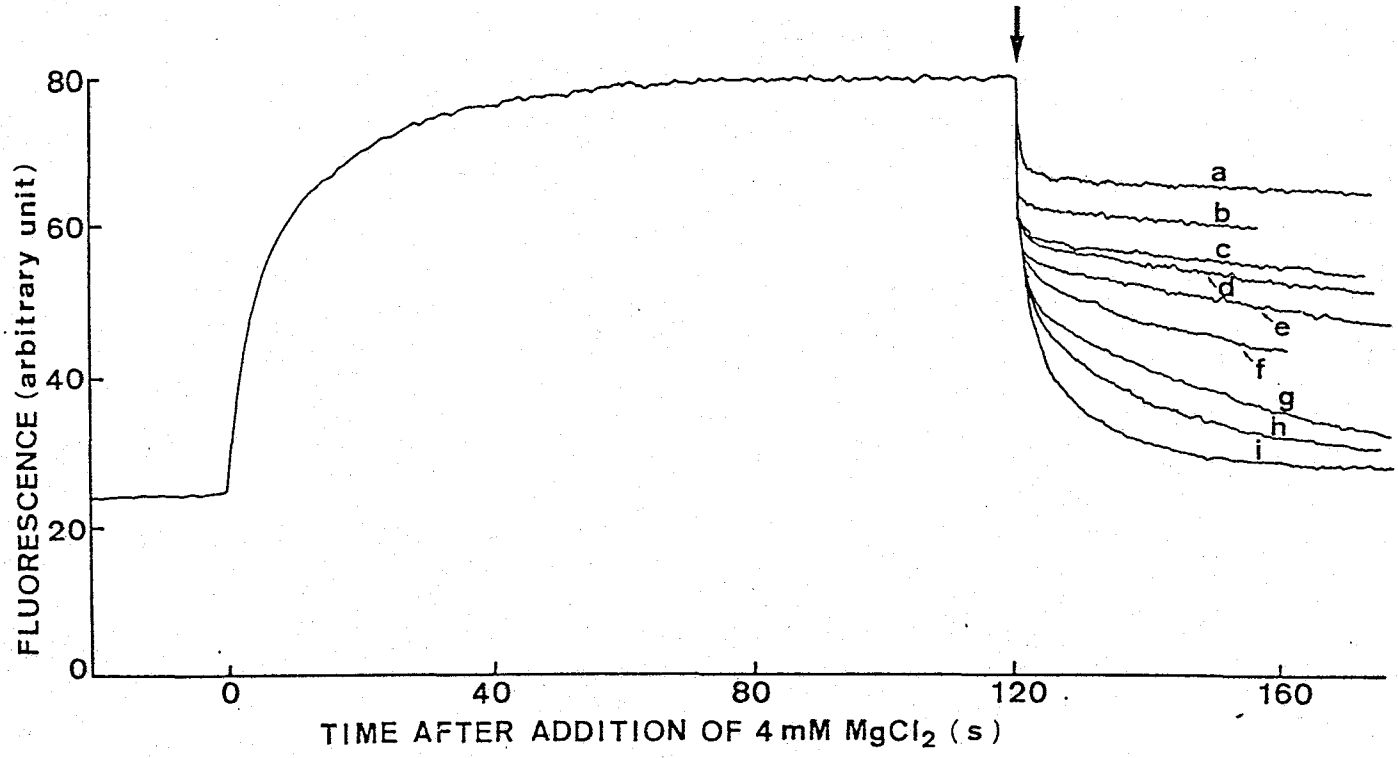

Fig. 17. Fluorescence decay on addition of various concentrations of ATP to F_1-DNS-nucleotide. The reaction mixture contained 1.1 μM DNS-ATP and 1.1 μM F_1 in 2 mM EDTA, 50 mM Tris-HCl at pH 8.0. At the arrow (2 min), following concentrations of ATP were added; 0.5 μM (a), 1.0 μM (b), 1.5 μM (c), 2.0 μM (d), 5.0 uM (e), 10 μM (f), 40 μM (g), 80 μM (h), 0.2 mM (i).

phases (Fig. 18). CTP at 0.2 mM yielded only a slow phase, and its rate was of the same order of magnitude as the second slow phase observed with 0.2 mM ATP. At the same time, the rate of TCA-$^{32}P_i$ liberation from F_1-DNS-nucleotide (Fig. 19) was accelerated slightly.

On addition of 7 mM EDTA to F_1-DNS-nucleotide in the presence 4 mM $MgCl_2$, the fluorescence intensity decreased very slowly as previously shown in Fig. 11 (Fig. 20). Further addition of 0.1 mM ATP or 0.1 mM ADP markedly increased the rate of the fluorescence decrease. The time course of the fluorescence decrease induced by 0.1 mM ADP followed simple kinetics, whereas that induced by 0.1 mM ATP showed both rapid and slow phases as in the presence of Mg^{2+} (Fig. 17).

As previously described, PP_i binds to F_1 competitively with DNS-ATP but with a much lower affinity than that of DNS-ATP. As shown in Fig. 21, the fluorescence intensity of F_1-DNS-nucleotide decreased on addition of PP_i with a single slow phase, and the extent of the fluorescence change increased with increasing concentration of PP_i. The rate of the fluorescence decrease in the presence of 10 mM PP_i was almost equal to that induced by 0.2 mM ATP in its slow phase. Furthermore, 1 mM PP_i did not accelerate TCA-$^{32}P_i$ liberation from F_1-DNS-nucleotide (see Fig. 14). AMP at 0.2 mM had no effect on the fluorescence intensity of F_1-DNS-nucleotide in the presence of Mg^{2+} (Fig. 22), did not change the rate of TCA-$^{32}P_i$ liberation from F_1-DNS-nucleotide (Fig. 19).

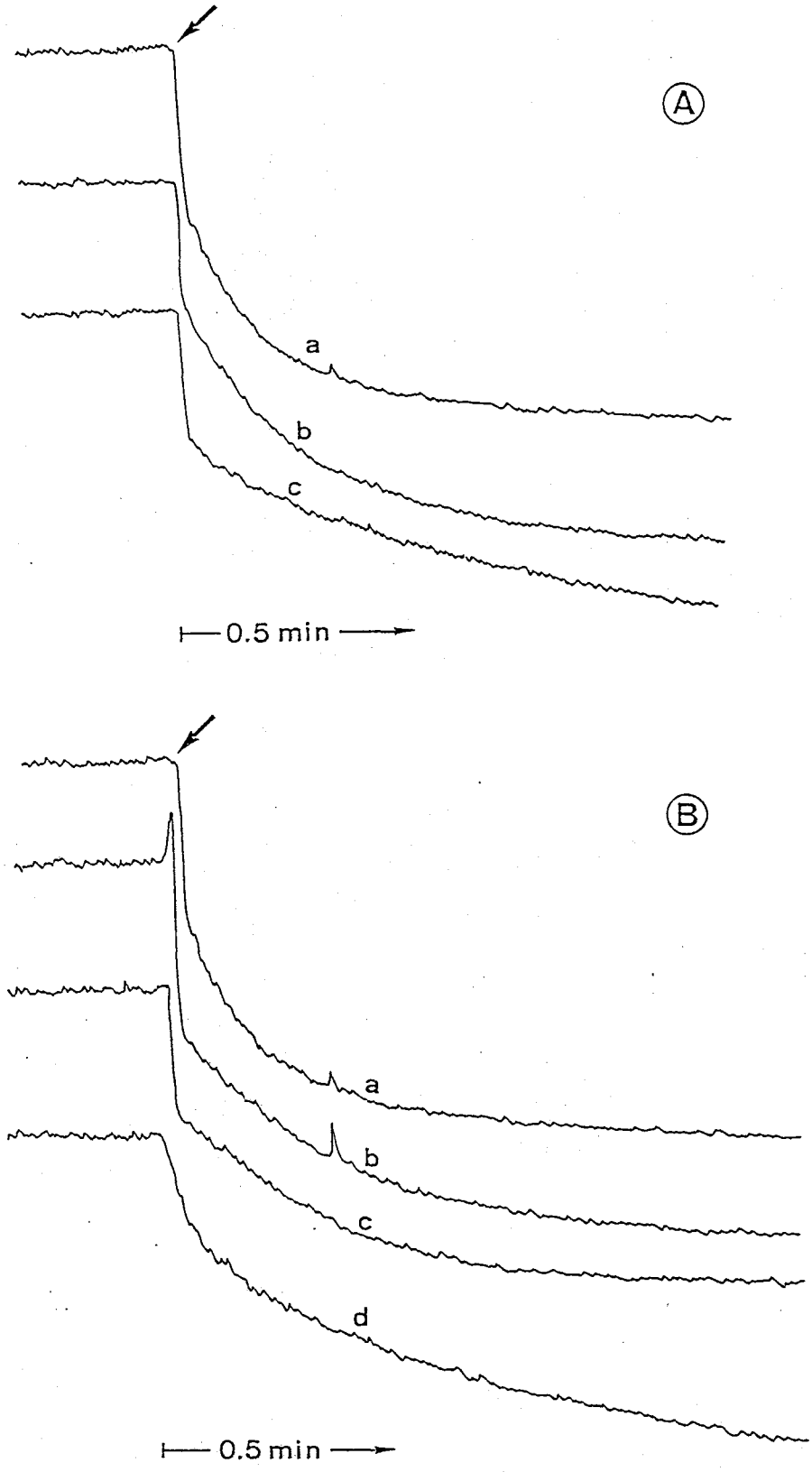

Fig. 18. Fluorescence decay on addition of various nucleotides to F_1-DNS-nucleotide. A mixture containing 2.1 μM DNS-ATP and 1.5 μM F_1 was incubated in the presence of 5 mM $MgCl_2$ for 2 min, and then (at the arrow) following additions were made. A: 0.2 mM ATP (a); 0.2 mM ADP (b); 0.2 mM AMPPNP (c). B: 0.2 mM ATP (a); 0.19 mM GTP (b); 0.22 mM ITP (c); 0.18 mM CTP (d).

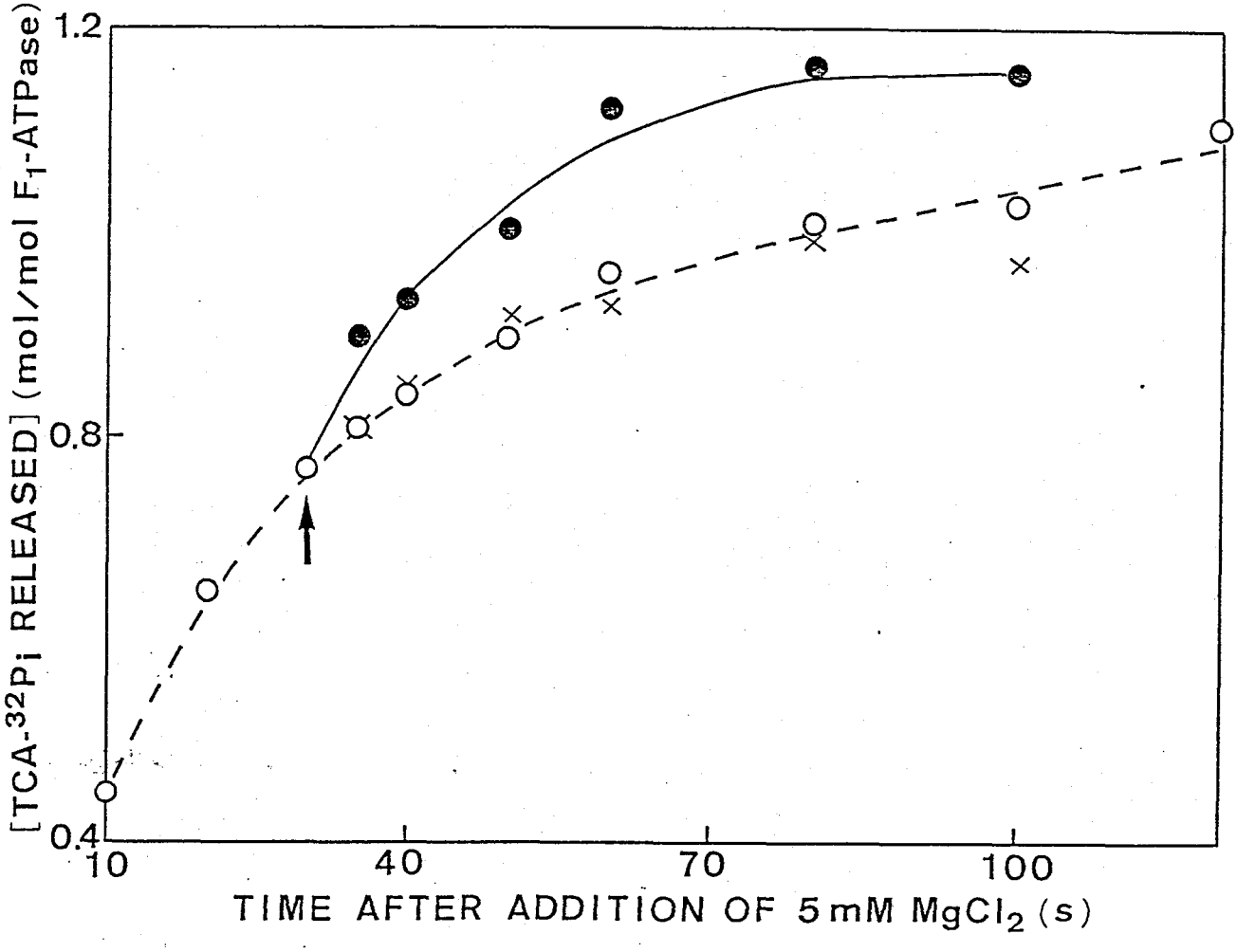

Fig. 19. Effect of CTP and AMP on TCA-$^{32}P_i$ liberation from the F_1-DNS-AT^{32}P system. The reaction mixture contained 1.8 μM DNS-AT^{32}P and 1.2 μM F_1 in 2 mM EDTA, 50 mM Tris-HCl at pH 8.0. The reaction was started by addition of 5 mM $MgCl_2$. At the arrow (30 s), 0.2 mM CTP (●) or 0.2 mM AMP (×) was added. The control (○) is also indicated.

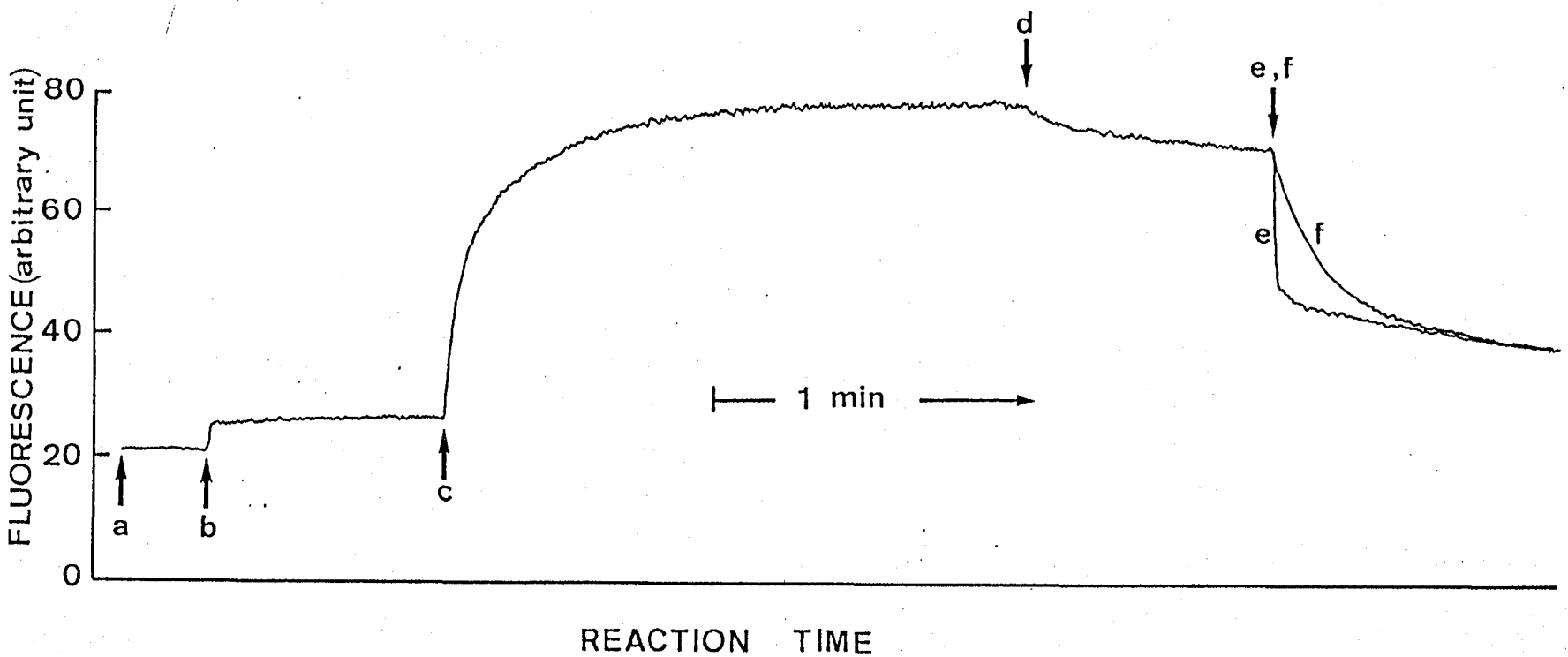

Fig. 20. Fluorescence decay of F_1-DNS-nucleotide on addition of ATP or ADP in the presence of EDTA. To a mixture containing 2 mM EDTA and 50 mM Tris-HCl at pH 8.0, following additions were made; a, 2.1 μM DNS-ATP; b, 1.4 μM F_1; c, 4 mM $MgCl_2$; d, 7 mM EDTA (final concentration); e, 0.1 mM ATP; f, 0.1 mM ADP.

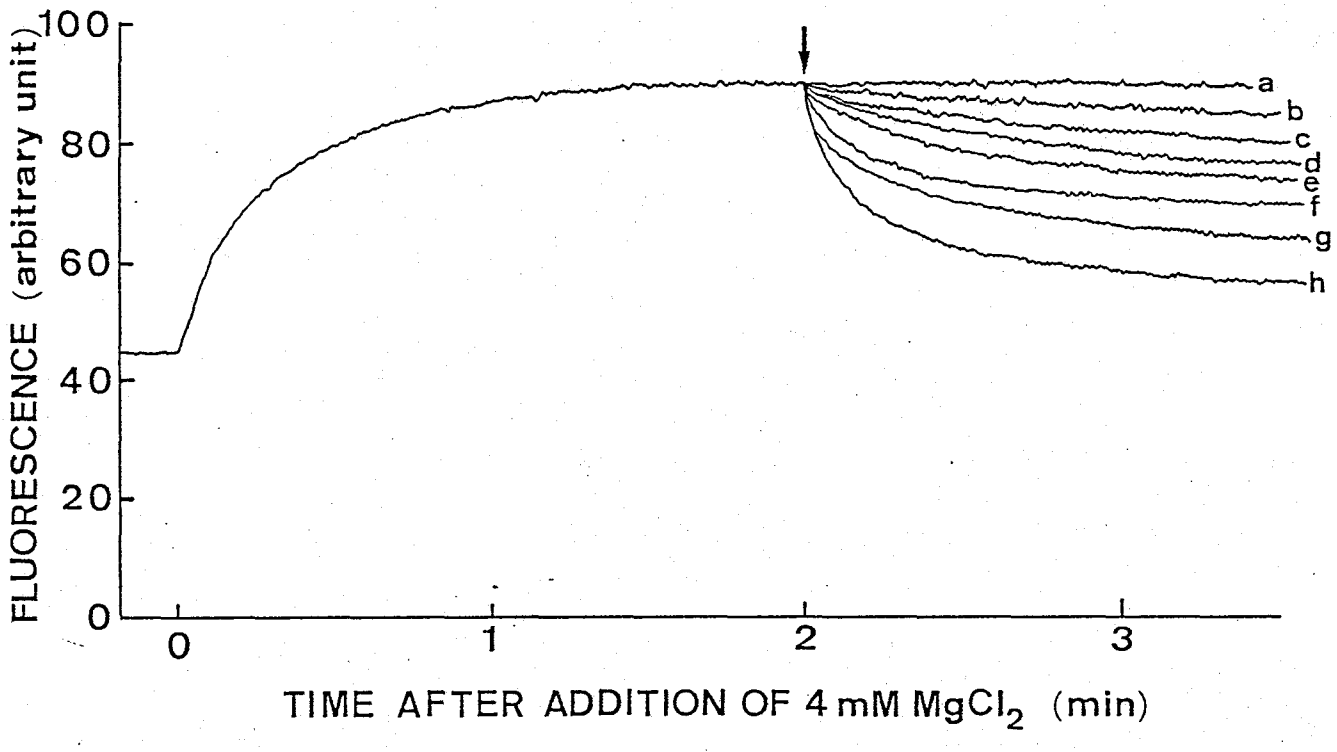

Fig. 21. Fluorescence decay of F_1-DNS-nucleotide on addition of various concentrations of PP_i. The reaction mixture contained 4.0 μM DNS-ATP and 0.75 μM F_1. At the arrow (2 min), following concentrations of PP_i were added; 0 (a), 4 μM (b); 10 μM (c); 40 μM (d); 100 μM (e); 400 μM (f); 4 mM (g); 10 mM (h).

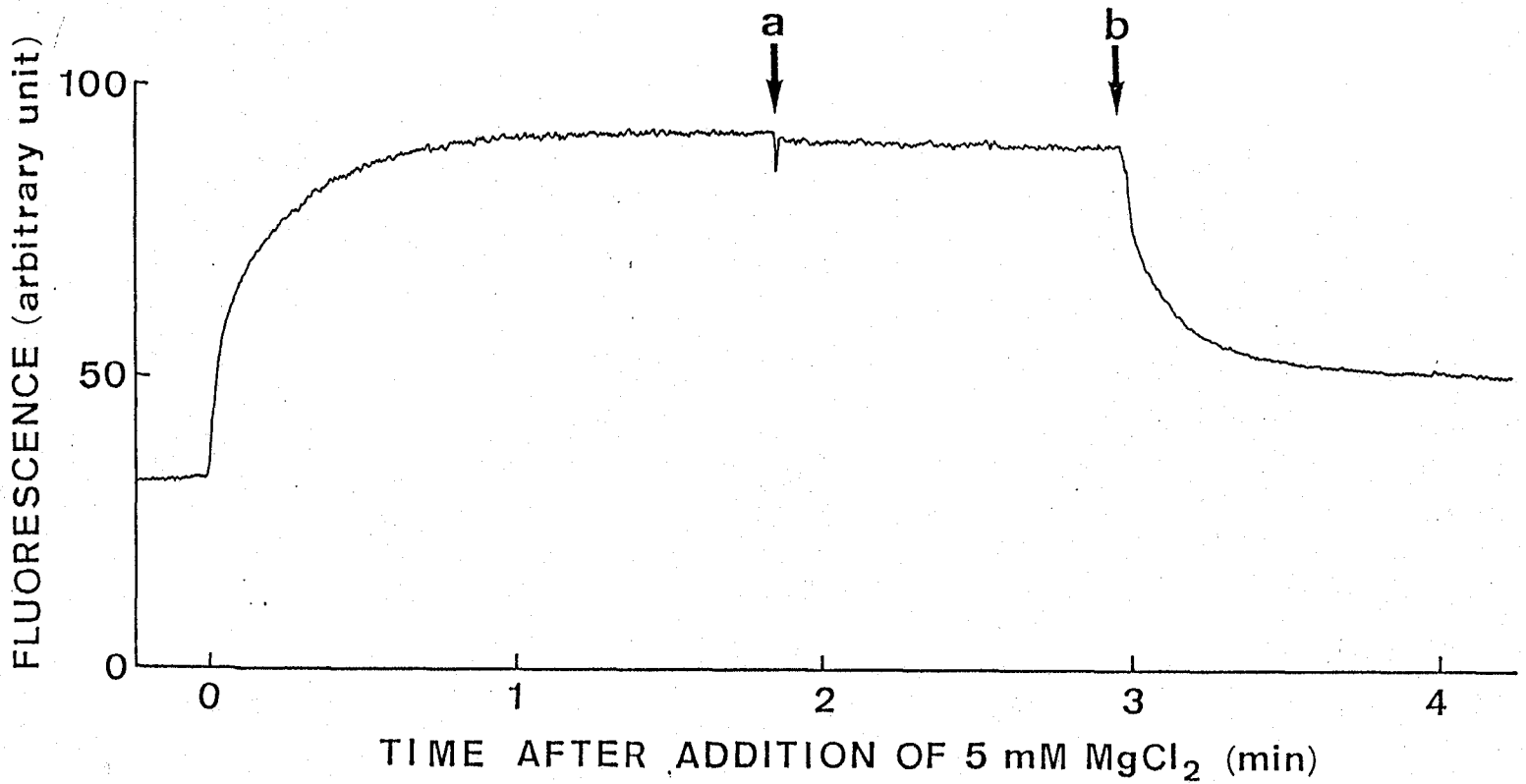

Fig. 22. Effect of AMP on fluorescence of F_1-DNS-nucleotide. The reaction mixture contained 2.1 μM DNS-ATP and 1.5 μM F_1. After addition of 5 mM $MgCl_2$, following additions were made; a, 0.2 mM AMP; b, 0.2 mM ATP.

Dependence of the Steady-State Rate of F_1-DNS-ATPase on Substrate Concentration---As shown in Fig. 23, the steady-state rate, v_o, increased in proportion to the DNS-AT^{32}P concentration up to 200 μM, where the v_o value was 1.0 s^{-1} accounting for about 0.5% of that of F_1-ATPase reaction at 200 μM ATP (cf. Fig. 24). If we assume that the F_1-DNS-ATPase reaction at the steady state follows a simple Michaelis-Menten kinetics, this result indicates that the values of K_m for DNS-ATP and V_{max} are much larger than 200 μM and 1 s^{-1}, respectively.

Comparison of Time Course of ATP Hydrolysis with That of DNS-ADP Release from F_1-DNS-Nucleotide Complex after Addition of ATP — DNS-ATP (6.42 μM) was allowed to react with F_1 (0.3 μM) in the presence of Mg^{2+}, PEP, and pyruvate kinase for 90 s. It was confirmed that ADP but not DNS-ADP can be converted into NTP by pyruvate kinase (16). Then 0.2 mM ATP was added, and both fluorescence decrease and TCA-P_i liberation were followed in parallel experiments. Under the condition used, almost all TCA-P_i was derived by ATP hydrolysis. At the moment of the ATP addition, more then 95% of F_1 added was estimated to have bound DNS-nucleotide on the basis of $\phi_{DNS\text{-}ATP}$ = 0.44 μM. As shown in Fig. 24, the fluorescence intensity decreased in two phases. If we assume that ATP is mainly hydrolyzed at the same site(s) where DNS-nucleotides bind to F_1, the TCA-P_i liberation should have a lag phase corresponding to the release of DNS-ADP (about 3.5 min). However, no such lag phase was observed.

Effect of P_i on Fluorescence of F_1-DNS-Nucleotide Complex — As already shown in Fig. 2, the fluorescence of F_1-Mg^{2+}-DNS-nucleotide was further enhanced by addition of P_i. Figure 25A

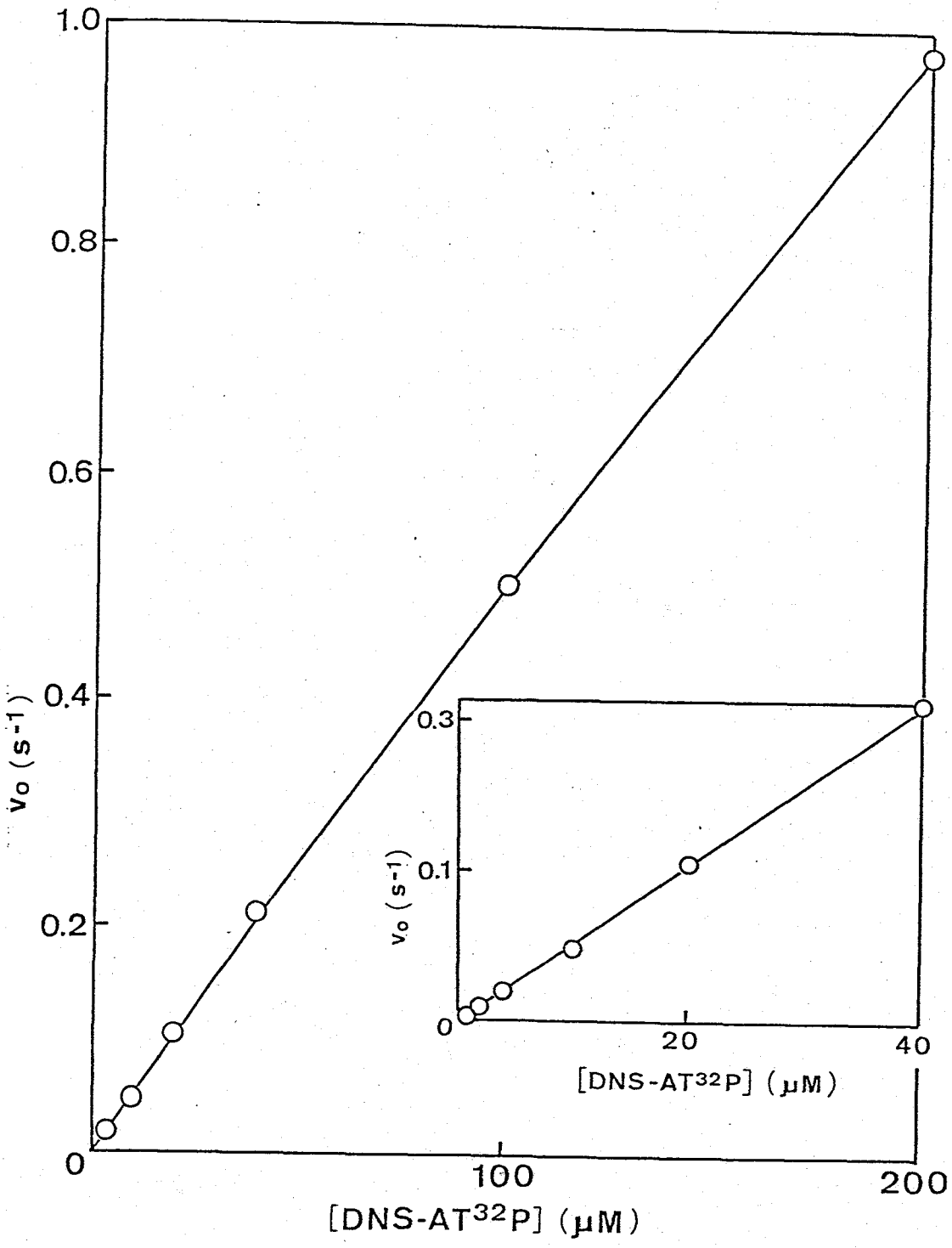

Fig. 23. Dependence on DNS-ATP concentration of the steady-state rate of F_1-DNS-ATPase reaction. The reaction mixture contained 0.30 μM F_1, various concentrations of DNS-$AT^{32}P$, 2.5 mM $MgCl_2$, and 50 mM Tris-HCl at pH 8.0 and 30°C. The reaction was started by addition of DNS-$AT^{32}P$.

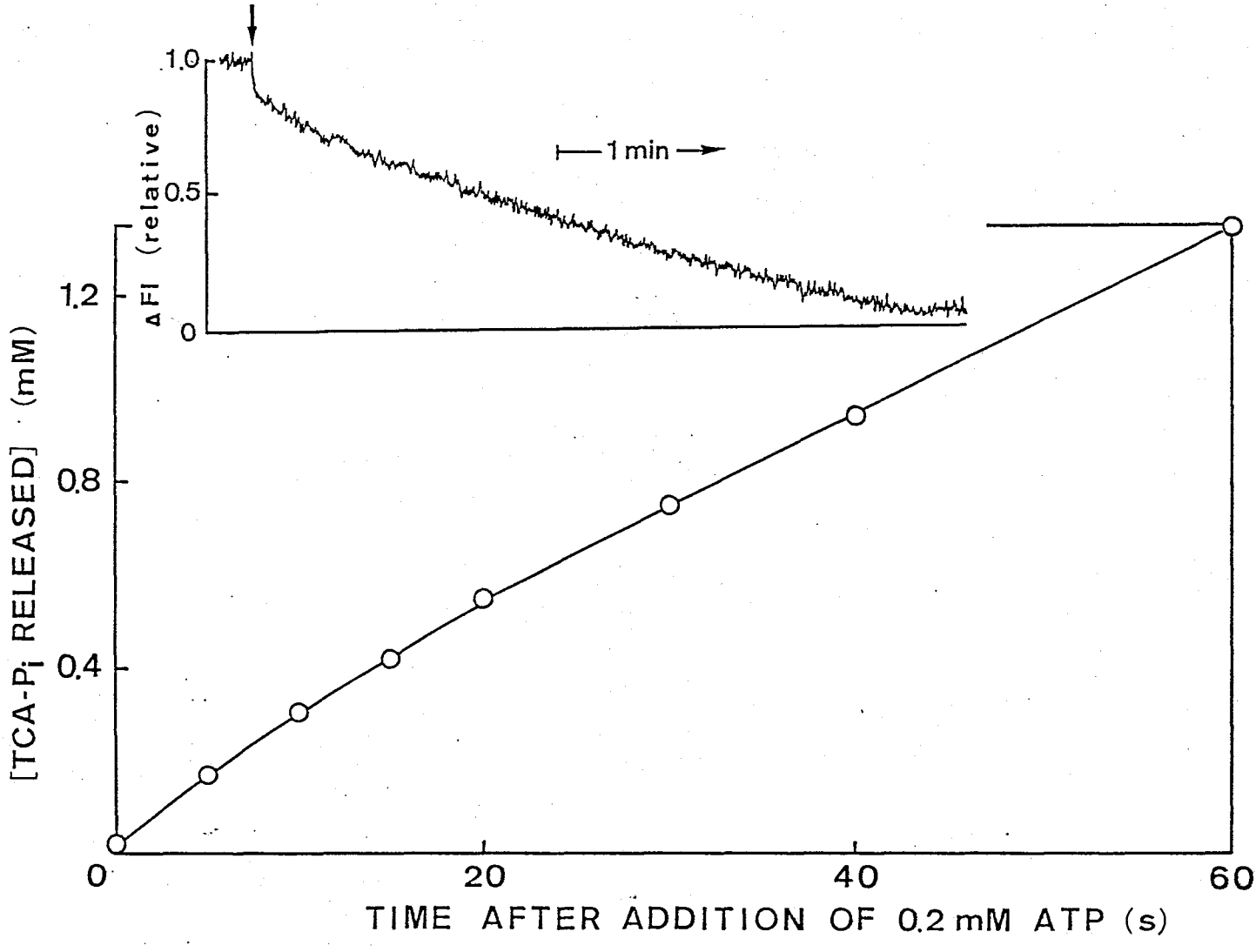

Fig. 24. Comparison of the time course of ATP hydrolysis with that of the DNS-ADP release from F_1-DNS-nucleotide after addition of ATP. A mixture containing 6.42 μM DNS-ATP, 0.31 μM F_1, 0.48 mg/ml pyruvate kinase, and 4 mM PEP in 2 mM EDTA, 50 mM Tris-HCl at pH 8.0 was incubated with 5 mM $MgCl_2$ for 90 s, and 0.2 mM ATP was added. The reaction was stopped by addition of 5% TCA at the time indicated. The time course of the DNS-ADP release was measured separately as a fluorescence change under the same conditions (inset). The arrow in the inset shows the time of addition of 0.2 mM ATP.

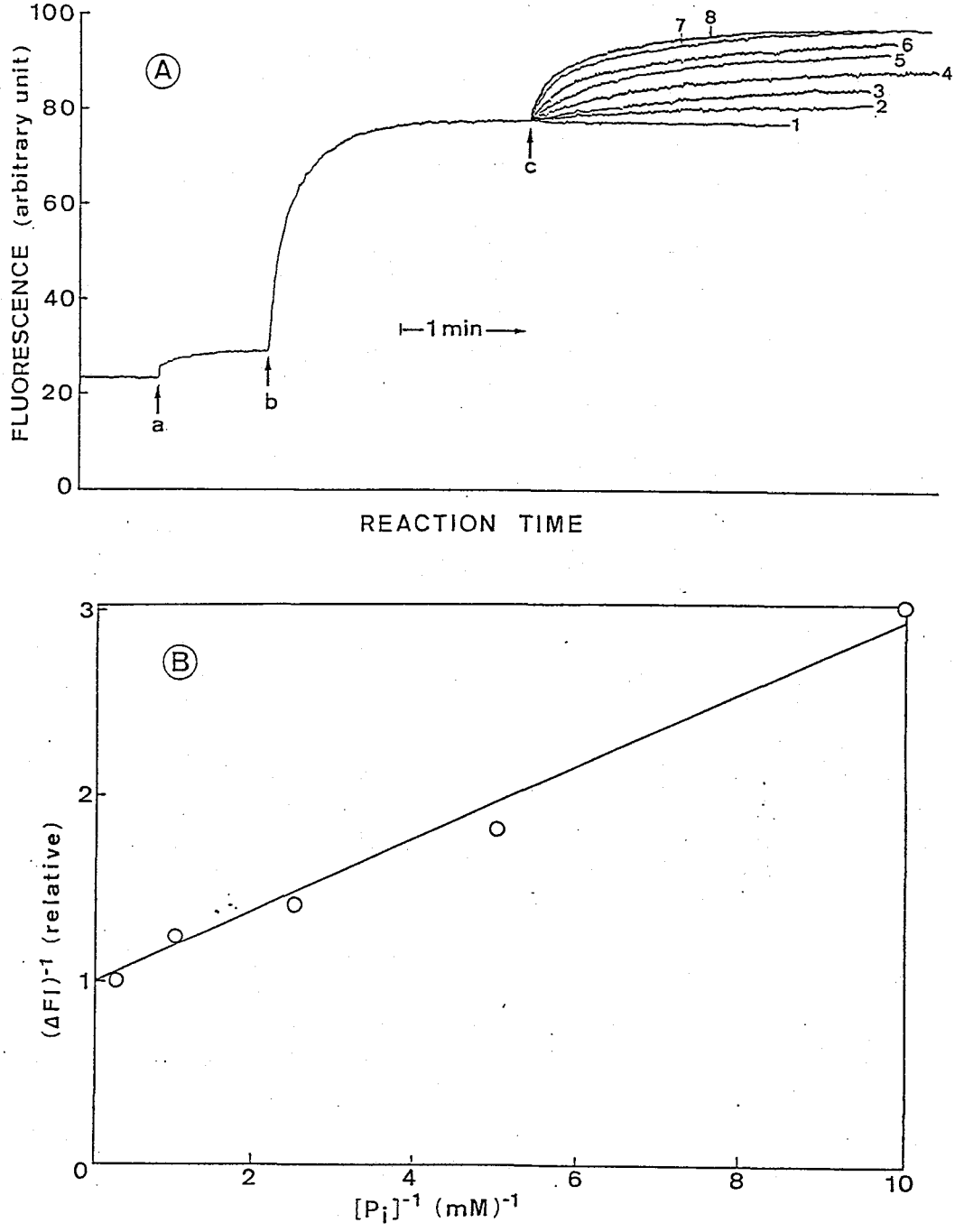

Fig. 25. Fluorescence enhancement of F_1-DNS-nucleotide on addition of P_i. The concentration of DNS-ATP added was 3.2 μM. A: Following additions were made; a, 1.5 μM F_1; b, 5 mM $MgCl_2$; c, K-P_i at concentrations of 0 (1), 40 μM (2), 0.1 mM (3), 0.2 mM (4), 0.4 mM (5), 1 mM (6), 4 mM (7), 10 mM (8). B: The reciprocal of the extent of fluorescence enhancement at 2 min after K-P_i addition (ΔFl) was plotted against the reciprocal of the concentration of K-P_i added.

shows the time courses of the fluorescence enhancement of F_1-DNS-nucleotide on addition of various concentrations of P_i at pH 8.0. With increasing concentrations of P_i, the extent of the fluorescence enhancement increased, and was saturated at about 4 mM P_i. Figure 25B shows a double reciprocal plot of the extent of the fluorescence enhancement at 2 min after P_i addition and the P_i concentration. A single straight line enabled an estimation of an apparent dissociation constant of P_i from F_1-DNS-nucleotide (ϕ_{P_i}) as 195 μM. The affinity of F_1-DNS-nucleotide for P_i increased with decreasing pH (Fig. 4). At pH 6.5 the fluorescence enhancement was saturated at least with 50 μM P_i (data not shown). The rate of DNS-AT^{32}P hydrolysis in the presence of 4.3 μM DNS-AT^{32}P, 1.7 μM F_1, and 5 mM $MgCl_2$ was unaffected by the addition of 1 mM P_i (data not shown).

We also examined effects of various anions on the fluorescence intensity of F_1-DNS-nucleotide (Fig. 26). These anions are known to accelerate the F_1-ATPase activity (28). The fluorescence intensity was almost unaffected by 5 mM HCO_3^- or 2 mM maleate, and slightly increased on addition of 0.5 mM HSO_3^-. The effect of HSO_3^- was maximal at 2 mM.

Binding of DNS-Nucleotide to F_1 in the Presence of P_i —

The fluorescence intensity of DNS-ATP after addition of F_1, $MgCl_2$, P_i, and ATP, as added in this order, was measured in the presence of different concentrations of DNS-ATP (see Fig. 2), and the fluorescence intensities at each step were plotted against the DNS-ATP concentration (Fig. 27A). The extent of the fluorescence enhancement induced by P_i was replotted in

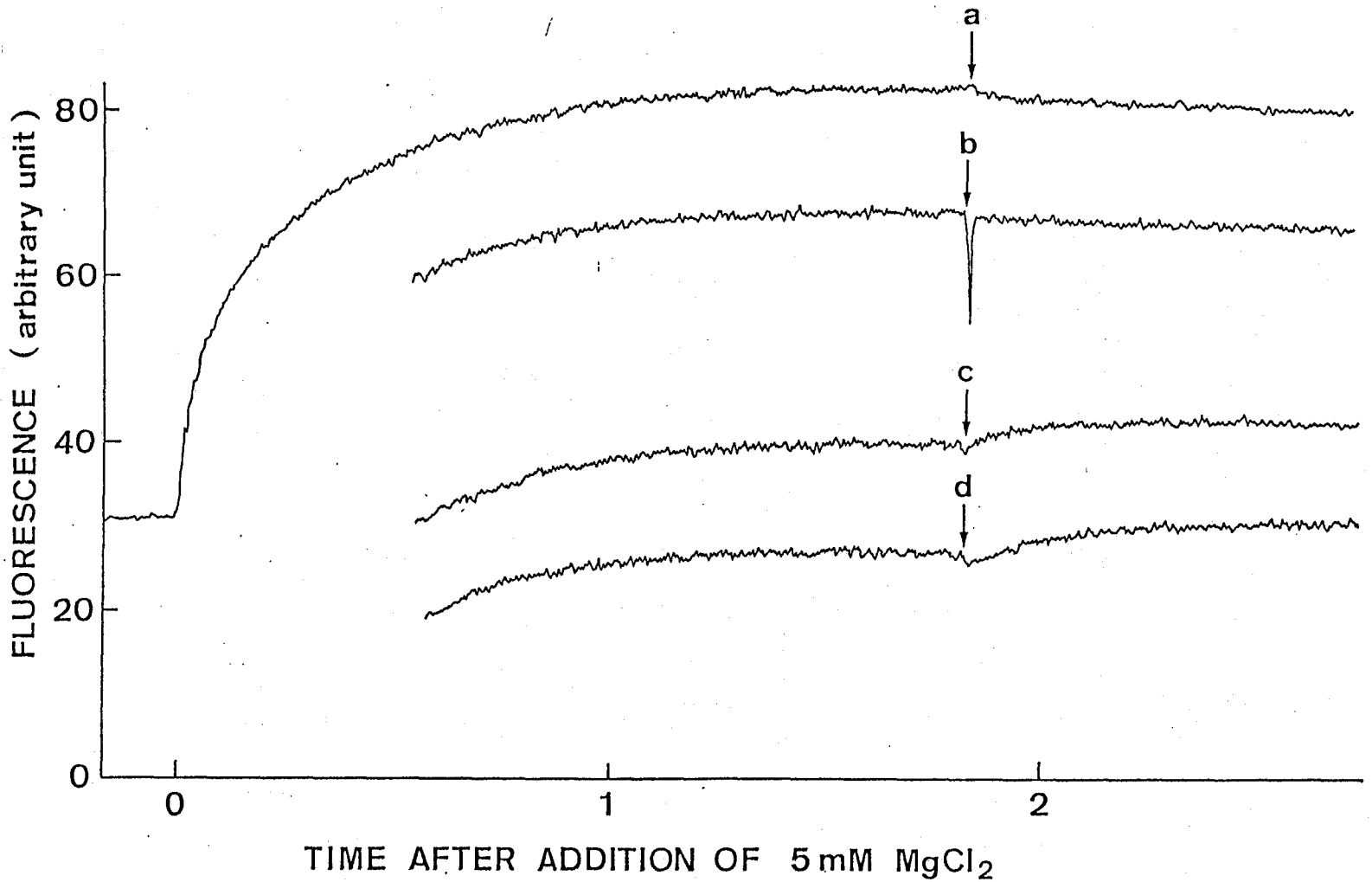

Fig. 26. Fluorescence change of F_1-DNS-nucleotide induced by various anions. The reaction mixture contained 2.1 μM DNS-ATP and 1.5 μM F_1. After addition of 5 mM $MgCl_2$, following additions were made; a, 5 mM HCO_3^-; b, 2 mM maleate; c, 0.5 mM HSO_3^-; d, 2 mM HSO_3^-.

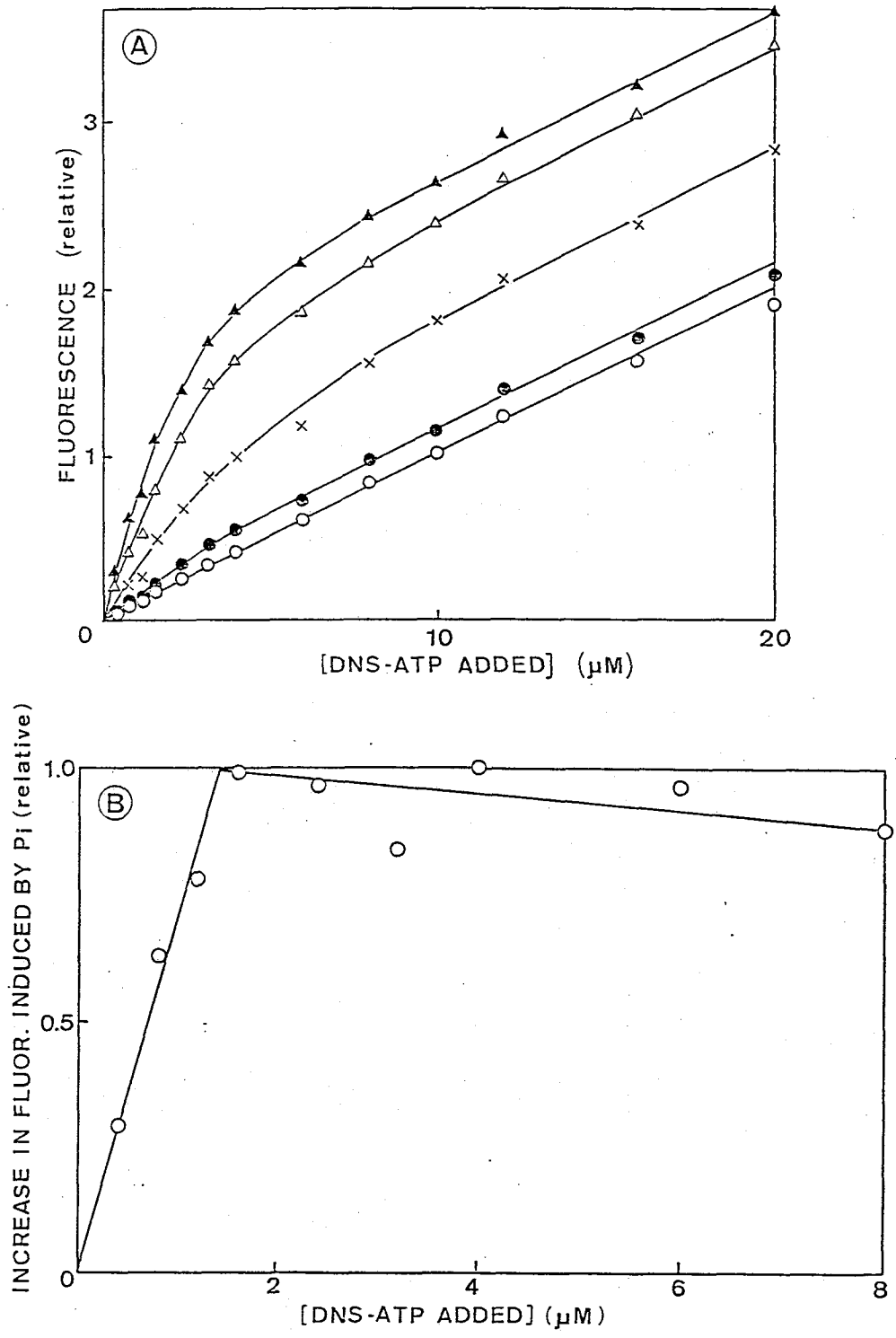

Fig. 27. Fluorometric titration of F_1 by DNS-ATP in the presence of P_i. A: The fluorescence intensity was measured sequentially as follows; DNS-ATP alone (○); 1 min after addition of 1.5 μM F_1 (●); 2 min after addition of 5 mM $MgCl_2$ (△); 2 min after addition of 8 mM K-P_i (▲); the level decreased rapidly on addition of 0.2 mM ATP (×). B: The extent of fluorescence enhancement after addition of 8 mM K-P_i (▲ minus △) was plotted against the concentration of DNS-ATP added.

Fig. 27B. With an equimolar concentration of DNS-ATP to F_1 (1.5 μM), the enhancement was saturated.

Figure 28 shows the effect of 4 mM P_i on the release of DNS-nucleotide from F_1 induced by PP_i (A) or ATP (B). The fluorescence decrease on addition of 1 mM PP_i showed only a slow phase, as already mentioned (cf. Fig. 21), and its rate was remarkably reduced by addition of 4 mM P_i. P_i also inhibited the second slow change of the DNS-ADP release on addition of ATP. After the fluorescence intensity of F_1-DNS-nucleotide was enhanced by addition of 4 mM P_i, 0.2 mM ATP was added. The fluorescence decreased in two phases as observed in the absence of P_i. However, the extent of the rapid phase was larger and the rate of the second slow phase was much smaller than those in the absence of P_i.

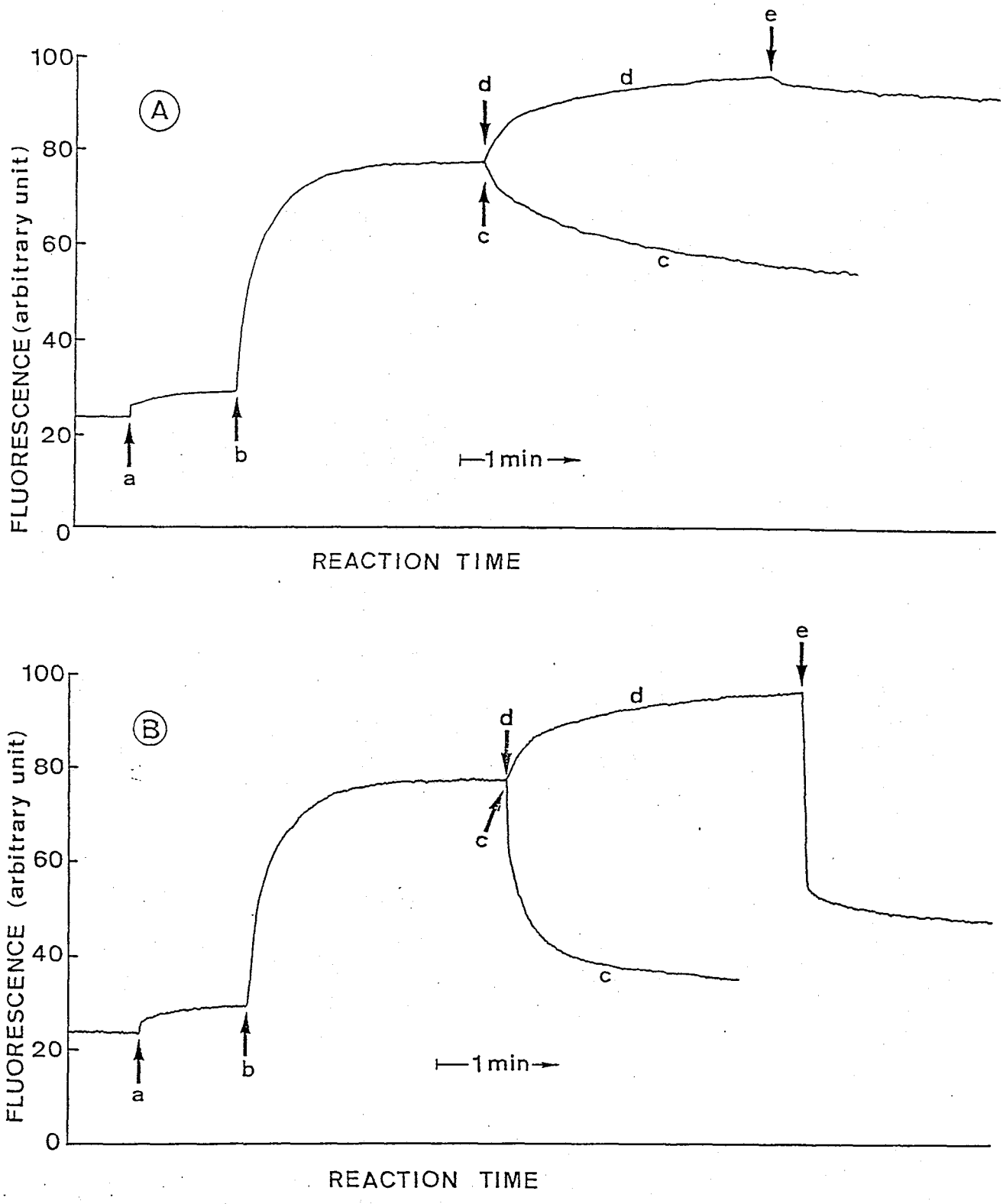

Fig. 28. Time course of a decrease in fluorescence of F_1-DNS-nucleotide in the presence and absence of P_i on addition of PP_i or ATP. The concentration of DNS-ATP added was 3.2 μM. A: Following additions were made; a, 1.5 μM F_1; b, 5 mM $MgCl_2$; c, 1 mM PP_i, d, 4 mM K-P_i; e, 1 mM PP_i. B: Following additions were made; a, 1.5 μM F_1; b, 5 mM $MgCl_2$; c, 0.2 mM ATP; d, 4 mM K-P_i; e, 0.2 mM ATP.

DISCUSSION

Recently, Slater et al. reported that purified F_1 contains 2 mol of unexchangeable ATP/mol F_1 and proposed that these ATP are indispensable in maintaining the conformation of F_1 (4). The amount of ATP tightly bound to our purified F_1 preparation was 2.3 mol/mol F_1. In this paper, we assumed that these tightly bound ATP were not directly involved in the F_1-DNS-ATPase reaction (4). Our purified F_1 preparation contained no intrinsic ATPase inhibitor protein (Fig. 1, 27).

So far there are several reports that the nucleotide binding sites on energy-transducing ATPases form hydrophobic clefts (29-31). Upon binding to F_1, DNS-ATP showed a similar change in fluorescence emission spectrum as when it was brought into dioxane (see Fig. 3 and also Table I). This change was reversed by adding several nucleotides including ATP. Therefore, we concluded that the nucleotide binding site of F_1 was in a hydrophobic cleft. The present fluorometric titration studies of F_1 by DNS-ATP in the presence of Mg^{2+} indicated that 2 mol of DNS-ATP were bound to 1 mol of F_1 with an apparent dissociation constant of 0.44 μM (Fig. 5). This finding is consistent with the $\alpha_2\beta_2$ stoichiometry of F_1 subunits reported by Vershoor et al. (32). However, we cannot deny the possibility that our purified F_1 preparation was partially inactivated, so that the $\alpha_3\beta_3$ stoichiometry (33) cannot be ruled out.

Binding of various phosphate compounds to F_1 are affected markedly by divalent cations and pH (34,35). The properties of fluorescence emission spectra of various complexes of DNS-ATP

with F_1 are summarized in Table I. The apparent dissociation constant of DNS-ATP bound to F_1 in the absence of Mg^{2+} was about 16 μM (Fig. 15), which was much higher than the ∅ value of 0.44 μM in the presence of Mg^{2+}. In Table I, the dioxane concentrations giving the same fluorescence emission peak and intensity at 520 nm that were obtained with free DNS-ATP and F_1-DNS-ATP in aqueous solution are also included. Thus, the hydrophobicity of environment around the DNS group in E·DNS-ATP and E·Mg^{2+}·DNS-ATP was equivalent to that of 20-30 and 58-76% dioxane, respectively. It is also suggested that Mg^{2+} increases both the affinity of F_1 for DNS-nucleotide and the hydrophobicity of the DNS-nucleotide binding site on F_1. A further increase in the extent of the fluorescence enhancement of DNS-ATP by reaction with F_1 in the absence of Mg^{2+} by lowering the pH (Fig. 4) suggests that the conformation around the nucleotide binding site on F_1 is altered by changing pH.

DNS-ADP was also bound to F_1 with a high affinity in the presence of Mg^{2+}, but the titration curve showed some heterogeneity (Fig. 7). One possibility is that two molecules of DNS-ADP bound to F_1 are not equivalent in terms of fluorescence intensity even if there is no interaction between them.

In this study, various elementary steps in the F_1-DNS-ATPase reaction were identified. The initial rate of fluorescence enhancement on addition of Mg^{2+} to F_1 increased with increasing concentration of DNS-ATP, following typical Michaelis-Menten kinetics (Fig. 8). Thus, we assumed the following reaction scheme to explain the formation of a complex of DNS-ATP and F_1 having enhanced fluorescence intensity ($E^{DNS\text{-}ATP*}$):

Table I. Properties of fluorescence emission spectra of various complexes of DNS-ATP and F_1. All the indicated values are for the bound forms of DNS-ATP except for free DNS-ATP.

Complex	Fluor. Max. (nm)	Fluor. Intensity at 520 nm (relative)	ø (μM)	Dioxane (v/v %)[b] Position of Peak	Intensity at 520 nm
Free DNS-ATP	555	1.0	–	0	0
E·DNS-ATP[a]	545	1.3-1.9	16[a]	20	30
$E \cdot Mg^{2+} \cdot$DNS-ATP	525	4.8	0.44	58	76
$P_i \cdot E \cdot Mg^{2+} \cdot$DNS-ATP	520	5.8	–	66	100

[a] The ø value was calculated from the data of Fig. 15. Fluorescence intensity at 520 nm was calculated from the data of Figs. 2 and 15.

[b] Concentration of dioxane which induces the same change in fluorescence properties of free DNS-ATP as that induced by formation of complex with F_1.

$$E + \text{DNS-ATP} \underset{K_f}{\rightleftharpoons} E^{\text{DNS-ATP}} \xrightarrow[V_f]{} E^{\text{DNS-ATP}*}$$

On addition of Mg^{2+} to a mixture containing DNS-ATP and F_1 the enhancement of fluorescence intensity of DNS-ATP, liberation of TCA-$^{32}P_i$ and free $^{32}P_i$ occurred consecutively (Fig. 9). Even after that the fluorescence intensity still maintained its enhanced level. All these findings are easily explained by the proposed reaction scheme shown in Fig. 29. $E_P^{\text{DNS-ADP}*}$ is a TCA-unstable intermediate, and its formation is measured as TCA-P_i. The rate of liberation of DNS-ADP from $E^{\text{DNS-ADP}*}$ is assumed to be very small, since the enhanced fluorescence level was maintained even after the release of free P_i.

The mechanism is supported by the following findings. (1) TCA-P_i burst of 2 mol/mol F_1 was observed with various concentrations of DNS-ATP (Fig. 10). The burst size agreed with the binding stoichiometry of 2 mol DNS-ATP/mol F_1 obtained from the fluorometric titration of F_1 (Fig. 5). (2) Boyer and coworkers (6) found $^{18}O/P$ ratio of more than three for P_i formed during ATP hydrolysis by F_1 at low concentrations of ATP, suggesting a rapid equilibrium of $E^{ATP} \rightleftharpoons E_P^{ADP}$. Notably the present reaction scheme resembles strikingly that of myosin ATPase (12-15). This similarity was originally pointed out by Boyer and coworkers (36). When Ca^{2+} was used as a divalent cation instead of Mg^{2+}, the release of DNS-ADP was accelerated (Fig. 12). This is also found with myosin ATPase.

There are several pieces of evidence to indicate the regulatory effect of ATP on ATP hydrolysis by F_1 (6-10). Boyer and coworkers (6) found that an increase in the ATP concentration

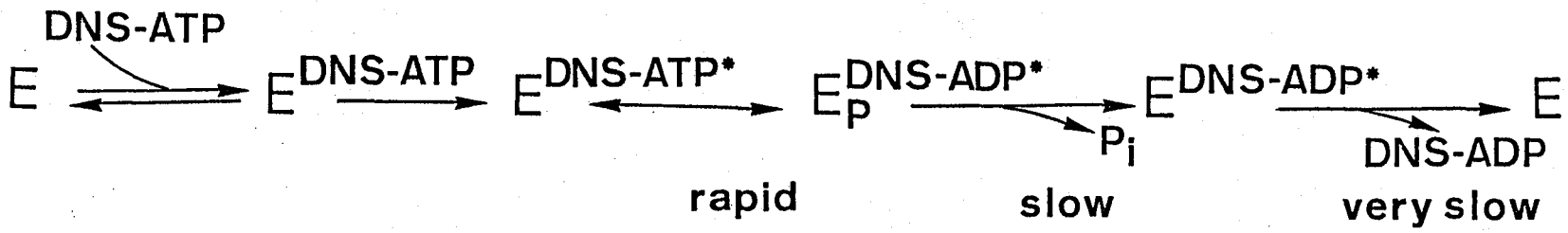

ADDITION OF ATP

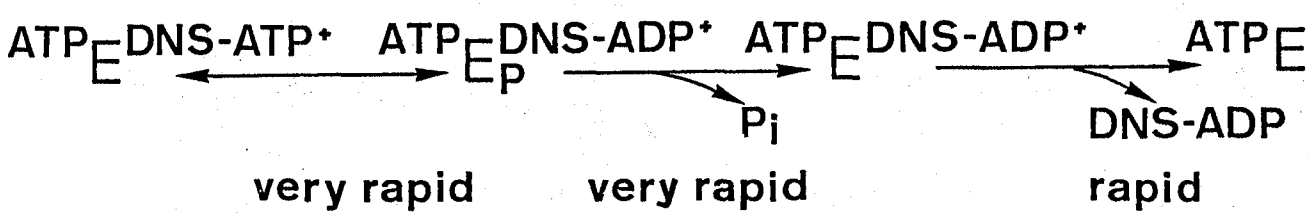

Fig. 29. The reaction mechanism of F_1-DNS-ATPase. Although two identical catalytic sites are postulated on F_1, only one of them is indicated here.

during ATP hydrolysis by F_1 decreased the extent of water oxygen incorporated into each P_i formed, as if ADP and P_i were released at one site when ATP was bound to another. In this study, we found that ATP accelerated markedly the formation of $E_P^{DNS\text{-}ADP*}$ from $E^{DNS\text{-}ATP*}$ (Fig. 13), release of P_i from $E_P^{DNS\text{-}ADP*}$ (Fig. 15), and also release of DNS-ADP from $E^{DNS\text{-}ADP*}$ (Fig. 16). This acceleration will be explained by a mechanism that a conformational change is induced by binding of ATP to regulatory site(s) which are different from the catalytic site(s) binding DNS-ATP.

When ATP was added to F_1-DNS-nucleotide under conditions where most of the DNS-ATP was bound to F_1, all the DNS-ATP was liberated rapidly as TCA-P_i (Fig. 13). However, when ATP was added at the initial phase of the F_1-DNS-ATPase reaction, the TCA-P_i liberation was only slightly accelerated, and then stopped (Fig. 14). These findings indicate that the rate of the reverse reaction, $E^{DNS\text{-}ATP*} \longrightarrow E^{DNS\text{-}ATP}$, is very small.

The rapid fluorescence decrease observed on addition of ATP, ADP, AMPPNP, ITP, or GTP to the reaction mixture containing DNS-ATP, F_1, and Mg^{2+} (Fig. 18) is suggested to be derived by the release of DNS-ADP induced by a conformational change of the catalytic site on F_1. The second slow phase will be due to the displacement of bound DNS-ADP by other nucleotides. ADP and AMPPNP also accelerated the TCA-P_i liberation, although the extent of the acceleration was smaller than that by ATP. Thus, the effects of nucleotides to accelerate the TCA-P_i liberation and to release DNS-ADP in the first rapid phase can be summarized as follows in the decreasing order of their efficiency:

$$\text{ATP} \gtrapprox \text{ADP} \approx \text{ITP} \gtrapprox \text{GTP} \approx \text{AMPPNP}$$

CTP accelerated slightly the step, $E^{DNS-ATP*} \longrightarrow E_P^{DNS-ADP*}$ (Fig. 19), and induced only a slow release of DNS-ADP from F_1 (Fig. 18B). These findings suggest that the affinity of the regulatory site for CTP is very low or a conformational change of the catalytic site is not induced by the CTP binding to the regulatory site. AMP accelerated neither the TCA-P_i liberation (Fig. 19) nor the DNS-ADP release (Fig. 22).

Recently, interactions of nucleotides with isolated subunits of F_1-ATPase from thermophilic bacteria were investigated by Kagawa and coworkers (37). They found that ATP were bound to both α and β, the affinity of the former being higher than that of the latter. They also found that CTP was bound to α subunit but not to β subunit, or that the conformational change of β subunit was not induced by CTP. Neither α nor β subunit bound AMP. If we assume that beef heart F_1 and thermophilic bacterial F_1 have essentially the same structure and function, our results strongly suggest that the catalytic site and the regulatory site exist on α and β subunits, respectively. This propose is apparently contrast to a widely accepted view that the catalytic site and the non-catalytic nucleotide binding site of F_1-ATPase are located on β and α subunits, respectively (38-42). However, it should be noted that this hypothesis was derived mainly by analyzing the effects of chemical modifications of F_1 only on the over-all reaction of F_1-ATPase. But this discrepancy will be removed by postulating that the hydrolysis of NTP by F_1 occurs at different catalytic sites.

If we assume that hydrolysis of DNS-ATP occurs only through the pathway *via* $E_P^{DNS\text{-}ADP*}$ in the steady-state, V_{max} has to be smaller than or equal to the maximum rate, V_f, for formation of $E^{DNS\text{-}ATP*}$. However, V_f was 0.34 s^{-1} (Fig. 8), which is much smaller than V_{max} ($\gg 1$ s^{-1}) (Fig. 23). Therefore, another pathway is also suggested for hydrolysis of DNS-ATP. Furthermore, when ATP was added under the conditions where most of F_1 was in the form of $E^{DNS\text{-}ADP*}$, ATP hydrolysis occurred without a lag phase (Fig. 24). If ATP is mainly hydrolyzed *via* E^{ADP}, a lag phase corresponding to the release of DNS-ADP should be observed contrary to the present finding. Thus, it is highly probable that hydrolysis of NTP occurs *via* different catalytic pathways and at different catalytic sites in F_1 as is observed with myosin ATPase (12,13).

E_P^{ADP} is widely accepted as a key intermediate in the energy-transducing process of myosin ATPase, and the present investigation clearly demonstrated that this type of intermediate is involved in the F_1-ATPase reaction. Therefore, it is speculated that the reverse process of the present reaction mechanism functions in the ATP synthesis. Differential effects of inhibitors on ATP synthesis on hydrolysis have been interpreted by several workers (43,44) as showing that the catalytic route for ATP synthesis is separate from that involved in ATP hydrolysis, although this view has been disputed by Boyer (11) from several lines of consideration.

The fluorescence enhancement of F_1-DNS-nucleotide induced by P_i in the presence of Mg^{2+} suggests that the environment of the nucleotide-binding sites on F_1 becomes more hydrophobic by

the action of P_i, thus diminishing the rate of the DNS-ADP release (Table I, Fig. 28). An apparent dissociation constant of this complex at pH 8 was 195 μM (Fig. 25) and this value decreased on lowering the pH. These results are in good agreement with those of Kasahara and Penefsky (45) who obtained the dissociation constant of 285 μM. Another interesting feature of the P_i effect is the distinction of the two DNS-ATP binding sites on F_1 which otherwise seem to be equivalent; that is, the saturation of the fluorescence enhancement induced by P_i at 1 mol DNS-ATP/mol F_1 implies the heterogeneity of the two binding sites, at least with respect to the interaction with P_i.

REFERENCES

1. Senior, A.E. (1973) Biochim. Biophys. Acta 301, 249-277
2. Kagawa, Y., Sone, N., Hirata, H., & Yoshida, M. (1979) J. Bioenerg. Biomem. 11, 39-78
3. Futai, M. (1977) Biochem. Biophys. Res. Commun. 79, 1231-1237
4. Slater, E.C., Kemp, A., Van der Kraan, I., Muller, J.L.M., Roveri, O.A., Verschoor, G.J., Wagenvoord, R.J., & Wielders, J.P.M. (1979) FEBS Lett. 103, 7-11
5. Harris, D.A. (1978) Biochim. Biophys. Acta 463, 245-273
6. Hutton, R.L. & Boyer, P.D. (1979) J. Biol. Chem. 254, 9990-9993
7. Roveri, O.A., Muller, J.L.M., Wilms, J., & Slater, E.C. (1980) Biochim. Biophys. Acta 589, 241-255
8. Vasilyeva, E.A., Fitin, A.F., Minkov, I.B., & Vinogradov, A.D. (1980) Biochem. J. 188, 807-815
9. Penefsky, H.S. (1977) J. Biol. Chem. 252, 2891-2899
10. Schuster, S.M., Ebel, R.E., & Lardy, H.A. (1975) J. Biol. Chem. 250, 7848-7853
11. Boyer, P.D. (1979) Membrane Bioenergetics (Lee, C.P., Schatz, G., & Ernster, L. eds.) pp. 461-479, Addison-Wesley Publishing Company Inc., London
12. Inoue, A., Takenaka, H., Arata, T., & Tonomura, Y. (1979) Adv. Biophys. (Kotani, M. ed.) Vol. 13, pp. 1-194, Japan Sci. Soc. Press and University Park Press, Tokyo and Baltimore
13. Tonomura, Y. (1972) Muscle Proteins, Muscle Contraction and Cation Transport, University of Tokyo Press and University Park Press, Tokyo and Baltimore

14. Trentham, D.R., Eccleston, J.F., & Bagshaw, C.R. (1976) Quart. Rev. Biophys. 9, 217-281

15. Taylor, E.W. (1979) CRC Crit. Rev. Biochem. 6, 103-164

16. Watanabe, T., Inoue, A., Tonomura, Y., Uesugi, S., Ohtsuka, E., & Ikehara, M. (1981) submitted to J. Biochem.

17. Glynn, I.M. & Chappell, J.B. (1964) Biochem. J. 90, 147-149

18. Tietz, A. & Ochoa, S. (1958) Arch. Biochem. Biophys. 78, 477-494

19. Furukawa, K.-I., Ikebe, M., Inoue, A., & Tonomura, Y. (1980) J. Biochem. 88, 1629-1641

20. Beyer, R.E. (1967) Methods in Enzymology (Colowick, S.P. & Kaplan, N.O., eds.) Vol. 10, pp. 186-194, Academic Press, New York

21. Beechey, R.B., Hubbard, S.A., Linnett, P.E., Mitchell, A.D., & Munn, E.A. (1975) Biochem. J. 148, 533-537

22. Gornall, A.G., Bardwill, C.S., & David, M.M. (1949) J. Biol. Chem. 177, 751-766

23. Weber, K. & Osborn, M. (1969) J. Biol. Chem. 244, 4406-4412

24. Nakamura, H. & Tonomura, Y. (1968) J. Biochem. 63, 279-294

25. Yamaguchi, M. & Tonomura, Y. (1979) J. Biochem. 86, 509-523

26. Fiske, C.H. & Subbarow, Y. (1925) J. Biol. Chem. 66, 375-400

27. Pullman, M.E. & Monray, G.C. (1963) J. Biol. Chem. 238, 3762-3769

28. Ebel, R.E. & Lardy, H.A. (1975) J. Biol. Chem. 250, 191-196

29. Takashi, R., Tonomura, Y., & Morales, M.F. (1977) Proc. Natl. Acad. Sci. USA 74, 2334-2338

30. Karlish, S.J.D., Yates, D.W., & Glynn, I.M. (1976) Nature 263, 251-253

31. Shoshan, V., Shavit, N., & Chipman, D.M. (1978) Biochim. Biophys. Acta 504, 108-122

32. Verschoor, G.J., van de Sluis, P.R., & Slater, E.C. (1977) Biochim. Biophys. Acta 462, 422-437

33. Each, F.S. & Allison, W.S. (1979) J. Biol. Chem. 254, 10740-10746

34. Wagenvoord, R.J., Kemp, A., & Slater, E.C. (1980) Biochim. Biophys. Acta 593, 204-211

35. Harris, D.A., Gomez-Fernandez, J.C., Klungsøyr, L., & Radda, G.K. (1978) Biochim. Biophys. Acta 504, 364-383

36. Boyer, P.D., Cross, R.L., & Momsen, W. (1973) Proc. Natl. Acad. Sci. USA 70, 2837-2839

37. Ohta, S., Tsuboi, M., Oshima, T., Yoshida, M., & Kagawa, Y. (1980) J. Biochem. 87, 1609-1617

38. Esch, F.S. & Allison, W.S. (1978) J. Biol. Chem. 253, 6100-6106

39. Ferguson, S.J., Lloyd, W.J., Lyons, M.H., & Radda, G.K. (1975) Eur. J. Biochem. 54, 117-126

40. Pougeois, R., Satre, M., & Vignais, P.V. (1979) Biochemistry 18, 1408-1413

41. Drutsa, V.L., Kozolov, I.A., Milgrom, Y.M., Shabarova, Z.A., & Sokolova, N.I. (1979) Biochem. J. 182, 617-619

42. Kozlov, I.A. & Milgrom, Y.M. (1980) Eur. J. Biochem. 106, 457-462

43. Penefsky, H.S. (1972) J. Biol. Chem. 249, 3579-3585

44. Steinmeier, R.C. & Wang, J.H. (1979) Biochemistry 18, 11-18

45. Kasahara, M. & Penefsky, H.S. (1978) J. Biol. Chem. 253, 4180-4187

PART II.

Reactions of a Fluorescent ATP Analog, 2'-(5-Dimethylamino-naphthalene-1-Sulfonyl) Amino-2'-DeoxyATP, with *E. coli* F_1-ATPase and Its Subunits: Evidence Suggesting the High Affinity Catalytic Site in α Subunit and Low Affinity Regulatory Site in β Subunit.

SUMMARY

We performed kinetic studies on the reactions of fluorescent ATP analog, 2'-(5-dimethyl-aminonaphthalene-1-sulfonyl) amino-2'-deoxyATP (DNS-ATP), with E. coli F_1-ATPase (EF_1) and its subunits, to clarify the role of each subunit in the ATPase reaction. The following results were obtained.

1. In the presence of Mg^{2+}, 3 mol of DNS-ATP binds to 1 mol of EF_1 with an apparent dissociation constant of 0.23 μM. Upon binding, the fluorescence intensity of DNS-ATP at 520 nm increased exponentially with $t_{1/2}$ of 35 s and reached 3.5 times the original fluorescence level. Following the fluorescence increase, DNS-ATP was hydrolyzed, and the fluorescence intensity maintained its enhanced level.

2. The addition of an excess of ATP over EF_1-DNS-nucleotide complex in the presence of Mg^{2+} decreased the fluorescence intensity rapidly, indicating the acceleration of DNS-nucleotide release from EF_1. ADP and GTP also decreased the fluorescence intensity.

3. DCCD inhibited markedly the accelerating effect of ATP on DNS-nucleotide release from EF_1 and the EF_1-ATPase activity at steady state. On the other hand, DCCD inhibited only slightly the fluorescence increase of DNS-ATP due to its binding to EF_1 and the rate of single turnover of DNS-ATP hydrolysis catalyzed by EF_1.

4. In the presence of Mg^{2+}, 0.65-0.82 mol of DNS-ATP binds to 1 mol of isolated α subunit of EF_1 with an apparent dissociation constant of 0.06-0.07 μM. Upon binding, the fluorescence intensity of DNS-ATP at 520 nm increased 1.55 fold very rapidly ($t_{1/2} < 1$ s). The fluorescence intensity of DNS-ATP was unaffected by the addition of the isolated β subunit.

5. The kinetic properties of the fluorescence change of DNS-ATP's reaction with EF_1-ATPase reconstituted from α, β and γ subunits were quite similar to that of native EF_1.

These findings strongly support the previous proposal that the high affinity catalytic site and low affinity regulatory site exist in the α and β subunit, respectively

INTRODUCTION

F_1-ATPase [EC 3.6.1.3] is composed of five subunits, designated α through ε in order of decreasing molecular weight (1,2). The stoichiometry of either $\alpha_3\beta_3\gamma$ or $\alpha_2\beta_2\gamma$ is proposed for the major subunits of F_1 (3-5). Recent reconstitution studies on F_1's from thermophilic bacterium PS3 (TF_1) (6,7) and E. coli (EF_1) (8,9) shed light on the role of each subunit of F_1. The complex of α with β and γ subunits possesses the ATPase activity, and the δ and ε subunits are essential for the binding of the $\alpha\beta\gamma$ complex to the membranous component, F_o. The α and β subunits each have nucleotide-binding sites, which are different in their affinity and specificity for nucleotides (9,10), and the total number of nucleotide-binding site in F_1 is 4-7 (11,12). The different nucleotide-binding sites in F_1 have been revealed by steady-state kinetics of the ATPase reaction (13), binding measurements (11,14), and the affinity labelling of nucleotide-binding sites (15-17). The F_1-ATPase activity was found to be inhibited by the modification of the β subunit which has a low affinity binding site for nucleotides (15,16,18-23). This finding suggests that the low affinity binding site in β subunit is the calatytic site. This suggestion is supported by the finding that the steady-state F_1-ATPase activity has a high K_m value for ATP (13,24).

Recently, we have synthesized a fluorescent ATP analog DNS-ATP, 2'-(5-dimethyl-aminonaphthalene-1-sulfonyl) amino-2'-deoxyATP (25), and studied the mechanism of the DNS-ATPase reaction of beef heart F_1 (26). We found that the reaction mechanism of F_1-ATPase is very similar to that of myosin ATPase, and that the nucleotide at high

concentrations accelerate the rates of three elementary steps in F_1-ATPase (26). These findings were interpreted as showing the existence of low affinity regulatory site(s) as well as high affinity catalytic sites (26). Together with the results on the direct nucleotide binding measurements of the isolated α and β subunit (9,10), this view can be extended to the subunit localization of the high affinity catalytic site in the α subunit and the low affinity regulatory site in the β subunit. However, this view is quite opposite to the widely accepted hypothesis as mentioned above.

To determine whether the catalytic site exists in the α or β subunit, we performed kinetic studies on the reactions of DNS-ATP with EF_1 and isolated active subunits. The results obtained strongly supported our hypothesis that the high affinity catalytic site and low affinity regulatory site exist in the α and β subunits, respectively.

MATERIALS AND METHODS

Materials —— DNS-ATP, DNS-ADP and [γ-^{32}P]DNS-ATP (DNS-AT^{32}P) were synthesized as described previously (25). Pyruvate kinase [EC 2.7.1.40] was prepared according to the method of Tietz and Ochoa (27). ATP, ADP and AMP were purchased from Khojin Ltd. (Tokyo). AMPPNP, ITP, GTP, CTP and phosphoenolpyruvate were purchased from Sigma Chemicals Co. (St. Louis, MO). All other chemicals were of reagent grade purity.

Preparation of EF_1, α and β Subunit, and Reconstituted EF_1-ATPase — EF_1 was purified as described previously (28) from E. coli KY7485 (λasn -5) after thermoinduction of the transducing phage carrying a set of structural genes for the proton translocating ATPase (29). Purified EF_1 was precipitated by 55% ammonium sulfate and dissolved in 50mM Tris-acetate (pH 7.0) and 2mM EDTA, at a concentration of 5-10 mg/ml. The EF_1 solution was dialyzed against the same buffer solution at 20°C for 20 h before use. The α, β and γ subunits were purified from EF_1 as described previously (9). Reconstituted EF_1-ATPase was prepared from a mixture of the α, β and γ subunits as described previously (8), and concentrated to 2 mg/ml by Diaflo XM-100A membrane purchased from Amicon Ltd. (Lexington, MA). The concentrated enzyme was dialyzed against the above buffer solution at 20°C for 20 h before use. The protein concentration was determined by biuret method (30) or by the method of Bradford (31) with bovine serum albumin as a standard. The molecular weights of EF_1, α, β subunits, and reconstituted EF_1-ATPase were taken as 376,000, 58,000, 52,000, and 364,000, respectively (9,28).

Fluorescence Measurements — Measurement solutions were prepared by addition of reagents in 5-20 µl portions to 2 ml of 2 mM EDTA, 100 mM NaCl and 50 mM Tirs-acetate at pH 7.0 and 30°C. The fluorescence intensity of DNS-ATP at 520 nm with excitation at 340 nm was measured as described previously (26).

DNS-ATPase and ATPase Activity — EF_1 at 0.87-1.6 µM was allowed to react with 2.8 µM DNS-AT^{32}P in 2 mM EDTA, 100 mM NaCl and 50 mM Tris-acetate at pH 7.0 and 30°C for 1 min. Then, the hydrolysis was started by the addition of 5 mM $MgCl_2$. The amount of $^{32}P_i$ liberated when the reaction was terminated by TCA (TCA-$^{32}P_i$) was measured as described previously (26). The steady-state ATPase activity of EF_1 was measured in the presence of an ATP-feeder system (0.1 mg/ml pyruvate kinase and 5 mM phosphoenolpyruvate) at pH 8.0 and 30°C (26). The amount of TCA-P_i liberated was measured by the method of Fiske and Subbarow (32).

Binding of DNS-AT^{32}P to α Subunit — To measure the binding of DNS-AT^{32}P to α subunit, the equilibrium dialysis was performed at room temperature using chambers consisting of two wells separated by a layer of dialysis membrane (9). One side of the chamber contained subunit and both wells contained 2 mM EDTA, 100 mM NaCl and 50 mM Tris-acetate at pH 7.0.

RESULTS

Fluorescence Change of DNS-ATP on Its Binding to EF_1 — Figure 1(A) shows a typical time course of change in the fluorescence intensity of DNS-ATP at 520 nm during its reaction with EF_1 in the presence of 3 mM free Mg^{2+}. The fluorescence intensity of 1.1 μM DNS-ATP in the presence of 2 mM EDTA increased only slightly on addition of 0.99 μM EF_1 [arrow a in Fig. 1(A); compare curves a and b in Fig. 2]. On further addition of 5 mM $MgCl_2$ [arrow b in Fig. 1(A)], the fluorescence increased exponentially with a $t_{1/2}$ of 35 s, and reached a plateu level, which was 3.2 fold the fluorescence intensity of free DNS-ATP. Being observed only in the presence of EF_1, the Mg^{2+}-dependent fluorescence increase of DNS-ATP reflects the binding of DNS-ATP to the nucleotide-binding sites in EF_1 (cf. DISCUSSION). On a further addition of 2 mM P_i [arrow c in Fig. 1(A)], the fluorescence intensity increased rapidly to the level of 5.1 fold that of free DNS-ATP. When 2 mM ATP was added to the reaction mixture [arrow d in Fig. 1(A)], the fluorescence intensity decreased rapidly to about 50% of the original level, then decreased slowly. When a small amount of DNS-ATP was added to EF_1 ($\lesssim$0.5 mol/mol EF_1), the fluorescence intensity decreased to a level almost identical to that of free DNS-ATP within 5 min after the addition of ATP. However, when a large amount of DNS-ATP was used, the second phase of the decrease occurred very slowly, and even 10 min after the addition of ATP, the fluorescence intensity was not the same as that of free DNS-ATP.

Figure 1(B) shows a time course of change in the fluorescence intensity of DNS-ATP in the presence of 3 mM Ca^{2+}. When 5 mM $CaCl_2$

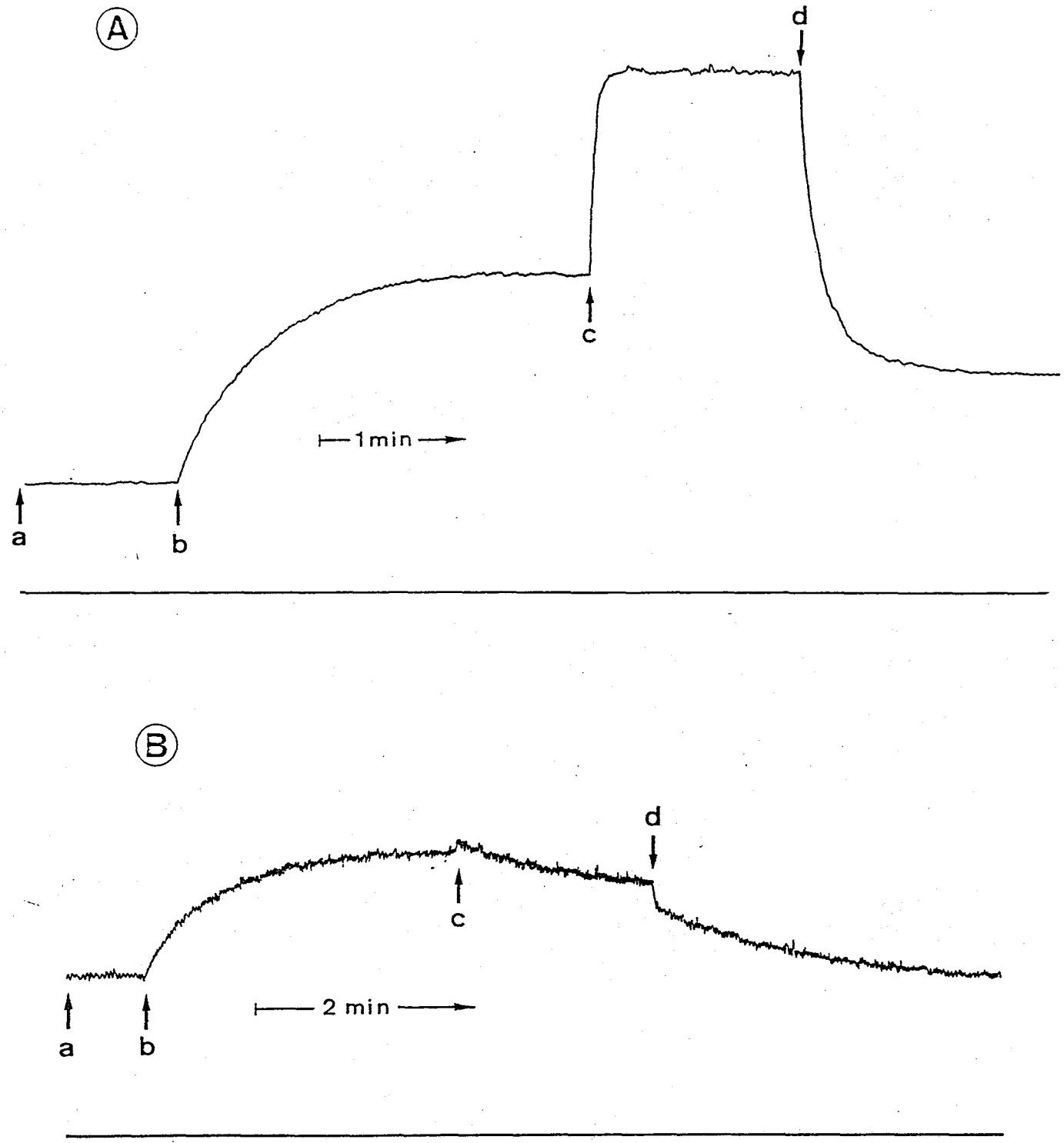

Fig. 1. Time course of fluorescence intensity change of DNS-ATP in the presence of EF_1. To a mixture containing 1.1 μM DNS-ATP, 2 mM EDTA, 0.1 M NaCl and 50 mM Tris-acetate at pH 8.0 and 30°C, the following additions were made at time indicated by arrows (a-d). (A): a, 0.99 μM EF_1; b, 5 mM $MgCl_2$; c, 2 mM K-P_i; d, 2 mM ATP. (B): a, 0.94 μM EF_1; b, 5 mM $CaCl_2$; c, 2 mM K-P_i; d, 2 mM ATP. The emission and excitation wavelengths were 520 and 340 nm, respectively.

was added to a reaction mixture containing 1.1 μM DNS-ATP, 0.94 μM EF_1 and 2 mM EDTA (b), the fluorescence intensity of DNS-ATP increased exponentially with almost the same value of $t_{1/2}$ as that in the case of 5 mM $MgCl_2$ addition. The plateu level of fluorescence in the presence of Ca^{2+} was 2 fold that of free DNS-ATP. Further addition of 1 mM P_i (c) did not cause any fluorescence increase, but caused a slow decrease. On further addition of 2 mM ATP (d), the fluorescence intensity decreased rapidly by about 10%, then approached slowly to the level of free DNS-ATP.

Figure 2 shows the fluorescence emission spectra of free DNS-ATP and various complexes of DNS-ATP with EF_1. As previously described (25), DNS-ATP had an emission peak at 555 nm (trace a). On addition of EF_1, the emission peak shifted to around 550 nm with a slight increase in the fluorescence intensity (trace b). Addition of 5 mM $MgCl_2$ markedly increased the fluorescence intensity, and the maximum shifted to 530 nm (trace c). Further addition of 2 mM P_i caused a further increase of the fluorescence and the shift of the maximum to around 520 nm (trace d). Addition of 2 mM ATP reversed these fluorescence changes almost backward to the state of free DNS-ATP (trace e). These fluorescence changes of DNS-ATP on its reactions with EF_1 are almost equal to those observed for beef heart F_1.

Stoichiometry of DNS-ATP Binding to EF_1 — The stoichiometry of DNS-ATP binding to EF_1 was determined by fluorometric titration of 1.1 μM DNS-ATP with EF_1 in the presence of 3 mM free Mg^{2+} (Fig. 3). Several kinds of reaction intermediates are produced by the reaction of EF_1 with DNS-ATP, as will be mentioned in "DISCUSSION." However, we (26) previously found that in the case of beef heart F_1, the fluorescence intensity of one intermediate is only slightly higher

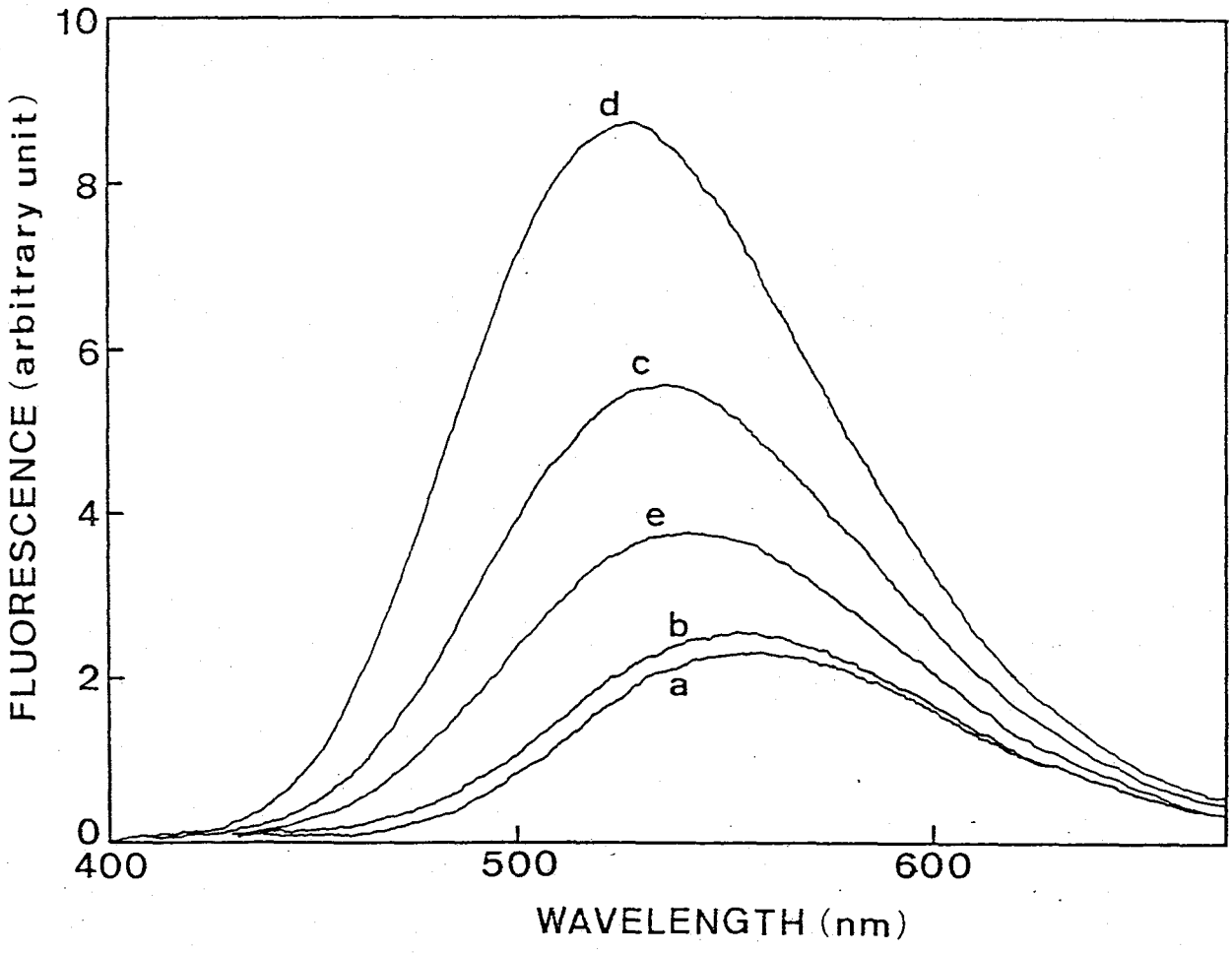

Fig. 2. Fluorescence emission spectra recorded during the course of reaction of DNS-ATP with EF_1. Spectra were recorded in the following order; curve a, 1.1 μM DNS-ATP alone; curve b, 1 min after addition of 1.6 μM EF_1; curve c, 2 min after addition of 5 mM $MgCl_2$; curve d, 1 min after addition of 2 mM K-P_i; curve e, 1 min after addition of 2 mM ATP. Other conditions were the same as described in Fig. 1 or in the text.

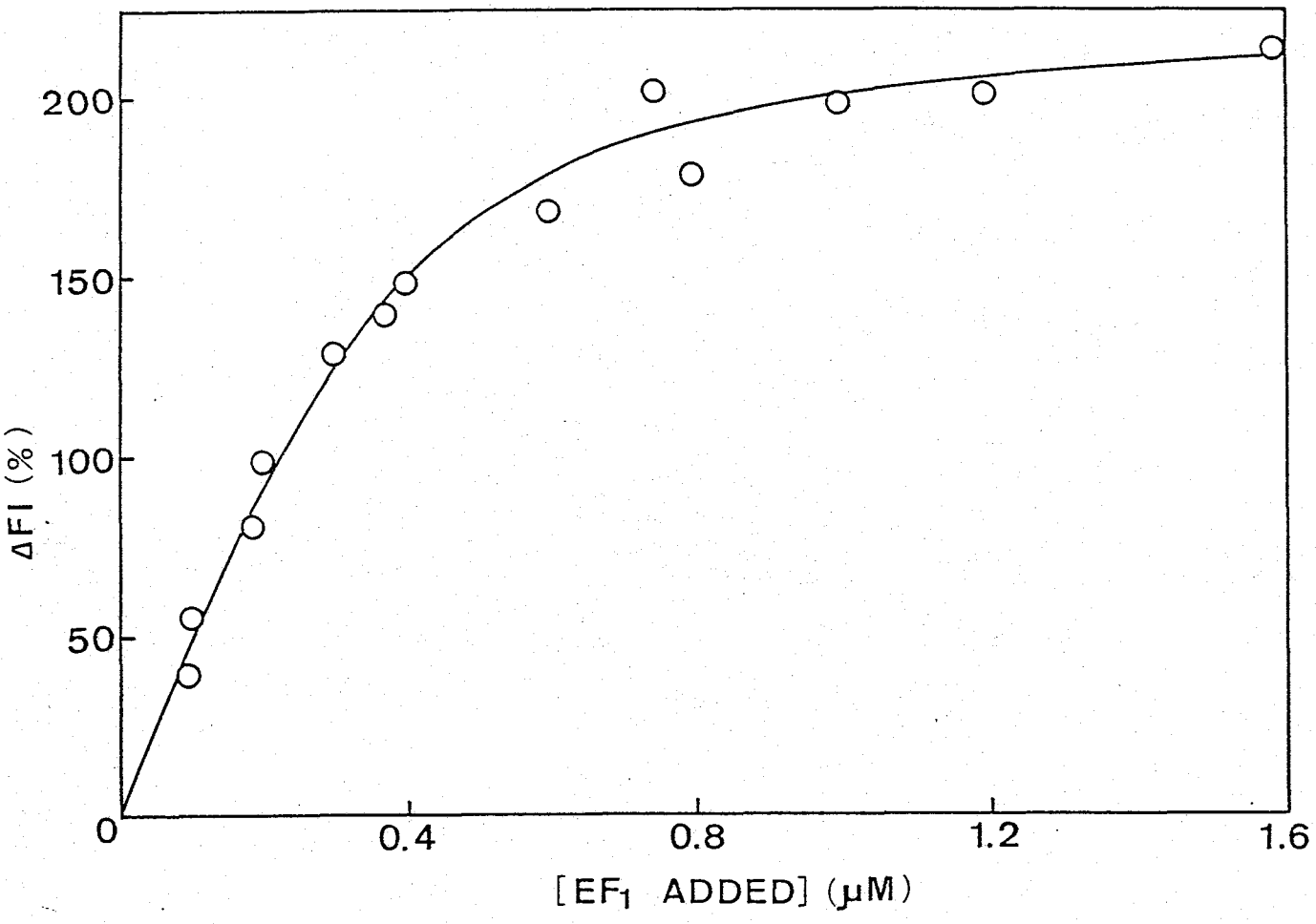

Fig. 3. Fluorometric titration of DNS-ATP with EF_1 in the presence of $MgCl_2$. The extent of fluorescence increase 2 min after addition of 5 mM $MgCl_2$ was plotted against the amount of EF_1 added. The reaction mixture contained 1.1 μM DNS-ATP in 2 mM EDTA, 0.1 M NaCl and 50 mM Tris-acetate at pH 7.0 and 30°C. The solid line is the theoretical curve (see the text).

than that of free DNS-ATP and the intensities of other intermediates are much higher than that of free DNS-ATP and are equal to each other. Therefore, the data were analyzed based on the quadratic equation:

$$\Delta F = \frac{\Delta F_{max}}{2}\left\{(nE_o+S_o+\phi_{DNS\text{-}ATP})-[(nE_o+S_o+\phi_{DNS\text{-}ATP})^2-4nE_oS_o]^{\frac{1}{2}}\right\} \quad \text{(Eq. 1)}$$

where ΔF is the extent of fluorescence increase, and is assumed to be proportional to the amount of EF_1-DNS-nucleotide complex. ΔF_{max} is the maximum value of ΔF, and is obtained when all the DNS-ATP binds to EF_1. Both the ΔF and ΔF_{max} values are expressed as percentage of the fluorescence intensity of free DNS-ATP in the absence of Mg^{2+}. E_o and S_o are the total concentrations of EF_1 and DNS-ATP, respectively. n is the number of independent and equivalent binding sites of DNS-ATP in EF_1, and $\phi_{DNS\text{-}ATP}$ is their dissociation constant. The solid line in Fig. 3 is the best fit of the data to Eq. 1 with ΔF_{max} = 250%, n = 3, and $\phi_{DNS\text{-}ATP}$ = 0.23 μM. With n values other than 3, the fit was poor.

Hydrolysis of DNS-ATP by EF_1 — We found that in the absence of free Mg^{2+}, DNS-ATP is not hydrolyzed by EF_1. Therefore, we measured the time course of TCA-$^{32}P_i$ liberation after addition of 5 mM $MgCl_2$ to a reaction mixture containing 2.8 μM DNS-AT^{32}P, 1.6 μM EF_1 and 2 mM EDTA (Fig. 4). The amount of TCA-$^{32}P_i$ liberated at 120 s was 0.47 mol/mol α. The amount of DNS-nucleotide bound to EF_1 under the conditions used was estimated to be 0.53 mol/mol α by using n = 3 and $\phi_{DNS\text{-}ATP}$ = 0.23 μM. Under these conditions the fluorescence increase was found to be almost completed after 120 s of reaction. When ATP at 2 mM was added 60 s after starting the reaction (arrow in Fig. 4),

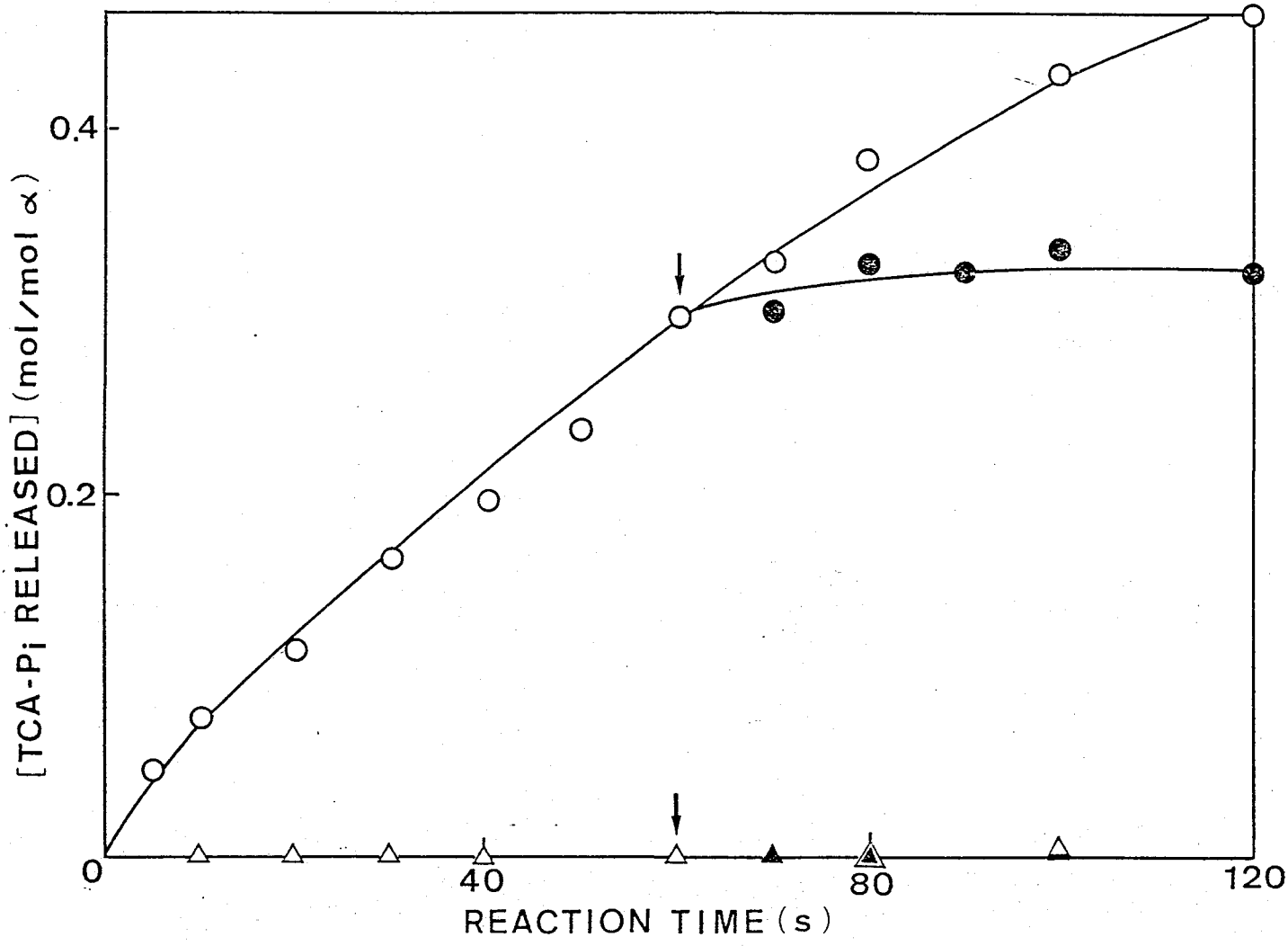

Fig. 4. Initial phase of TCA-$^{32}P_i$ liberation from DNS-AT^{32}P catalyzed by EF_1 or purified α subunit. The reaction mixture contained 2.8 μM DNS-AT^{32}P and 1.6 μM EF_1 (○, ●) or 2.3 μM α subunit (△, ▲) in 2 mM EDTA, 0.1 M NaCl and 50 mM Tris-acetate at pH 7.0 and 30°C. The reaction was started by the addition of 5 mM $MgCl_2$. At the time indicated by an arrow (60 s after addition of $MgCl_2$), 2 mM ATP was added (●, ▲).

the TCA-$^{32}P_i$ liberation ceased immediately, showing no acceleration such as observed on beef heart F_1 (26).

Acceleration of DNS-Nucleotide Release from EF_1-Nucleotide Complex by Addition of Nucleotides and Pyrophosphate — The fluorescence intensity of EF_1-DNS-nucleotide complex maintained its enhanced level after liberation of TCA-$^{32}P_i$. Because of a very small rate of release of DNS-ADP from the complex, it is clear that DNS-ADP formed by hydrolysis of DNS-AT^{32}P was still bound to EF_1. In the presence of 3 mM Mg^{2+}, DNS-ATP at 1.1 μM was allowed to react with 0.98 μM EF_1 for 2 min. Then, various nucleotides (0.2 mM) or pyrophosphate (2 mM) were added, and the following decrease in the fluorescence intensity was measured (Fig. 5). The addition of ATP caused a fluorescence decrease with first rapid and second slow phases (trace a). In the case of beef heart F_1, we found that the time course of the fluorescence decrease after addition of ATP was identical to that of the release of DNS-ADP from F_1-DNS-nucleotide in both rapid and slow phases (26). Therefore, we assumed that the fluorescence decrease after addition of ATP corresponds to the release of DNS-nucleotide from EF_1-DNS-nucleotide in the case of EF_1 as well. ADP (trace b) and GTP (trace c) also induced a fluorescence decrease, but the rates of the decrease were smaller than that induced by ATP. The rates of the fluorescence decrease on addition of AMPPNP (trace d), PP_i (trace e), and CTP (trace f) became smaller in this order. AMP (trace g) had no effect on the fluorescence intensity of EF_1-DNS-nucleotide.

Effects of DCCD on the Reaction of DNS-ATP with EF_1 — Figure 6 shows the time course of the change in the fluorescence intensity of

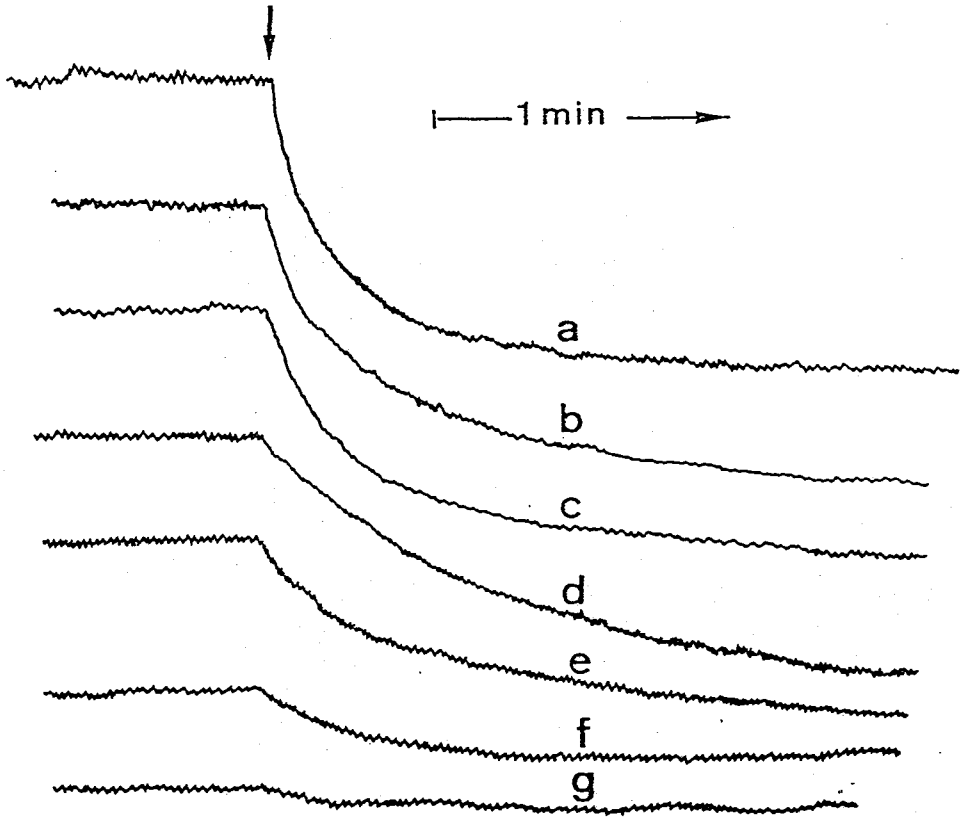

Fig. 5. Fluorescence decrease on addition of various phosphate compounds to EF_1-DNS-nucleotide complex. DNS-ATP at 1.1 μM was allowed to react with 0.98 μM EF_1 in the presence of 3 mM Mg^{2+} for 2 min, then at the time indicated by an arrow, the following additions were made; a, 0.2 mM ATP; b, 0.2 mM ADP; c, 0.2 mM GTP; d, 0.2 mM AMPPNP; e, 2 mM PP_i; f, 0.2 mM CTP; g, 0.2 mM AMP. Other conditions were the same as described in Fig. 1.

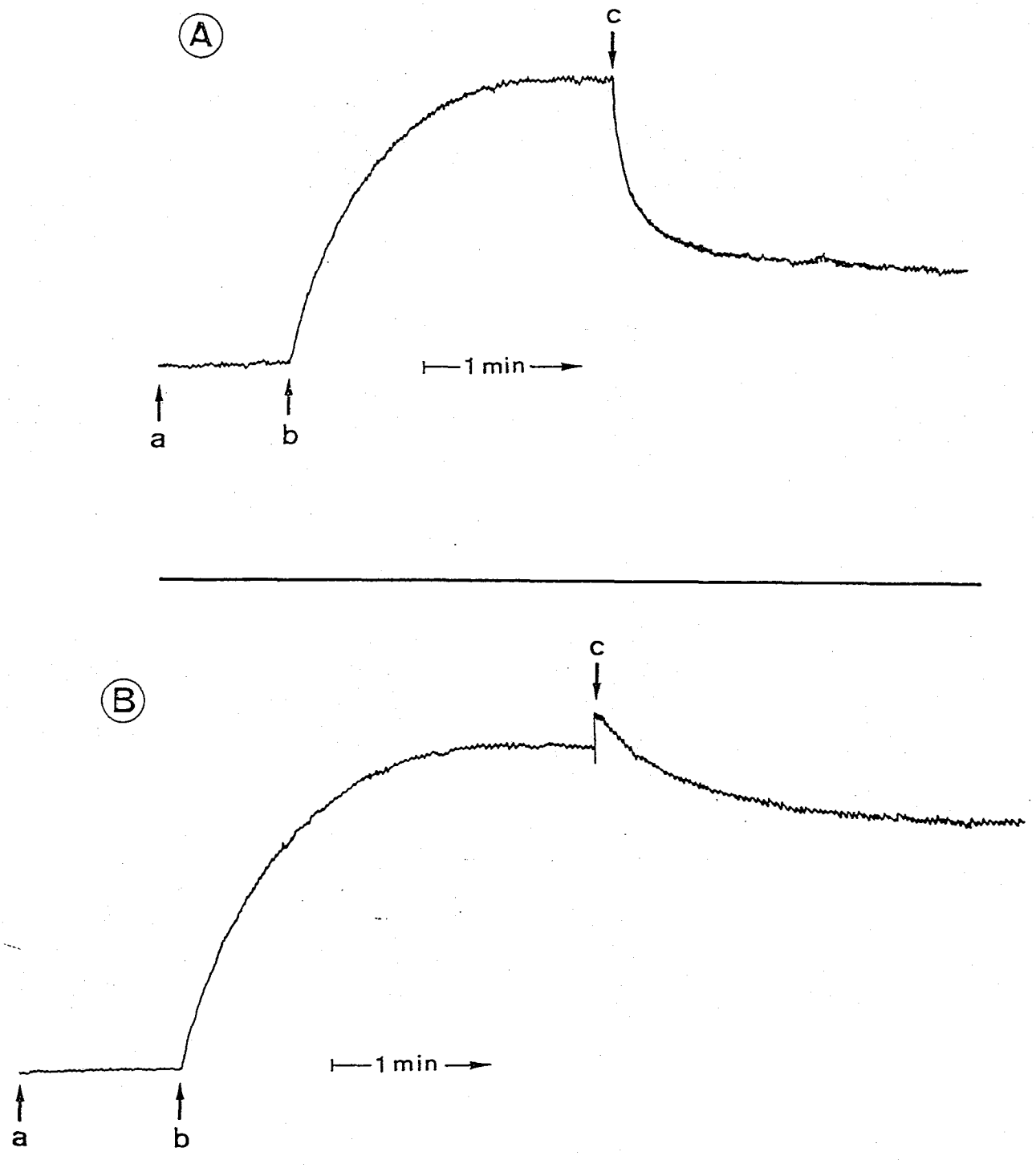

Fig. 6. Inhibition by DCCD-treatment of decrease in the fluorescence intensity of EF_1-DNS-nucleotide upon addition of ATP. After incubation of 0.98 μM EF_1 without (A) or with (B) 0.2 mM DCCD in 2 mM EDTA, 100 mM NaCl and 50 mM Tris-acetate at pH 7.0 and 30°C for 20 min, the following additions were made at the time indicated by arrows (a-c) a, 1.1 μM DNS-ATP; b, 5 mM $MgCl_2$; c, 2 mM ATP.

1.1 μM DNS-ATP during its reaction with 0.98 μM EF_1, which was preincubated with 0 (A) or 0.2 mM DCCD (B) at pH 7.0 and 30°C for 20 min. The time course of increase in the fluorescence intensity after addition of 5 mM $MgCl_2$ (b) was almost unaffected by the DCCD-treatment. On the other hand, the decrease of the fluorescence intensity upon subsequent addition of 2 mM ATP (c) was inhibited markedly by the DCCD-treatment (Fig. 6B).

Figure 7 shows the effects of DCCD on the steady-state rate of EF_1-ATPase and the initial rate of EF_1-DNS-ATPase. The steady-state rate of the Mg^{2+}-ATPase reaction of EF_1 was inhibited almost completely by the DCCD-treatment [Fig. 7(A)], as already reported by Satre et al. (21). The initial rate of TCA-$^{32}P_i$ liberation in the presence of a low concentration of DNS-ATP was only slightly inhibited by the DCCD-treatment of EF_1 [Fig. 7(B)]. It must be noted that in both experiments EF_1 of the same concentration range was preincubated with DCCD (legend of Fig. 7).

Fluorescence Change of DNS-ATP on Its Binding to α Subunit of EF_1 — Fig. 8(A) shows a typical time course of change in the fluorescence intensity of DNS-ATP at 520 nm during its reaction with α subunit of EF_1. The fluorescence intensity of 1.1 μM DNS-ATP in the presence of 2 mM EDTA did not change on addition of 0.8 μM α subunit [arrow a in Fig. 8(A), cf. Fig. 9]. On further addition of 5 mM $MgCl_2$ [arrow b in Fig. 8(A)], the fluorescence intensity increased very rapidly ($t_{1/2} < 1$ s) by 19%. No fluorescence increase was observed in the absence of this subunit or in the presence of an excess amount of ATP with the subunit. On further addition of 2 mM P_i [arrow c in Fig. 8(A)], the fluorescence intensity changed only slightly and maintained its level. When 2 mM ATP was finally added [arrow d in

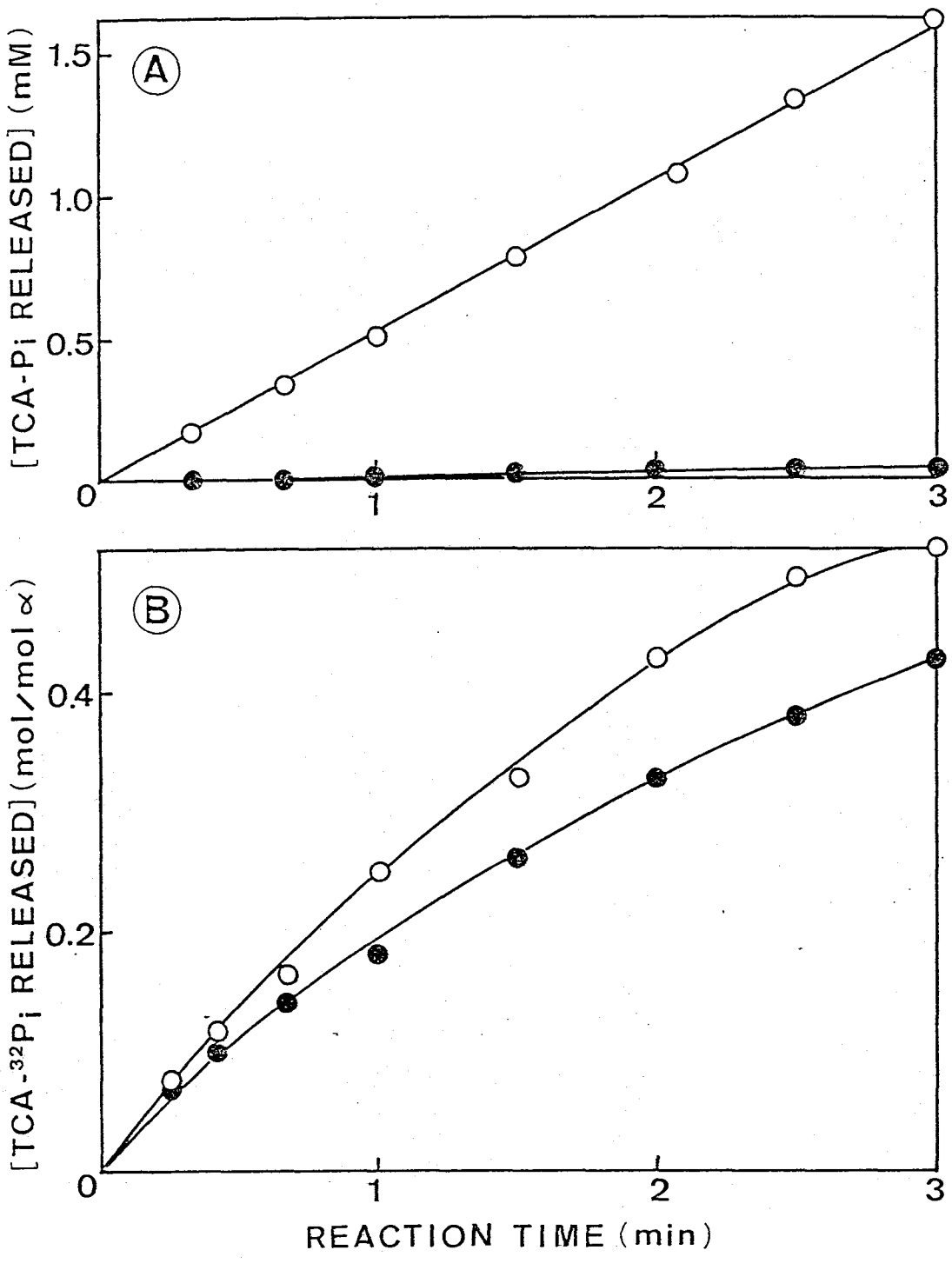

Fig. 7. Effects of DCCD-treatment of EF_1 on its steady-state ATPase and single turnover of DNS-ATP hydrolysis. (A) EF_1 at 0.87 μM was preincubated with (●) or without (○) 0.2 mM DCCD in 2 mM EDTA and 50 mM Tris-acetate at pH 7.0 and 30°C for 20 min. Then, EF_1 solution was diluted to 0.087 μM in 5 mM phosphoenolpyruvate, 0.11 mg/ml pyruvate kinase, 2.5 mM $MgCl_2$, 0.2 mM EDTA and 50 mM Tris-HCl at pH 8.0 and 30°C. The reaction was started by addition of 5 mM ATP. (B) EF_1 at 1.6 μM was preincubated with (●) or without (○) 0.2 mM DCCD under the same conditions as A, then allowed to react with 2.8 μM DNS-AT^{32}P for 1 min. The reaction was started by addition of 3 mM Mg^{2+}.

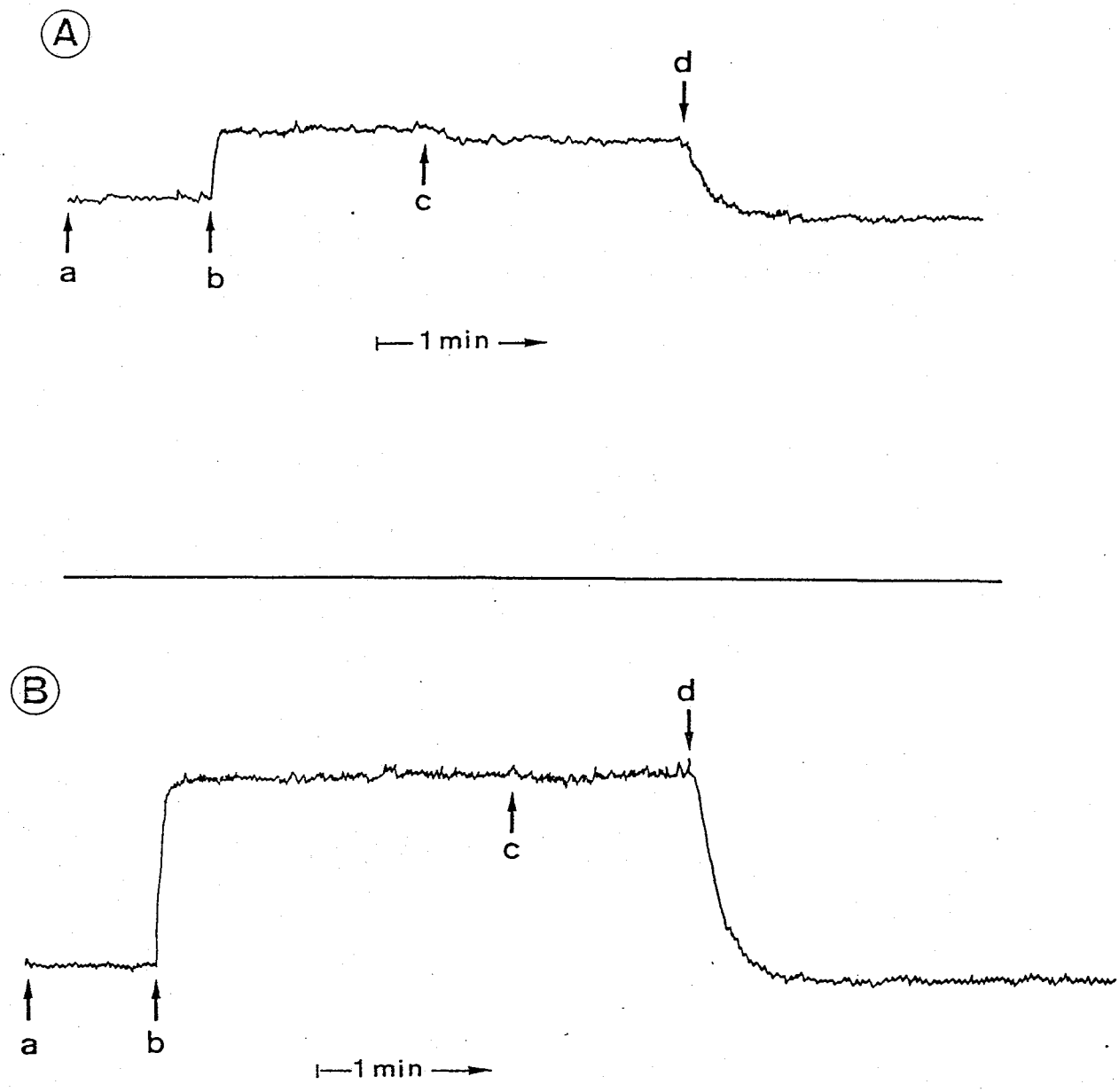

Fig. 8. Time course of fluorescence intensity change of DNS-ATP in the presence of α subunit. (A) To a reaction mixture containing 0.8 μM α subunit in a buffer solution (2 mM EDTA, 0.1 M NaCl and 50 mM Tris-acetate at pH 7.0 and 30°C), the following additions were made at the time indicated by arrows (a-d); a, 1.1 μM DNS-ATP; b, 5 mM $MgCl_2$; c, 2 mM K-P_i; d, 2 mM ATP. (B) To a reaction mixture containing 4 μM α subunit in the buffer solution, the following additions were made at the time indicated by arrows (a-d); a, 1.1 μM DNS-ATP; b, 5 mM $MgCl_2$; c, 0.2 mM AMP; d, 0.2 mM ATP.

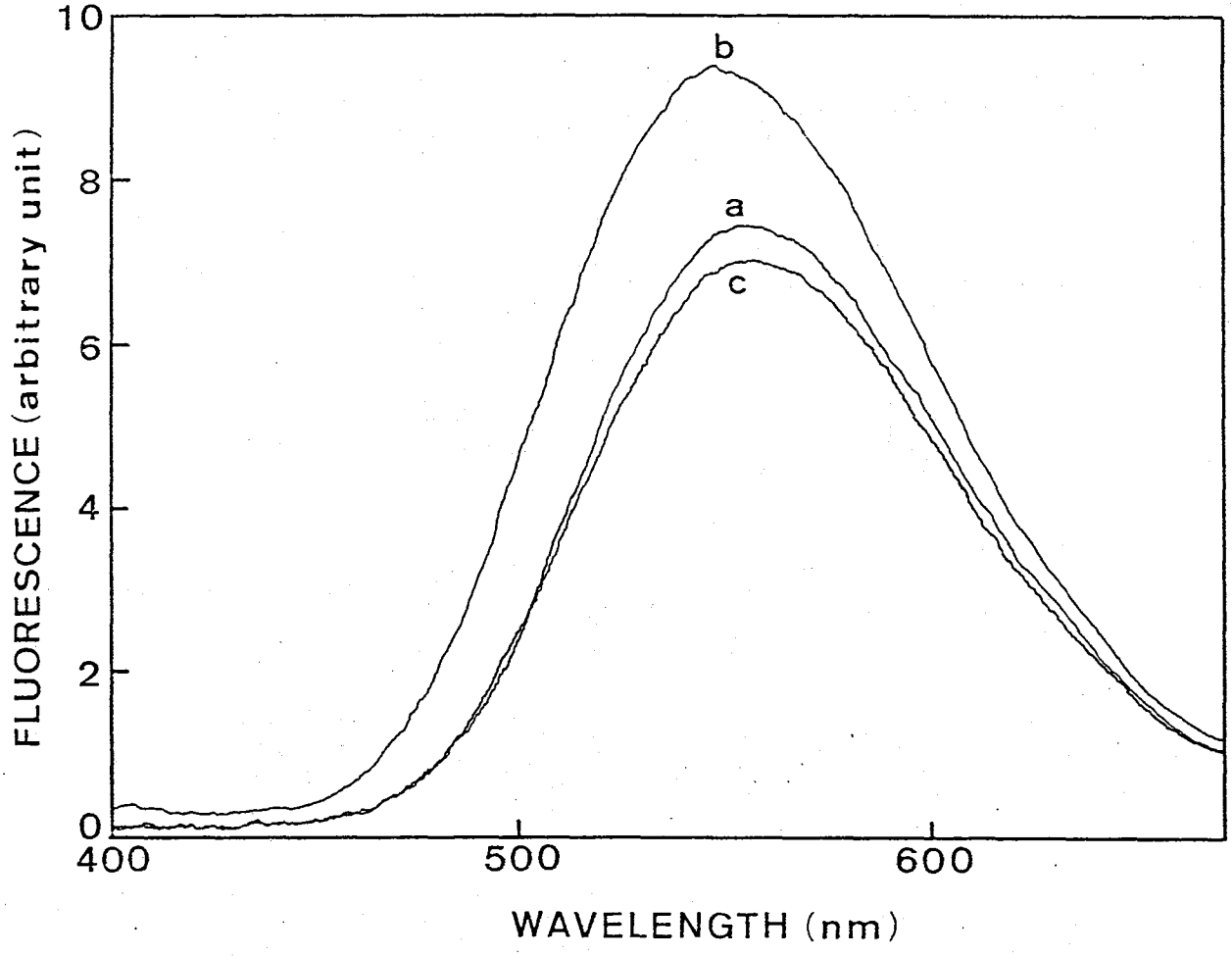

Fig. 9. Fluorescence emission spectra recorded during the course of reaction of DNS-ATP with α subunit. Spectra were recorded in the following order; curve a, 1 min after addition of 4 μM α subunit to 1.1 μM DNS-ATP; curve b, 1 min after addition of 5 mM $MgCl_2$; curve c, 1 min after addition of 2 mM ATP. The fluorescence emission spectra of 1.1 μM DNS-ATP alone in 2 mM EDTA and in 2 mM EDTA + 5 mM $MgCl_2$ were the same as the curve a and c, respectively. Other conditions are the same as described in Fig. 8.

Fig. 8(A)], the fluorescence intensity decreased exponentially with a $t_{1/2}$ of 8 s to a level which was about 5% lower than that before the addition of 5 mM $MgCl_2$. The final level was found to be equal to that of free DNS-ATP in the presence of free Mg^{2+}.

Essentially the same experiment was carried out with 4.0 μM α subunit; as shown in Fig. 8(B) the fluorescence intensity increased very rapidly by 50% upon addition of 5 mM $MgCl_2$ [arrow b in Fig. 8(B)]. Addition of 0.2 mM AMP [arrow c in Fig. 8(B)] had no effect on the fluorescence intensity, whereas subsequent addition of 0.2 mM ATP [arrow d in Fig. 8(B)] decreased the intensity as observed in Fig. 8(A). When 5 mM $CaCl_2$, instead of $MgCl_2$, was added to the reaction mixture, no change of the fluorescence intensity was observed (data not shown).

Fluorescence emission spectra were recorded during the course of reaction of DNS-ATP with α subunit (Fig. 9). Addition of 4.0 μM α subunit to 1.1 μM DNS-ATP in the presence of 2 mM EDTA did not change the fluorescence emission spectrum of the free DNS-ATP (trace a). Further addition of 5 mM $MgCl_2$ increased the fluorescence intensity, and the emission maximum shifted to around 530 nm (trace b). Addition of 2 mM ATP decreased the fluorescence intensity to the level of free DNS-ATP in the presence of Mg^{2+} (trace c), which was slightly lower than that in the absence of Mg^{2+} (trace a).

Stoichiometry of DNS-ATP Binding to α Subunit — The stoichiometry of DNS-ATP binding to α subunit was determined by fluorometric titration of 1.1 μM DNS-ATP with α subunit in the presence of 3 mM Mg^{2+} at 4° or 30°C (Fig. 10). Data were analyzed based on Eq. 1, where the parameters for $_{-}EF_1$ were taken as those for α subunit. The solid lines in Fig. 10 are the best fits of the data of the DNS-ATP titration with α subunit at 4° (●) and 30°C (○). The parameters

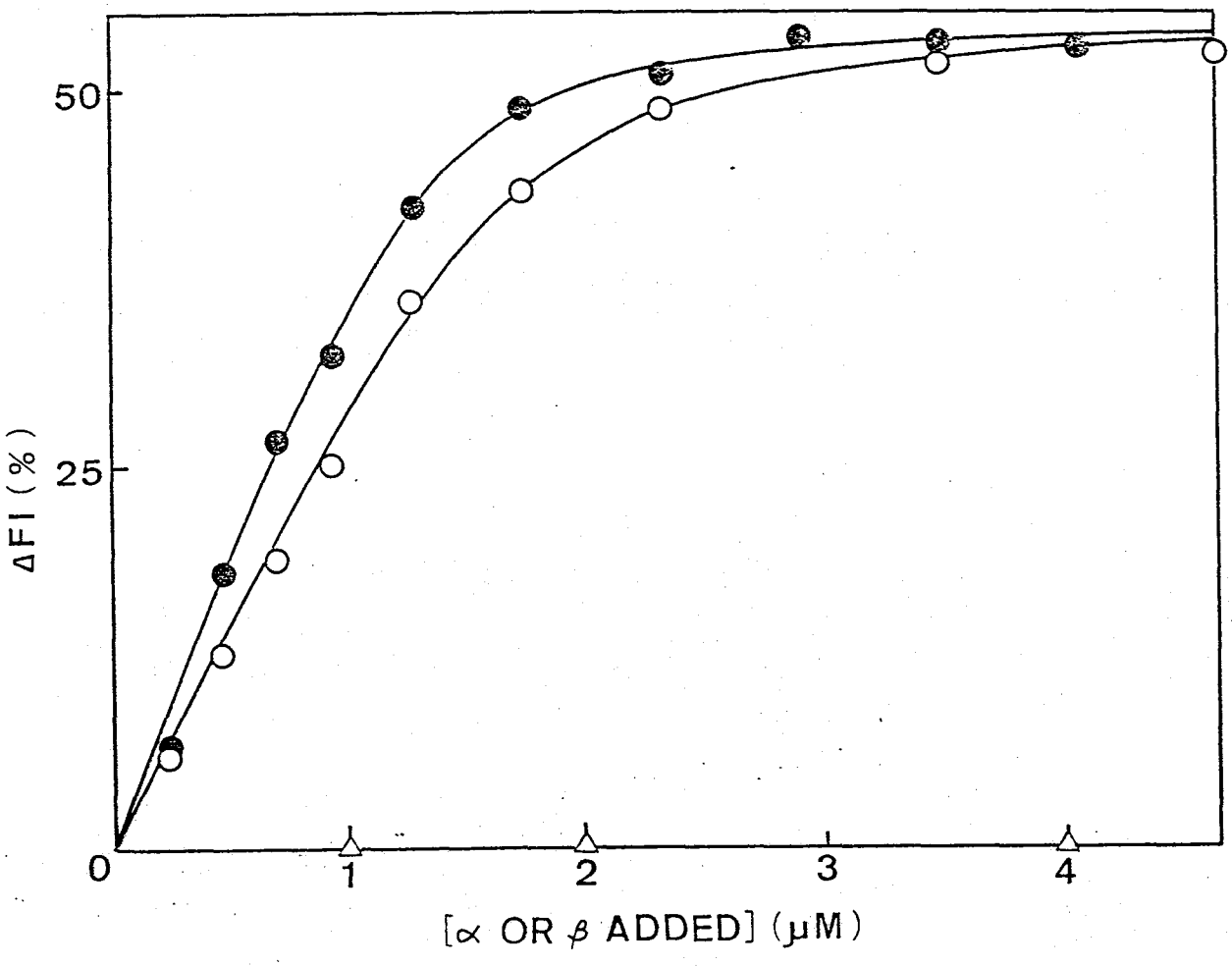

Fig. 10. Fluorescence titration of DNS-ATP with α subunit in the presence of Mg^{2+}. The extent of fluorescence increase of 1.1 μM DNS-ATP after addition of 3 mM Mg^{2+} was plotted against the amount of α subunit at 30° (○) or 4°C (●). Other conditions are the same as described in Fig. 8. The extent of fluorescence decrease of free DNS-ATP in the presence of free Mg^{2+} (cf. Fig. 9, curve c) was corrected. The solid lines are the theoretical curves (see the text). When 1.1 μM DNS-ATP was allowed to react with β subunit in the presence of Mg^{2+} at 30°C, no fluorescence change was observed (△).

obtained from the data are n = 0.82, and $\phi_{DNS\text{-}ATP}$ = 0.06 μM at 4°C, and n = 0.65 and $\phi_{DNS\text{-}ATP}$ = 0.07 μM at 30°C. The value of ΔF_{max} was 55% at both temperatures. When β subunit up to 4 μM was added to 1.1 μM DNS-ATP, no Mg^{2+}-dependent fluorescence increase was observed (Δ).

The DNS-ATP binding to α subunit was also measured at room temperature by the equilibrium dialysis. We found that even in the absence of Mg^{2+}, DNS-ATP can bind to α subunit with an apparent dissociation constant of about 5 times higher than that in the presence of Mg^{2+}. However, during the equilibration we noticed some denaturation of α subunit, and therefore could not analyze the data quantitatively.

Effects of Nucleotides and Pyrophosphate on DNS-ATP Bound to α Subunit — The fluorescence intensity of DNS-ATP increased by addition of 5 mM $MgCl_2$ to the mixture containing 1.1 μM DNS-ATP, 0.8 μM α subunit and 2 mM EDTA. Then, ADP, AMPPNP, GTP, ITP, CTP at 0.2 mM or PP_i at 2 mM was added. All these compounds decreased the fluorescence intensity exponentially with $t_{1/2}$ = 7-8 s to a level almost equal to that of free DNS-ATP (data not shown), as was observed upon the addition of 0.2 mM ATP (Fig. 8).

DCCD inhibited the steady-state rate of EF_1-ATPase activity at high ATP concentrations, but did not inhibit EF_1-DNS-ATPase activity at low DNS-ATP concentrations, as mentioned above (Fig. 7). On the contrary we found that DCCD at 2 mM did not affect the Mg^{2+}-dependent fluorescence increase and the ATP-dependent fluorescence decrease of DNS-ATP in the presence of α subunit (data not shown), suggesting that the results obtained above (Figs. 6 & 7) were not due to the reaction of DCCD to this subunit.

Inability of α Subunit to Hydrolyze DNS-ATP and ATP — No TCA-$^{32}P_i$ liberation was observed on either addition of 5 mM $MgCl_2$ to the reaction mixture containing 2.8 μM DNS-AT^{32}P, 2.3 μM α subunit and 2 mM EDTA (△), or subsequent addition of 2 mM ATP (▲) (Fig. 4). Even when 5 mM $MgCl_2$ was added to the mixture containing 7.6 μM AT^{32}P and 1.6 μM α or 1.8 μM β subunit in 2 mM EDTA, no TCA-$^{32}P_i$ liberation was observed (data not shown). These results are in agreement with the previous finding that the isolated α, β or γ subunit did not have ATPase activity (7,8).

Fluorescence Change of DNS-ATP on Its Binding to Reconstituted EF_1-ATPase — To determine what kind of subunit interactions are needed for the EF_1-ATPase activity, we further investigated the reaction of DNS-ATP with the reconstituted EF_1-ATPase. Figure 11 shows the time course of change in the fluorescence intensity of DNS-ATP at 520 nm during its reaction with reconstituted EF_1-ATPase. The fluorescence intensity of 1.1 μM DNS-ATP in the presence of 2 mM EDTA increased slightly on addition of 0.36 mg/ml reconstituted EF_1-ATPase [arrow a in Fig. 11, compare curves a and b in Fig. 12]. On further addition of 5 mM $MgCl_2$ [arrow b in Fig. 11], the fluorescence intensity increased very rapidly ($t_{1/2} < 1$ s), then slowly with $t_{1/2}$ of about 30 s. The plateu level was 1.83 fold the intensity of free DNS-ATP. On further addition of 2 mM P_i [arrow c in Fig. 11], the fluorescence increased rapidly to a level of 2.4 fold that of free DNS-ATP. On addition of 2 mM ATP [arrow d in Fig. 11], the fluorescence intensity decreased to the level of free DNS-ATP.

When 5 mM $CaCl_2$ was added to the mixture containing 1.1 μM DNS-ATP and 0.36 mg/ml reconstituted EF_1-ATPase in the presence of 2 mM EDTA, the fluorescence intensity increased exponentially with

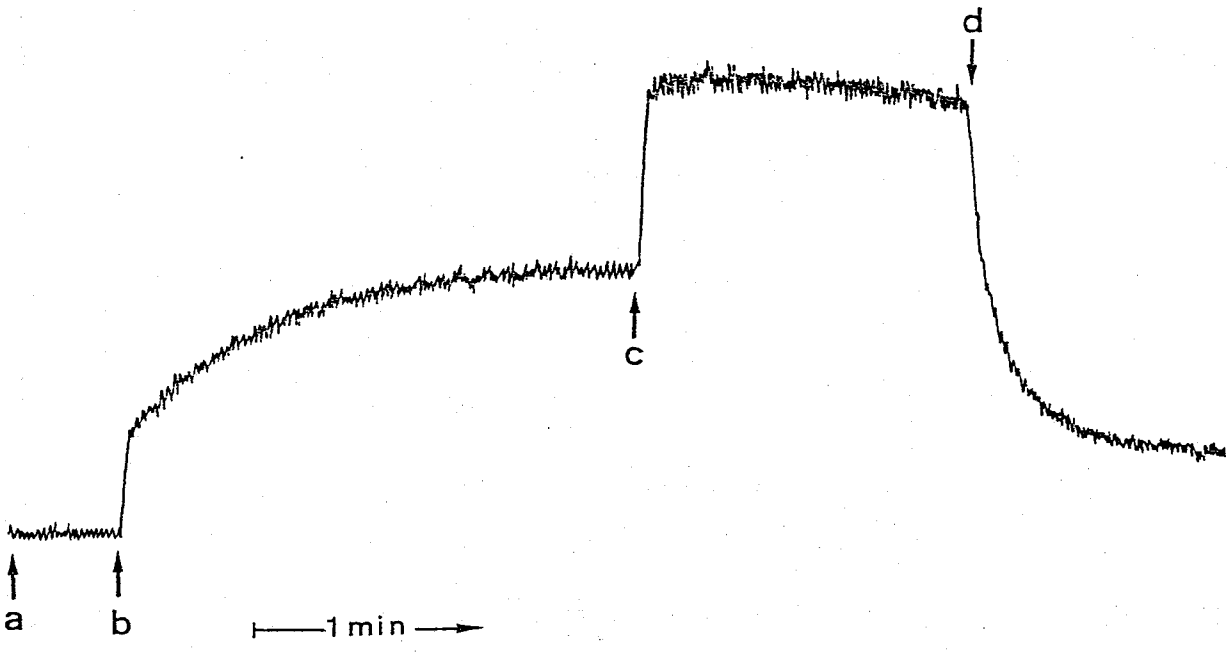

Fig. 11. Time course of fluorescence intensity change of DNS-ATP in the presence of reconstituted EF_1-ATPase. To a mixture containing 0.36 mg/ml reconstituted EF_1-ATPase in 2 mM EDTA, 100 mM NaCl and 50 mM Tris-acetate at pH 7.0 and 30°C, the following additions were made at the time indicated by arrows (a-d); a, 1.1 μM DNS-ATP; b, 5 mM $MgCl_2$; c, 2 mM K-P_i; d, 2 mM ATP. Specific activity of the reconstituted EF_1-ATPase was 30 U/mg protein. The concentration of the reconstituted EF_1-ATPase was shown by the protein concentration, because the recon= stitution was not complete [note that the specific activity of purified EF_1 is about 100 U/mg protein (28)].

$t_{1/2}$ of 40 s to reach a plateu level, which was 1.5 fold the intensity of free DNS-ATP. Further addition of 2 mM P_i induced a small increase (6%) in the fluorescence intensity (data not shown).

Figure 12 shows the fluorescence emission spectra of free DNS-ATP (trace a) and complexes of DNS-ATP with reconstituted EF_1-ATPase. When 0.53 mg/ml reconstituted EF_1-ATPase was added to 1.1 μM DNS-ATP in the presence of 2 mM EDTA, the fluorescence intensity increased slightly with a shift of the emission maximum from 555 to 550 nm (trace b). Further addition of 5 mM $MgCl_2$ markedly increased the fluorescence intensity, and the maximum shifted to 535 nm (trace c). The addition of 2 mM ATP reversed these fluorescence changes backward to the state of free DNS-ATP (trace d).

Figure 13 shows the result of fluorescence titration of DNS-ATP with reconstituted EF_1-ATPase in the presence of 3 mM Mg^{2+}. The extent of the Mg^{2+}-dependent fluorescence increase of 1.1 μM DNS-ATP increased with increase in the amount of reconstituted EF_1-ATPase added. When the amount of reconstituted EF_1-ATPase added was 1.5 μM (0.54 mg/ml), the extent of the Mg^{2+}-dependent fluorescence increase was 88% of the intensity of free DNS-ATP. However, we could not obtain a good fit to the data based on Eq. 1, since we could not measure the saturation level of the fluorescence increase.

Acceleration of DNS-Nucleotide Release from Reconstituted EF_1-ATPase-DNS-Nucleotide Complex by Nucleotides and Pyrophosphate — DNS-ATP at 1.1 μM was allowed to react with 0.42 mg/ml reconstituted EF_1-ATPase for 2 min in the presence of 3 mM Mg^{2+}. Then, 0.2 mM of nucleotide or 2 mM pyrophosphate was added [arrow c in Fig. 14], and the following decrease in the fluorescence intensity was measured

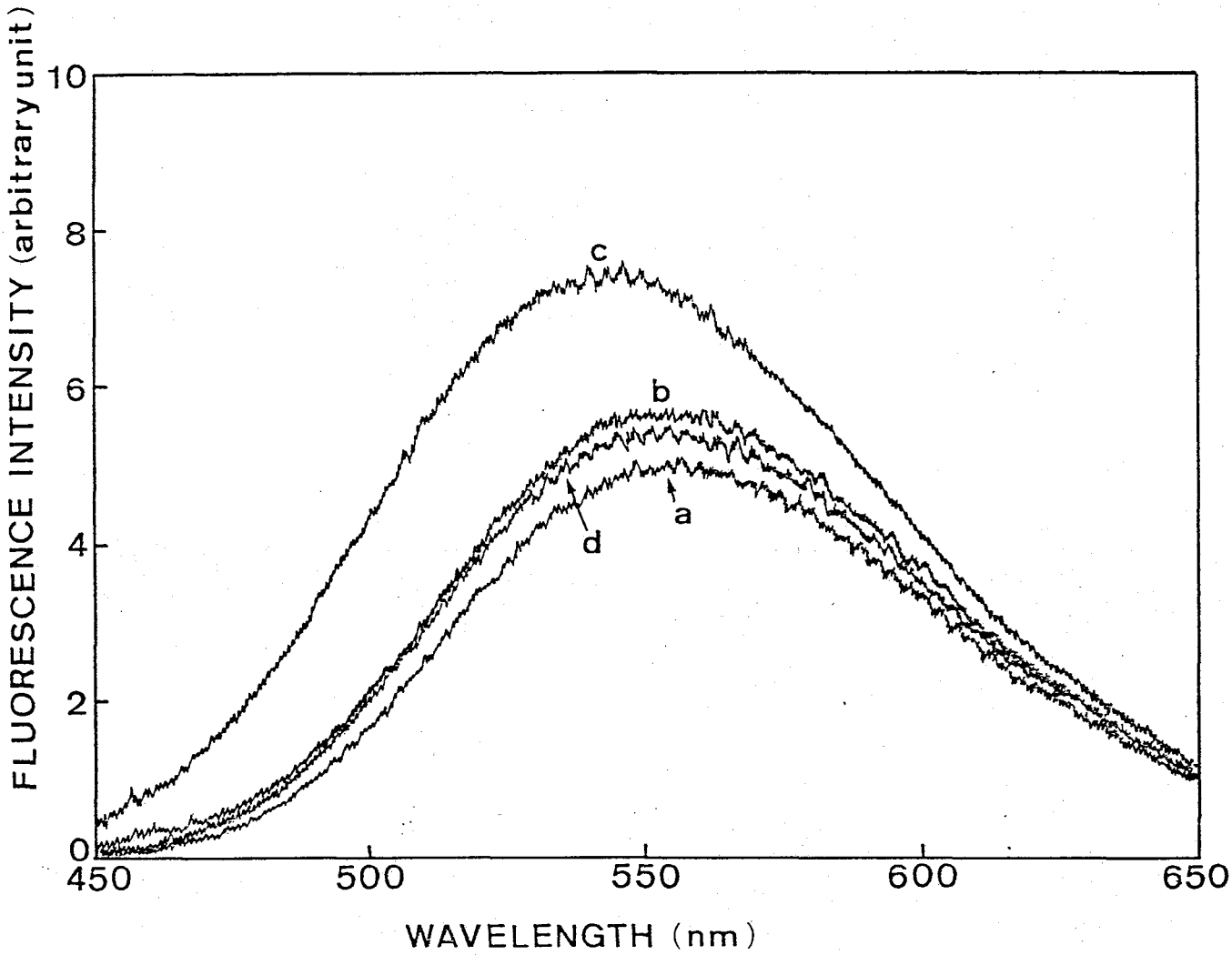

Fig. 12. Fluorescence emission spectra recorded during the course of reaction of DNS-ATP with reconstituted EF_1-ATPase. Spectra were recorded in the following order; curve a, 1.1 μM DNS-ATP; curve b, 1 min after addition of 0.53 mg/ml reconstituted EF_1; curve c, 2 min after addition of 3 mM Mg^{2+}; curve d, 1 min after addition of 2 mM ATP. Other conditions are the same as described in Fig. 11.

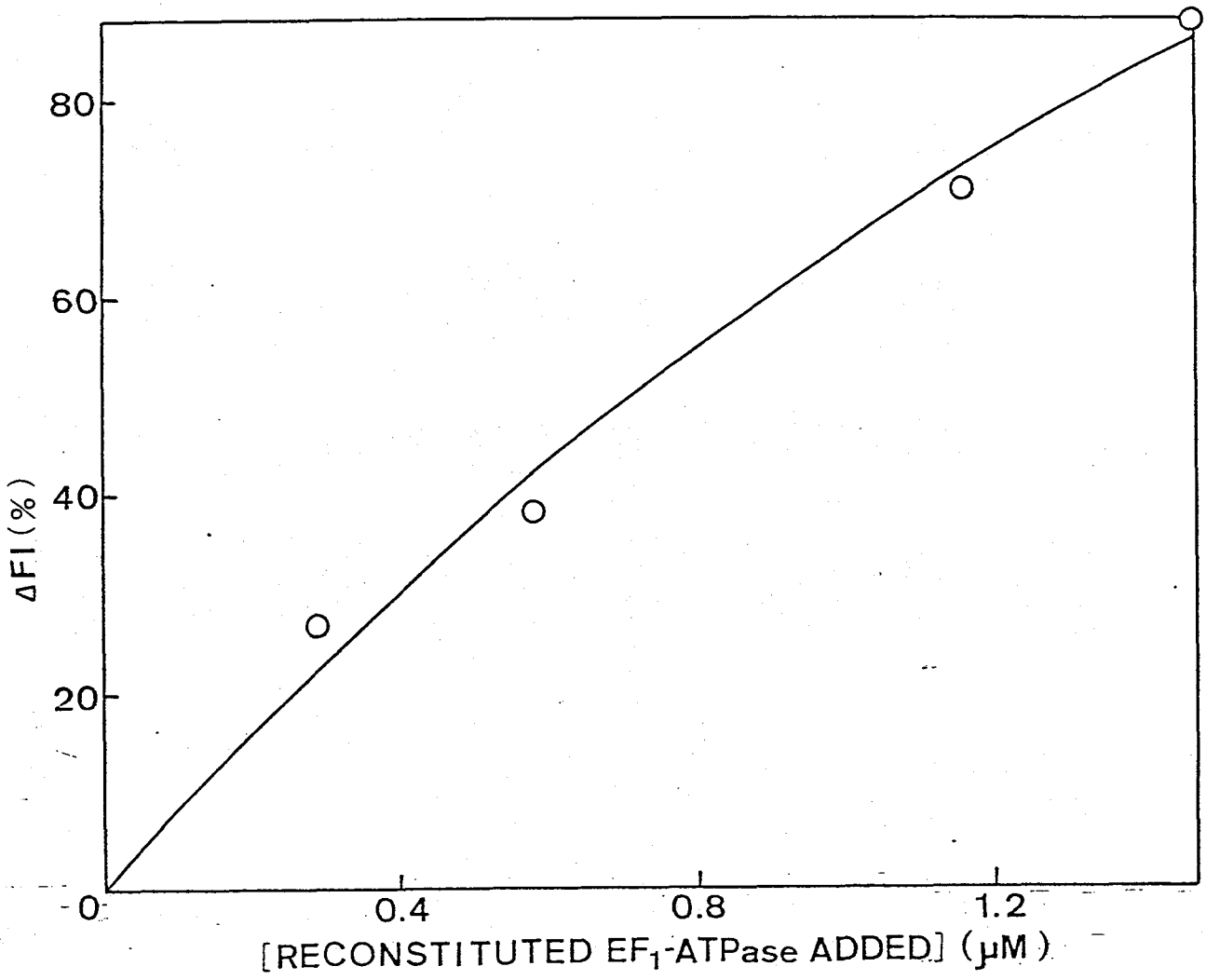

Fig. 13. Fluorometric titration of DNS-ATP with reconstitured EF_1-ATPase in the presence of Mg^{2+}. The extent of fluorescence enhancement of 1.1 μM DNS-ATP 2 min after addition of 3 mM Mg^{2+} was plotted against the amount of reconstituted EF_1-ATPase added. Other conditions are the same as described in Fig. 11.

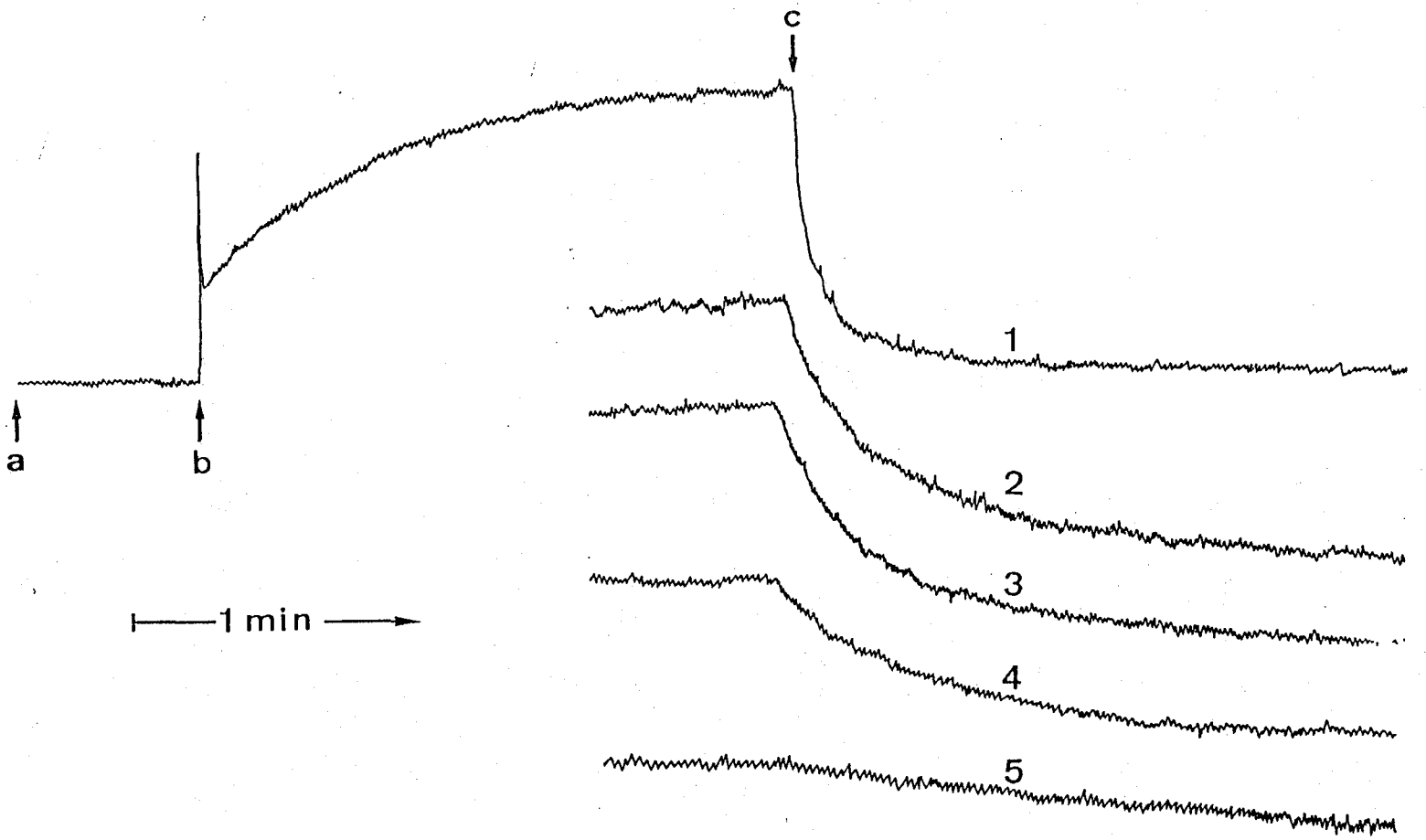

Fig. 14. Fluorescence decrease on addition of various phosphate compounds to reconstituted EF_1-ATPase-DNS-nucleotide. DNS-ATP at 1.1 μM was added to 0.42 mg/ml reconstituted EF_1-ATPase (indicated by arrow a), then 3 mM Mg^{2+} was added (indicated by arrow b). At the time indicated by arrow c, the following additions were made; 0.2 mM ATP (1), 0.2 mM ADP (2), 2 mM PP_i (3), 0.2 mM CTP (4) or 0.2 mM AMP (5). Other conditions are the same as described in Fig. 11.

(Fig. 14). The addition of ATP caused a fluorescence decrease, first rapidly ($t_{1/2} < 1$ s) and then slowly, and the final level was almost equal to that of free DNS-ATP (trace 1). When ADP (trace 2), PP_i (trace 3) or CTP (trace 4) was added, the fluorescence decreased almost exponentially. The rate of the fluorescence change decreased in the order of ATP ADP PP_i CTP. AMP (trace 5) had no effect on the fluorescence intensity of the reconstituted EF_1-ATPase-DNS-nucleotide.

DISCUSSION

We have previously performed kinetic studies on the single turnover of DNS-ATPase of beef heart F_1 (26), and proposed the following reaction scheme for the F_1-DNS-ATPase reaction:

$$E + \text{DNS-ATP} \rightleftharpoons E^{\text{DNS-ATP}} \rightarrow E^{\text{DNS-ATP*}} \rightleftharpoons E_P^{\text{DNS-ADP*}} \xrightarrow[P_i]{} E^{\text{DNS-ADP*}} \xrightarrow[\text{DNS-ADP}]{} E$$

The asterisk designates the reaction intermediate with enhanced fluorescence intensity of DNS-nucleotide. In the presence of Mg^{2+}, DNS-ATP binds to the high affinity site of F_1 to form a loose complex without enhanced fluorescence ($E^{\text{DNS-ATP}}$). The loose complex is converted to a tight complex with enhanced fluorescence ($E^{\text{DNS-ATP*}}$), then bound DNS-ATP is cleaved on the enzyme ($E_P^{\text{DNS-ADP*}}$). The apparent affinity of DNS-ATP to the enzyme is very high. Nucleotides such as ATP at high concentrations markedly accelerate the following three steps in the reaction sequence:

$$E^{\text{DNS-ATP*}} \rightleftharpoons E_P^{\text{DNS-ADP*}} \xrightarrow[P_i]{} E^{\text{DNS-ADP*}} \xrightarrow[\text{DNS-ADP}]{} E$$

Therefore, we suggested that there are low affinity regulatory site(s) as well as the high affinity catalytic sites in F_1. The purified EF_1 contained 2 mol ATP and 0.5 mol ADP per mol enzyme (33). These bound adenine nucleotides were found to be nonexchangeable with nucleotides in the medium (33). Therefore, in analyzing the results on the reaction of EF_1 with DNS-ATP, we neglected the effect of these tightly bound adenine nucleotides.

The first issue investigated in this study is the similarity of the reaction mechanism of EF_1-DNS-ATPase to that of F_1-DNS-ATPase. In the presence of Mg^{2+}, DNS-ATP reacted with EF_1 to induce a

fluorescence increase similar to that observed on beef heart F_1 (Figs. 1 & 2). This finding suggests that the environment of DNS-ATP binding sites in EF_1 is hydrophobic as is the case for F_1. The fluorescence intensity of EF_1-DNS-nucleotide complex increased on further addition of P_i, again as is the case for F_1-DNS-nucleotide complex. The fluorescence increase by P_i was observed even in the presence of excess amounts of DNS-ATP to EF_1. Furthermore, we (26) previously found that in the case of beef heart F_1, the affinity of DNS-ATP was unaffected by the addition of P_i. These findings indicate that the DNS-ATP binding site in EF_1 is made more hydrophobic by the action of P_i. The fluorometric titration of DNS-ATP with EF_1 in the presence of Mg^{2+} indicated that 3 mol of DNS-ATP was bound to 1 mol of EF_1 with an apparent dissociation constant of 0.23 μM (Fig. 3). Using the same method of fluorometric titration, we previously found that 2 mol of DNS-ATP binds to 1 mol of beef heart F_1 with an apparent dissociation constant of 0.44 μM (26). The stoichiometry of 3 mol DNS-ATP bound/mol EF_1 is consistent with the $\alpha_3\beta_3\gamma\delta\varepsilon$ stoichiometry of EF_1 subunits (34). When Mg^{2+} was added to a reaction mixture containing EF_1 and a low concentration of DNS-ATP, the fluorescence intensity was increased ($E^{DNS\text{-}ATP*}$; Fig. 1), and the increase was followed by liberation of P_i on termination of the reaction with TCA ($E_P^{DNS\text{-}ADP*}$ & $E^{DNS\text{-}ADP*}$; Fig. 4). The fluorescence intensity maintained its increased level after liberation of TCA-P_i, indicating that the rate of liberation of DNS-ADP from $E^{DNS\text{-}ADP*}$ is very small. These findings are quite similar to those of beef heart F_1 (26).

The mechanism of acceleration of EF_1-DNS-ATPase by high

concentrations of nucleotide was investigated using the same procedures as in the case of beef heart F_1. A biphasic decrease in the fluorescence intensity of EF_1-DNS-nucleotide complex was observed upon addition of high concentrations of ATP (Fig. 5). Therefore, it was suggested that ATP binding to low affinity regulatory site(s) in EF_1 induced a conformational change around the catalytic sites and accelerated the release of DNS-nucleotide, as in the case of beef heart F_1 (26). The rapid phase of the fluorescence decrease observed on addition of ATP, ADP, or GTP to EF_1-DNS-nucleotide complex (Fig. 5) is suggested to be due to the release of DNS-nucleotide induced by a conformational change of catalytic site on EF_1. The second slow phase will be due to the displacement of bound DNS-nucleotide by other nucleotide. This slow release of DNS-nucleotide was also observed in the case of addition of PP_i or CTP. Thus, the ability of phosphate compounds to release DNS-nucleotide from EF_1 was found to follow in the order of

$$\text{ATP} > \text{ADP} \approx \text{GTP} > \text{AMPPNP} > PP_i \approx \text{CTP} \gg \text{AMP}$$

This order was similar to that observed on beef heart F_1 (26):

$$\text{ATP} \gtrsim \text{ADP} \gtrsim \text{GTP} \approx \text{AMPPNP} > PP_i \approx \text{CTP} \gg \text{AMP}$$

In the case of beef heart F_1, ATP at high concentrations accelerated markedly the TCA-P_i liberation from $E^{DNS\text{-}ATP*}$ (26), whereas no acceleration of the TCA-P_i liberation by ATP was observed in the case of EF_1-DNS-ATPase (Fig. 4). This may suggests that the reaction mechanism of EF_1-DNS-ATPase is essentially different from that of F_1-DNS-ATPase. However, if we assume the reaction mechanisms of these ATPases are essentially the same, we can explain the discrepancy between the results of the two enzymes as due to the larger rate constant of the cleavage step ($E^{DNS\text{-}ATP*} \longrightarrow E_P^{DNS\text{-}ADP*}$) than the rates of the following steps in the case of EF_1-DNS-ATPase. Then, the

acceleration of TCA-P_i liberation due to acceleration of the cleavage step is not observed, since the amount of $E^{DNS\text{-}ATP*}$ at steady state is small.

The second issue is the subunit localization of the high affinity catalytic site and low affinity regulatory site. We previously suggested that the high affinity catalytic site and low affinity regulatory site exist in the α and β subunit, respectively (26). This suggestion is based on the information that the isolated α subunit of thermophilic F_1 or EF_1 and β subunit of thermophilic F_1 have high affinity and low affinity nucleotide-binding site, respectively (9,10). In this study, we found that the fluorescence intensity of DNS-ATP increased markedly on its reaction with α subunit but not with β subunit of EF_1 in the presence of Mg^{2+} (Figs. 8-10). The fluorometric titration of DNS-ATP with α subunit in the presence of Mg^{2+} indicated that 0.65-0.82 mol of DNS-ATP bound to 1 mol of α subunit very tightly (Fig. 10). This finding suggests that properties of DNS-ATP binding to α subunit are very similar to those of DNS-ATP binding to EF_1.

We investigated the possibility of the existence of a low affinity regulatory site in β subunit by using DCCD, a potent inhibitor of F_1-ATPase activity specific to β subunit (20-23). DCCD had no effect on the binding of DNS-ATP with α subunit. It inhibited only slightly the fluorescence increase of DNS-ATP by its binding to EF_1 (Fig. 6) and the single turnover of DNS-ATP hydrolysis by EF_1 [Fig. 7(B)]. DCCD inhibited markedly both the accelerating effect of ATP on DNS-nucleotide release from EF_1 (Fig. 6) and the EF_1-ATPase activity in the steady state [Fig. 7(A)]. These finding indicate that the modification of β subunit by DCCD blocks the function of the low affinity regulatory site, without affecting the binding of DNS-ATP to the high affinity catalytic site.

Thus, our findings strongly suggest that the high affinity catalytic site and the low affinity regulatory site exist in α and β subunits, respectively. This concept is apparently opposite to a widely accepted view that the catalytic site and the non-catalytic nucleotide binding site are located in β and α subunits, respectively (15,16,18-23). It should be mentioned that the latter view has been derived mainly from the inhibition of F_1-ATPase activity in the steady state by chemical modification of β subunit. However, we cannot determine the subunit localization of the catalytic site and regulatory site by measuring the effect of the modification of α or β subunit on the steady-state ATPase. This is because the low affinity nucleotide-binding to the regulatory site accelerates markedly the release of product bound to the catalytic site (26), and the F_1-ATPase activity in the steady state is markedly inhibited by the modification of the regulatory site as well.

In the previous paper, it was suggested that hydrolysis of nucleosidetriphosphate in the steady state occurs *via* different catalytic pathways and at different catalytic sites in F_1 because of the following two reasons (26). (a) The value of V_f (0.34 s^{-1}) for the formation of $E^{DNS\text{-}ATP*}$ was smaller than that of V_{max} ($\gg$1 s) for the steady-state rate of F_1-DNS-ATPase. (b) When ATP was added under conditions where most of F_1 was in the form of $E^{DNS\text{-}ADP*}$, ATP hydrolysis occurred without lag phase. For EF_1, the modification of β subunit by DCCD blocks both catalytic pathways, because DCCD inhibited the EF_1-ATPase in the steady state almost completely [Fig. 7(A)].

The third issue investigated in this paper is the difference between the structure and function of the isolated α subunit and those of integrated α in EF_1. Recently, Dunn and Futai (7), and Dunn

(35) reported that the isolated α subunit of EF_1 binds ATP in the absence of Mg^{2+} with very high affinity (K_d = 0.1 μM at 4°C). In this study, we found that the structure and function of the α subunit are altered when isolated from EF_1 in the following two respects: (a) In the presence of Ca^{2+}, DNS-ATP showed the fluorescence increase on its reaction with EF_1 [Fig. 1(B)], but not with isolated α subunit. The apparent dissociation constant of isolated α subunit for DNS-ATP in the presence of Mg^{2+} was 0.07 μM, which was about 1/3 of the value found with EF_1 (Figs. 3 & 10). The extent of the fluorescence increase of DNS-ATP bound to the isolated α subunit in the presence of Mg^{2+} was 55% of the fluorescence intensity of free DNS-ATP, which was about 1/5 of the value found with EF_1 (Figs. 3 & 10). These differences suggest that on isolation of α subunit, its affinity for DNS-ATP increased and the environment of the nucleotide-binding site became less hydrophobic. (b) P_i had no effect on the fluorescence intensity of DNS-ATP bound to the isolated α subunit [Fig. 8(A)], wherease P_i enhanced markedly the fluorescence intensity in the case of EF_1 [Fig. 1(A)]. This finding is consistent with the report that the P_i binding site exists in the subunit (36), and it also suggests an interaction between the α and β subunits in EF_1.

We found that the properties of the reaction of DNS-ATP with the isolated α subunit was unaffected by the addition of the β subunit, and that the fluorescence changes of DNS-ATP on its reaction with EF_1-ATPase reconstituted from α, β and γ subunit were quite similar to those on its reaction with native EF_1. On addition of Mg^{2+} to a reaction mixture containing DNS-ATP and the reconstituted EF_1-ATPase, the fluorescence intensity increased in two phases (Fig. 11). The

rapid phase ($t_{1/2} < 1$ s) of the increase was suggested to be due to the contamination by free α subunit, since the rapid phase was not observed on addition of Ca^{2+} instead of Mg^{2+}. It is suggested that the hydrophobicity of the nucleotide binding site is recovered to the level of native EF_1, since the extent of the Mg^{2+}-dependent fluorescence increase was larger than 88% of the intensity of free DNS-ATP (Fig. 13). Furthermore, the decrease in the fluorescence intensity of reconstituted EF_1-DNS-nucleotide complex after adding a phosphate compound showed a specificity quite aimilar to that of native EF_1: which is ATP > ADP $\approx$ PP_i > CTP $\gg$ AMP (Fig. 14). These findings clearly indicate that the subunit interactions in reconstituted EF_1-ATPase are similar to those in the native EF_1.

REFERENCES

1. Kagawa, Y., Sone, N., Hirata, H., & Yoshida, M. (1979) J. Bioenerg. Biomem. 11, 39-78
2. Penefsky, H.S. (1979) Adv. Enzymol. 49, 223-280
3. Baird, B.A. & Hammes, G.G. (1977) J. Biol. Chem. 252, 4743-4748
4. Verschoor, G.J., van de Sluis, P.R., & Slater, E.C. (1977) Biochim. Biophys. Acta 462, 422-437
5. Esch, F.S. & Allison, W.S. (1979) J. Biol. Chem. 254, 10740-10746
6. Yoshida, M., Okamoto, H., Sone, N., Hirata, H., & Kagawa, Y. (1977) Proc. Natl. Acad. Sci. U.S.A. 74, 936-940
7. Yoshida, M., Sone, N., Hirata, H., & Kagawa, Y. (1977) J. Biol. Chem. 252, 3480-3485
8. Futai, M. (1977) Biochem. Biophys. Res. Commun. 79, 1231-1237
9. Dunn, S.D. & Futai, M. (1980) J. Biol. Chem. 255, 113-118
10. Ohta, S., Tsuboi, M., Oshima, T., Yoshida, M., & Kagawa, Y. (1980) J. Biochem. 87, 1609-1617
11. Garret, N.E. & Penefsky, H.S. (1975) J. Biol. Chem. 250, 6640-6647
12. Slater, E.C., Kemp, A., Van der Kraan, I., Muller, J.L.M., Roveri, O.A., Verschoor, G.J., Wagenvoord, R.J., & Wielders, J.P.M. (1979) FEBS Lett. 103, 7-11
13. Schuster, S.M., Ebel, R.E., & Lardy, H.A. (1975) J. Biol. Chem. 250, 7848-7853
14. Wielders, J.P.M., Slater, E.C., & Muller, J.L.M. (1980) Biochim. Biophys. Acta 589, 231-240
15. Budker, V.G., Kozlov, I.A., Kurbatov, V.A., & Milgrom, Y.M. (1977) FEBS Lett. 83, 11-14

16. Drutsa, V.L., Kozlov, I.A., Milgrom, Y.M., Shabarova, Z.A., & Sokolova, N.I. (1979) Biochem. J. 182, 617-619

17. Wagenvoord, R.J., Kemp, A., & Slater, E.C. (1980) Biochim. Biophys. Acta 593, 204-211

18. Ferguson, S.J., Lloyd, W.J., & Radda, G.K. (1975) Eur. J. Biochem. 54, 127-133

19. Esch, F.S. & Allison, W.S. (1978) J. Biol. Chem. 253, 6100-6106

20. Pougeois, R., Satre, M., & Vignais, P.V. (1979) Biochemistry 18, 1408-1413

21. Satre, M., Lunardi, J., Pougeois, R., & Vignais, P.V. (1979) Biochemistry 18, 3134-3140

22. Shoshan, V. & Selman, B.R. (1980) J. Biol. Chem. 255, 384-389

23. Yoshida, M., Poser, J.W., Allison, W.S., & Esch, F.S. (1981) J. Biol. Chem. 256, 148-153

24. Hammes, G.G. & Hilborn, D.A. (1971) Biochim. Biophys. Acta 233, 580-590

25. Watanabe, T., Inoue, A., Tonomura, Y., Uesugi, S., Ohtsuka, E., & Ikehara, M. (1981) J. Biochem. 90, 956-965

26. Matsuoka, I., Watanabe, T., & Tonomura, Y. (1981) J. Biochem. 90, 967-989

27. Tietz, A. & Ochoa, S. (1958) Arch. Biochem. Biophys. 78, 477-494

28. Futai, M., Sternweis, P.C., & Heppel, L.A. (1974) Proc. Natl. Acad. Sci. U.S.A. 71, 2725-2729

29. Kanazawa, H., Miki, T., Tamura, F., Yura, T., & Futai, M. (1979) Proc. Natl. Acad. Sci. U.S.A. 76, 1126-1130

30. Gornall, A.G., Bardwill, C.S., & David, M.M. (1949) J. Biol. Chem. 177, 751-766

31. Bradford, M.M. (1976) Anal. Biochem. 72, 248-254

32. Fiske, C.H. & Subbarow, Y. (1925) J. Biol. Chem. 66, 375-400

33. Maeda, M., Kobayashi, H., Futai, M., & Anraku, Y. (1976) Biochem. Biophys. Res. Commun. 70, 228-234

34. Bragg, P.D. & Hou, C. (1975) Arch. Biochem. Biophys. 167, 311-321

35. Dunn, S.D. (1980) J. Biol. Chem. 255, 11857-11860

36. Lauquin, G., Pougeois, R., & Vignais, P.V. (1980) Biochemistry 19, 4620-4626

ACKNOWLEDGMENTS

I would like to express my great appreciation to Professor Y. Tonomura, Faculty of Science, Osaka University, and Professor M. Futai, Faculty of Pharmaceutical Sciences, Okayama University, and Dr. T. Nakamura, National Cardiovascular Center Research Institute, for their guidances, many valuable suggestions, and continuous encouragements during the course of this work.

I am greatly indebted to Dr. T. Watanabe, Faculty of Science, Osaka University, who performed the synthesis of DNS-ATP with his great ability in organic chemistry.

I am grateful to Dr. H. Kanazawa, Faculty of Pharmaceutical Sciences, Okayama University, and Dr. Y. Fukumori and Professor T. Yamanaka, Faculty of Science, Osaka University, for large scale culture of E. coli. Ms. K. Takeda, Faculty of Pharmaceutical Sciences, Okayama University, kindly supplied me the preparation of EF_1 and its subunits.

I am also grateful to many members of Professor Tonomura's laboratory for their help in the preparation of beef heart mitochondria.

Finally, I want to extend my thanks to Professor Y. Orii, Medical School, Kyoto University, and Dr. R. E. Yantorno, Faculty of Science, Osaka University, for their valuable discussion and help in the preparation of this thesis in English.

LIST OF PUBLICATIONS

1. Calorimetric studies of heat of respiration of mitochondria. Nakamura, T. & Matsuoka, I. (1978) J. Biochem. 84, 39-46

2. Calorimetric studies of the heat of respiration of mitochondria. Matsuoka, I., Watanabe, T., & Nakamura, T. (1978) Frontiers of Biological Energetics Vol. 1, pp. 689-697, Academic Press, Inc., New York

3. Reversible effects of fatty acids on respiration, oxidative phosphorylation, and heat production of rat liver mitochondria. Matsuoka, I. & Nakamura, T. (1979) J. Biochem. 86, 675-681

4. Comparative studies on the effects of linoleate and methyl linoleate and their hydroperoxides on the respiration and reactivities of rat heart mitochondria. Shiotani, A. Watanabe, T., Matsuoka, I., & Nakamura, T. (1980) J. Biochem. 88, 677-683

5. Reaction mechanism of the ATPase activity of mitochondrial F_1, studied by using a fluorescent ATP analog, 2'-(5-dimethyl-aminonaphthalene-1-sulfonyl) amino-2'-deoxyATP. Matsuoka, I., Watanabe, T., & Tonomura, Y. (1981) J. Biochem. 90, 967-989

6. Reactions of fluorescent ATP analog, 2'-(5-dimethylamino-naphthalene-1-sulfonyl) amino-2'-deoxyATP with E. coli F_1-ATPase and its subunits. Matsuoka, I., Takeda, K., Futai, M., & Tonomura, Y. submitted to J. Biochem.